INCREASING TREATMENT EFFICACY BY DRUG REPOSITIONING IN ACUTE LYMPHOBLASTIC LEUKEMIA

EZGİ YAĞMUR TÜKEL

Thesis for the Master's Program in Bioengineering

Graduate School

Izmir University of Economics

Izmir

2024

INCREASING TREATMENT EFFICACY BY DRUG REPOSITIONING IN ACUTE LYMPHOBLASTIC LEUKEMIA

EZGİ YAĞMUR TÜKEL

THESIS ADVISOR: ASST. PROF. DR. YAĞMUR KİRAZ DURMAZ

A Master's Thesis

Submitted to

the Graduate School of Izmir University of Economics

the Department of Bioengineering

Izmir

2024

ETHICAL DECLARATION

I hereby declare that I am the sole author of this thesis and that I have conducted my work in accordance with academic rules and ethical behaviour at every stage from the planning of the thesis to its defence. I confirm that I have cited all ideas, information and findings that are not specific to my study, as required by the code of ethical behaviour, and that all statements not cited are my own.

Name, Surname: EZGİ YAĞMUR TÜKEL

Date: 25.01.2024

Signature:

ABSTRACT

INCREASING TREATMENT EFFICACY BY DRUG REPOSITIONING IN ACUTE LYMPHOBLASTIC LEUKEMIA

Tükel, Ezgi Yağmur

Master's Program in Bioengineering

Advisor: Asst. Prof. Dr. Yağmur Kiraz Durmaz

Janurary, 2024

Acute lymphoblastic leukemia (ALL) is recognized for its heterogeneity, and diverse genetic abnormalities contributing to disease progression. The predominant subtype, high-risk and aggressive Philadelphia positive ALL (Ph+ ALL), is characterized by BCR/ABL translocation. Imatinib mesylate, a tyrosine kinase inhibitor (TKI), has been pivotal in treating Ph+ ALL. However, achieving sustainable therapeutic success is made difficult by TKI resistance. Therefore, there is an urgent need to identify targets that offer alternative ALL treatments. This thesis aims to propose a novel treatment strategy through drug repositioning, using a comprehensive analysis of transcriptome datasets of ALL and Ph(+) ALL to identify DEGs associated with disease progression. The research revealed Maytansine and Isoprenaline for ALL, and Glipizide and Desipramine for Ph(+) ALL as potential candidates for therapeutic intervention. MTT and Trypan blue assays were performed to confirm the cytotoxic effects of these drugs on both ALL (Jurkat) and Ph+ ALL (SUP-B15) cell lines. Additionally, the apoptotic

effects of these drugs have been determined using Annexin/FITC dual staining. Furthermore, tests were conducted on Imatinib-resistant SUP-B15/R cells to determine the impact of Imatinib resistance on the cytotoxic and apoptotic effects of Desipramine and Glipizide. According to results, all the drugs have exhibited cytotoxic and apoptotic effects on the cells. Additionally, synergistic doses with Imatinib were obtained in both SUP-B15 and SUP-B15/R cells. As such, the repositioned drugs, whose cytotoxic and apoptotic effects have been detected, may pave the way to increase the survival rate by increasing the treatment effectiveness in both Ph (-) ALL and Ph (+) ALL patients.

Keywords: Acute lymphoblastic leukemia, Philadelphia chromosome, drug resistance, imatinib, drug repurposing

ÖZET

Akut Lenfoblastik Lösemilerde İlaç Yeniden Konumlandırma Ile Tedavi Etkinliğinin Artırılması

Tükel, Ezgi Yağmur

Biyomühendislik Yüksek Lisans Programı

Tez Danışmanı: Dr. Öğr.Üyesi Yağmur Kiraz Durmaz

Ocak, 2024

Akut lenfoblastik lösemi (ALL), hastalığın ilerlemesine katkıda bulunan çeşitli genetik anormalliklerle işaretlenmiş, önemli ölçüde heterojenliği ile tanınmaktadır. Baskın alt tip olan Philadelphia pozitif ALL (Ph+ ALL), BCR/ABL translokasyonu ile karakterize olup hastalığı yüksek riskli ve agresif hale getirir. İmatinib mesilat, tirozin kinaz inhibitörü (TKI) olarak, Ph+ ALL'nin tedavisinde etkili olmuştur. Fakat, dikkate değer etkisine rağmen, sürdürülebilir terapötik başarıya ulaşması, TKI direncinin ortaya çıkması nedeniyle zorlaşmaktadır. Bu nedenle, ALL tedavisi için alternatif sunabilecek hedeflerin belirlenmesi konusunda acil bir ihtiyaç bulunmaktadır. Bu tez, ilaçların yeniden konumlandırılması yoluyla yenilikçi ve etkili bir tedavi stratejisi önermeyi amaçlamaktadır. Çalışma, hastalık ilerlemesi ile ilişkilendirilen DEG'leri belirlemek amacıyla ALL ve Ph (+) ALL ile ilgili transkriptom veri setlerinin kapsamlı bir analizini içermektedir. Araştırma ALL için Maytansin ve İzoprenalin, Ph(+) ALL

için Glipizid ve Desipramin'in terapötik müdahale için potansiyel adaylar olduğu belirlenmiştir. Seçilen ilaçların hem ALL (Jurkat) hem de Ph(+) ALL (SUP-B15) hücre hatları üzerindeki in vitro sitotoksik etkilerini doğrulamak için MTT ve Trypan blue deneyleri yapılmıştır. Ayrıca sitotoksik aktiviteye sahip olduğu belirlenen ilaçların hücreler üzerindeki apoptotik etkileri Annexin/FITC ikili boyama yöntemi kullanılarak belirlenmiştir. Bununla birlikte, Imatinib dirençli SUP-B15/R hücrelerinde Imatinib direncinin Desipramin ve Glipizid'in sitotoksik ve apoptotik aktiviteleri üzerineki etkisi belirlenmiştir. Deney sonuçlarına göre, belirlenen tüm ilaçların hücreler üzerinde sitotoksik ve apoptotik etkiler gösterdiği görülmüştür. Ayrıca, hem SUP-B15 hem de SUP-B15/R hücrelerinde İmatinib ile sinerjik dozlar elde edilmiştir. Sonuç olarak, sitotoksik ve apoptotik etkileri belirlenen yeniden konumlandırılmış ilaçların, hem Ph (-) ALL hem de Ph (+) ALL hastalarında tedavi etkinliğini artırarak sağkalım oranını artırma yolunu açabileceği düşünülmektedir.

Anahtar Kelimeler: Akut Lenfoblastik Lösemil, Philadelphia kromozomu,ilaç direnci,imatinib, ilaç yeniden konumlandırma

Dedicated to *all dreamers*…

ACKNOWLEDGEMENTS

I would like to extend my heartfelt gratitude to those who have played a pivotal role in the completion of this thesis. This academic journey has been a challenging yet rewarding experience, and I am fortunate to have received support from many incredible individuals.

First and foremost, I express my deepest appreciation to my advisor, Asst. Prof. Dr. Yağmur Kiraz Durmaz. Their guidance, expertise, and unwavering commitment to academic excellence have been the driving forces behind the success of this research. I am truly grateful for the invaluable mentorship provided throughout this process.

I am indebted to my parents, Ebru Tükel and Alper Tükel, for their constant encouragement and understanding during the ups and downs of this academic endeavor. Their belief in my abilities has been a constant source of motivation. Furthermore, I am grateful to them for always showing me the light even in the darkest of moments.

I extend my thanks to my partner, Melik Fırat, and my best friend, Başak Özay, who have provided insights, feedback, encouragement and for always trusting me even when I did not trust myself along the way. Your presence has made this academic journey more enriching and enjoyable.

I wish to express my sincere gratitude to all my lab colleagues, especially Onur Ateş, for all their help. Your helpful and friendly attitude made this process much easier.

Finally, I would like to thank Beste Turanlı and Betül Budak for all their contributions to this project.

TABLE OF CONTENTS

ABSTRACT……iv
ÖZET……...vi
ACKNOWLEDGEMENTS……... ix
TABLE OF CONTENTS……x
LIST OF TABLES…… xiii
LIST OF FIGURES……...xiv
CHAPTER 1: INTRODUCTION 1
1.1. Leukemia and Leukemia Classification 1
1.2. Acute Lymphoblastic Leukemia..... 2
1.2.1. T-lineage ALL 3
1.2.2. B-lineage ALL 5
1.3. Philadelphia Chromosome..... 9
1.4. Treatment Strategies for ALL and Ph (+) ALL..... 10
1.4.1. Treatment Strategies for ALL..... 11
1.4.2. Treatment Strategies for Ph (+) ALL..... 13
1.4.2.1. Imatinib 15
1.5. Imatinib Resistance on Acute Lymphoblastic Leukemia..... 16
1.6. Computational Approaches in Life Sciences 17
1.6.1. System Biology..... 18
1.6.2. Analyses Used in Systems Biology Studies 19
1.6.3. Drug Repurposing..... 23
2. The Aim of Study 29
CHAPTER 2: METHODS 31
2.1. Computational Studies 31
2.1.1. Obtaining transcriptome (gene expression) data sets 31
2.1.2. Identifying Differentially Expressed Genes at the mRNA Level..... 32
2.1.3. Functional Enrichment of Gene Sets 33
2.1.4. Establishing Protein-Protein Interaction Networks 33
2.1.5. Drug Repositioning for Candidate Drug Identification..... 34
2.2. Cell Culture 34

2.2.1. Thawing Frozen Cells 35
2.2.2. Subculturing of Cells 35
2.2.3. Freezing Cells 35
2.2.4. Cell Counting 36
2.2.5. Establishing an Imatinib-Resistant Cell Line Ph (+) ALL 36
2.2.6. Validating Imatinib Resistance with MTT Assay 37
2.2.7. Validating Imatinib Resistance with Growth Curve 37
2.2.8. Validating Imatinib Resistance with Flow Cytometry 38
2.3. Evaluating the Cytotoxic Activity of Drug Candidates for Ph (-) ALL on Jurkat Cell Line 38
2.3.1. Determination of Anti-Proliferative Effects of Drugs on Ph (-) ALL Cells with MTT Assay 38
2.3.2. Assessment of Cytotoxic Effects of Drugs Possessing Established 39
Anti-Proliferative Properties on Ph (-) ALL Cells with Trypan Blue Assay 39
2.4. Estimation of the Cytotoxic Effects of Drugs, Both Individually and in Combination with Imatinib, on Imatinib-Sensitive and Resistant Ph+ ALL Cells. 39
2.4.1. Determination of Cytotoxic Effects of Drugs on Both Sensitive and Imatinib Resistant Ph (+) ALL Cells with MTT Assay 39
2.4.2. Determination of the Cytotoxic Effect of Drugs Given in Combination with Imatinib by MTT Assay. 40
2.4.3. Confirmation of Cytotoxic Activity of Selected Synergistic Doses Using Trypan Blue Exclusion Assay 40
2.5. Assessment of the Apoptotic Effects of Synergic Doses of the Selected Drugs Determined To Have Potent Cytotoxic Effects on the Cells. 41
2.5.1. Determination of Apoptotic Cell Population via Annexin/FITC dual staining 41
2.6.1. Confirmation of Cytotoxic Activity of Selected Drugs on HUVEC Cells Using Trypan Blue Exclusion Assay 41
CHAPTER 3: RESULTS 43
3.1. Determination of the Drugs to be Repositioned 43
3.1.1. Identification of HUB Proteins 44
3.1.2. Gene Enrichment Analysis 45
3.1.3. Selected Repositioned Drugs 46

3.2. Generation of Imatinib Resistant Cell Line 48
3.2.1. Results of MTT assays 48
3.2.2. Representation of Growth Curve for Validating Imatinib Resistance 49
3.2.3. Flow cytometry for determining resistance 50
3.3. Cytotoxic Effects of Maytansine and Isoprenaline on Ph (-) ALL cell line 52
3.3.1. Ascertainment of Anti-Proliferative Effects of Maytansine and Isoprenaline With MTT Assay 52
3.3.2. Results of Trypan Blue Staining on Ph (-) ALL cell line after Drug Administrations 53
3.4. Assessment of the Cytotoxic Impact of Glipizide and Desipramine, Both Individually and in Conjunction with Imatinib, on Ph (+) ALL Cells 54
3.4.1. MTT Assay Results for Antiproliferative Effects Induced by Glipizide and Desipramine in Ph (+) ALL Cells 55
3.4.2. MTT Assay outcomes obtained with Glipizide and Desipramine combinations in conjunction with Imatinib administration on Ph (+) ALL Cells Respectively 57
3.4.3. Findings from Trypan Blue Staining at the Selected Synergistic Doses on Ph(+) ALL Cells 59
3.5. Evaluation of Apoptotic Effects of Selected Drugs on ALL Cells. 62
3.5.1 Determination of Apoptotic Effects of Maytansine and Isoprenaline on Jurkat Cells 62
3.5.2. Determination of Apoptotic Effects of Glipizide and Desipramine on SUP-15 and SUP-B15/R cells 63
3.6. Findings from Trypan Blue Staining at the Selected Drugs on HUVEC Cells .. 66
CHAPTER 4: DISCUSSION 69
CHAPTER 5: CONCLUSION 75
REFERENCES 78

LIST OF TABLES

Table 1. Who (2016) ALL Classification 2
Table 2. The table comprises GEO datasets utilized within the study's framework, encompassing ALL, Ph+ ALL, B-CLL , and CLL 31
Table 3. The first two drugs targeting core proteins in ALL disease..... 47
Table 4. The first two drugs targeting core proteins in Ph (+) ALL disease..... 48

LIST OF FIGURES

Figure 1. Illustrative representation genetic biomarkers associated with B-ALL… ... 9
Figure 2. Formation of Philadelphia chromosome..... 10
Figure 3. Generation of Imatinib resistant SUP-B15/R cell line by gradually exposing the cells to increasing concentrations of Imatinib over an extended period. 37
Figure 4. Schematic representation of the 6-well plate arrangement for the Trypan Blue experiment. 39
Figure 5. Representation of combination MTT assays with selected drugs on a 96-well plate. 40
Figure 6. Number of DEGs in the result of DEG analysis of each dataset A) in ALL and B) in Ph+ ALL..... 43
Figure 7. Representation of R/Robustrankaggreg analysis results with heatmap diagram of fold changes (logFC) of the top 20 genes with increased and decreased expression in the ALL (A) and Ph (+) ALL data sets (B)..... 44
Figure 8. A) The interaction network illustrating the connections of hub proteins (depicted by blue octagons) with other proteins in ALL. B) The interaction network showcasing the links of hub proteins (depicted by red octagons) with other proteins in Ph+ ALL. 45
Figure 9. Pathways/biological processes activated by genes exhibiting differential gene expression in ALL (A). Pathways/biological processes activated by genes exhibiting differential gene expression in Ph-positive ALL (B)..... 46
Figure 10. Determination of the viability of SUP-B15 and SUP-B15/R cells with imatinib treatment. Imatinib application was carried out for 72 hours, and viability analysis was performed using the MTT test. The experiments were repeated three times. Error bars indicate the standard deviation. 49
Figure 11. Representative growth curve created with data obtained from the trypan blue experiment on SUP-B15 and SUP-B15/R. Imatinib application was carried out for 72 hours, and viability analysis was performed using the MTT test. The experiments were repeated three times. Error bars indicate the standard deviation. . 50
Figure 12. Representation of apoptotic cells identified in SUP-B15 and SUP-B15/R cells treated with IC50 Imatinib dose using Annexin/PI staining. Imatinib application

was carried out for 72 hours, and viability analysis was performed using the MTT test. The experiments were repeated three times. Error bars indicate the standard deviation 51
Figure 13. Determination of the viability of Jurkat cells treated with Maytansine (A) and Isoprenaline (B). Both treatment was conducted for 48 hours, and viability analysis was performed using the MTT test. The experiments were repeated three times. Error bars indicate standard deviation. 52
Figure 14. Determination of the viability of Jurkat cells treated with Doxorubicin. treatment was conducted for 48 hours, and viability analysis was performed using the MTT test. The experiments were repeated three times. Error bars indicate standard deviation. 53
Figure 15. Determination of the cytotoxic effects of Maytansine (A) and Isoprenaline (B) on Jurkat cells based on the trypan blue staining results obtained from the assessment of their anti-proliferative activity. The experiment was repeated three times. Error bars indicate standard deviation. 54
Figure 16. Determination of the viability of SUP-B15 (A) and SUP-B15/R (B) cells treated with Desipramine. Desipramine treatment was carried out for 72 hours, and viability analysis was conducted using the MTT test. The experiments were repeated three times. Error bars indicate standard deviation. 55
Figure 17. Determination of the viability of SUP-B15 (A) and SUP-B15/R (B) cells treated with Glipizide. Glipizide treatment was carried out for 72 hours, and viability analysis was conducted using the MTT test. The experiments were repeated three times. Error bars indicate standard deviation. 56
Figure 18. Determination of the viability of SUP-B15 (A) and SUP-B15/R (B) cells treated with Dasatinib. Dasatinib treatment was carried out for 72 hours, and viability analysis was conducted using the MTT test. The experiments were repeated three times. Error bars indicate standard deviation. 57
Figure 19. Determination of the viability of SUP-B15 (A) and SUP-B15/R (B) cells treated with Imatinib (IC20), Desipramine, and Imatinib (IC20) plus Desipramine combination. All treatments were carried out for 72 hours, and viability analysis was conducted using the MTT test. The experiments were repeated three times. Error bars indicate standard deviation. 58

Figure 20. Determination of the viability of SUP-B15 (A) and SUP-B15/R (B) cells treated with Imatinib (IC20), Glipizide and Imatinib (IC20) plus Glipizide combination. All treatments were carried out for 72 hours, and viability analysis was conducted using the MTT test. The experiments were repeated three times. Error bars indicate standard deviation. 59
Figure 21. Determination of the cytotoxic effects of IC20 Imatinib, Desipramine 10 μM, and their combinations on SUP-B15 cells based on the trypan blue staining results obtained from the assessment of their anti-proliferative activity. The experiment was repeated three times. Error bars indicate standard deviation. 60
Figure 22. Determination of the cytotoxic effects of IC20 Imatinib, Glipizide 10 μM, and their combinations on SUP-B15 cells based on the trypan blue staining results obtained from the assessment of their anti-proliferative activity. The experiment was repeated three times. Error bars indicate standard deviation. 60
Figure 23. Determination of the cytotoxic effects of IC20 Imatinib, Glipizide 80 μM, and their combinations on SUP-B15 cells based on the trypan blue staining results obtained from the assessment of their anti-proliferative activity. The experiment was repeated three times. Error bars indicate standard deviation. 61
Figure 24. Determination of the cytotoxic effects of IC10 Imatinib, Glipizide 50μM, and their combinations on SUP-B15/R cells based on the trypan blue staining results obtained from the assessment of their anti-proliferative activity. The experiment was repeated three times. Error bars indicate standard deviation. 62
Figure 25. Determination of Apoptotic effects of Maytansine (A) and Isoprenaline (B) on Jurkat cell line based on the Annexin/PI double staining results. The experiment was repeated three times. Error bars indicate standard deviation. 63
Figure 26. Determination of the Apoptotic effects of IC20 Imatinib, Glipizide 10 μM and their combinations (A) and IC20 Imatinib, Glipizide 80 μM and their combinations (B) on SUP-B15 cells based on the Annexin/PI double staining experiment. The experiment was repeated three times. Error bars indicate standard deviation. 64
Figure 27. Determination of the Apoptotic effects of IC20 Imatinib,Desipramine 10 μM and their combinations on SUP-B15 cells based on the Annexin/PI double staining experiment. The experiment was repeated three times. Error bars indicate standard deviation. 65

Figure 28. Determination of the Apoptotic effects of IC10 Imatinib, Glipizide 50 μM and their combinations on SUP-B15/R cells based on the Annexin/PI double staining experiment. The experiment was repeated three times. Error bars indicate standard deviation. 65
Figure 29. Determination of the Apoptotic effects of IC10 Imatinib, Desipramine 15 μM and their combinations on SUP-B15/R cells based on the Annexin/PI double staining experiment. The experiment was repeated three times. Error bars indicate standard deviation. 66
Figure 30. Determination of the cytotoxic effects of Maytansine (A) and Isoprenaline (B) on HUVEC and Jurkat cells based on the trypan blue staining results obtained from the assessment of their anti-proliferative activity. The experiment was repeated three times. Error bars indicate standard deviation. 67
Figure 31. Determination of the cytotoxic effects of Glipizide (A) and Desipramine (B) on HUVEC and SUP-B15 cells based on the trypan blue staining results obtained from the assessment of their anti-proliferative activity. The experiment was repeated three times. Error bars indicate standard deviation. 68

CHAPTER 1: INTRODUCTION

1.1. Leukemia and Leukemia Classification

It is an established fact that leukemias are lethal disorders that originate from the bone marrow and blood. Types of leukemias can affect every segment of population from children to the elderly, at disparate degrees (Juliusson and Hough, 2016). The term 'leuk' (white) combined with 'emia' (blood) denotes the color of the blood in leukemia, which becomes whitish due to the accumulation of a high number of white blood cells (Sell, 2005). Leukemias encompass a diverse array of conditions resulting from the excessive growth of immature hematopoietic cells that become arrested at an early developmental stage, unable to mature into fully functional blood cells. These accumulated cell clones tend to occupy the bone marrow and can also migrate into the bloodstream. Analyzing the peripheral blood offers insights into identifying the specific cell lineage involved (Lightfoot et al., 2017). Leukemias can exhibit diverse courses of progression. They may present as rapidly advancing conditions with limited survival prospects in the absence of treatment, referred to as acute leukemia. Alternatively, these diseases can manifest as slow-growing forms, allowing patients to lead relatively long lives even without intervention, categorized as chronic leukemia. Beyond this chronic/acute distinction, leukemias are further categorized based on their cellular lineage. Myeloid leukemia pertains to leukemic cells originating from the bone marrow lineage, which causes granulocytes, macrophages, red blood cells, and platelets. In contrast, lymphoid leukemia involves leukemic cells derived from the lymphocyte lineage (Sabath, 2013). The most prevalent leukemia subtypes include acute myeloid leukemia (AML) and chronic myeloid leukemia (CML), which are associated with the myeloid lineage, as well as acute lymphoblastic leukemia (ALL) and chronic lymphocytic leukemia (CLL), which pertain to the lymphoid lineage. There are also less common variations, like mature B and T-cell leukemias, along with NK cell-related leukemias, among others, originating from mature white blood cells. Notably, in 2016, the World Health Organization (WHO) updated its classification due to identification of various biomarkers and resulting in significant alterations to the traditional categorization. In table 1, ALL classifications were given(Wang and He, 2016). The etiology of leukemia remains a subject of ongoing debate within the

scientific community. Presently, three factors have garnered significant attention in connection to leukemia development, specifically ionizing radiation, benzene exposure, and alkylating agents. Nevertheless, the established risk factors can account for only a limited subset of patients, leaving the pathogenesis of the majority of cases yet to be fully understood. Recent research suggests that smoking, exposure to electromagnetic fields, the use of hair dyes, contact with organic solvents, and viral infections may also present potential risk factors for leukemia (Guo et al., 2022)

Table 1. Who (2016) ALL Classification (Source: Wang and He, 2016)

B-cell lymphoblastic leukemia/lymphoma – not otherwise specified
B-cell lymphoblastic leukemia/lymphoma, with recurrent genetic abnormalities
B-cell lymphoblastic leukemia/lymphoma with hypodiploidy *B-cell lymphoblastic leukemia/lymphoma with hyperdiploidy* *B-cell lymphoblastic leukemia/lymphoma with t(9;22)(q34;q11.2)[BCR-ABL1]* *B-cell lymphoblastic leukemia/lymphoma with t(v;11q23)[MLL rearranged]* *B-cell lymphoblastic leukemia/lymphoma with t(12;21)(p13;q22)[ETV6-RUNX1]* *B-cell lymphoblastic leukemia/lymphoma with t(1;19)(q23;p13.3)[TCF3-PBX1] B-cell lymphoblastic leukemia/lymphoma with t(5;14)(q31;q32)[IL3-IGH]* *B-cell lymphoblastic leukemia/lymphoma with intrachromosomal amplification of chromosome 21 (iAMP21)* *B-cell lymphoblastic leukemia/lymphoma with translocations involving tyrosine kinases or cytokine receptors (BCR-ABL1–like ALL)*
T-cell lymphoblastic leukemia/lymphomas *Early T-cell precursor lymphoblastic leukemia*

1.2. Acute Lymphoblastic Leukemia

Acute lymphoblastic leukemia (ALL) represents a diverse spectrum of lymphoid conditions that arise from the uncontrolled growth of immature lymphoid cells in the bone marrow, bloodstream, and various other organs. Enhanced comprehension of the underlying biological mechanisms driving ALL has prompted revisions in its pathological categorization, the introduction of novel therapeutic approaches, and the implementation of treatment strategies tailored to individual risk profiles (Jacobson et

al., 2016). Clinically, ALL is considered an infrequent ailment, with nearly 6.000 new instances identified in the USA in 2019, constituting only 0.3% of all cancer cases. ALL have revealed it to be a genetically diverse disease, resulting in the emergence of various genetic subtypes that have refined our ability to assess risk. While most instances of ALL are detected among the pediatric population, the incidence exhibits a distinct pattern, with two notable peaks: One in those under 5 years old, and another around the age of 50 (DeAngelo et al., 2020). In the case of pediatric ALL, there is a comparatively favorable prognosis upon diagnosis, with approximately 80% of children experiencing extended periods of event-free survival. In stark contrast, adults diagnosed with ALL tend to face significantly less promising prospects for long-term outcomes(Jacobson et al., 2016). The distinction in outcomes primarily arises from risk-tailored therapeutic approaches that have evolved and fine-tuned chemotherapy dosages and schedules over the last four decades for pediatric patients. Conversely, equivalent treatment modalities have resulted in survival rates for adults in the long term around %40. This discrepancy is partly attributed to a higher incidence of co-morbidities and the presence of other high-risk characteristics upon diagnosis in adult ALL patients, rendering them less tolerant to chemotherapy and more resistant to its effects(Rafei et al., 2019). Furthermore, in adults diagnosed with ALL, there is notably a greater prevalence of unfavorable genetic subtypes, and wider array of mutations and epigenetic modifications compared to their pediatric ALL. These factors collectively contribute to the observed divergence in benefits of treatment between age groups (Liu et al., 2016). The development of ALL entails the aberrant multiplication and maturation of a lymphoid cells. Within the pediatric patients, research has uncovered certain syndromes that associated with a minority of ALL cases, including conditions like ataxia telangiectasia, Fanconi anemia, Down syndrome, and Bloom syndrome. Additional contributing factors encompass exposure to specific solvents, viral infections (like Epstein-Barr Virus), pesticides, or ionizing radiation. However, in most cases, ALL seems to emerge as a new malignancy in individuals who were in good health in the past.(Terwilliger and Abdul-Hay, 2017).

1.2.1. T-lineage ALL

ALL is separated into two broad categories T-lineage ALL (T-ALL) and B-lineage ALL (B-ALL). T-ALL is an uncommon and aggressive type of leukemia arising from

the cancerous transformation of T-lineage progenitor cells at different points in their development. Out of the estimated 6,660 new ALL diagnoses in the United States in 2022, T-ALL in adult patients constitutes approximately 10% to 25% of these cases. T-ALL primarily affects the adolescent and young adult population. Clinical features linked to T-ALL encompass conditions like hyperleukocytosis and extramedullary involvement, which may manifest as lymphadenopathy, a mediastinal mass, hepatosplenomegaly, and an increased occurrence of central nervous system participation, occurring in roughly 10% of adult patients at the point of diagnosis(O'Dwyer, 2022). The origin of T-ALL remains evasive and is currently the subject of thorough investigation, much like every single hematological cancer. The isolation of primitive tumor stems or initiating cells has proven pivotal in advancing our comprehension of leukemia's inception and pathobiology. Furthermore, the diverse clinical, molecular, and biological aspects of leukemia underscore the presence of multi-clonal diversity, underscoring its intricate and multifaceted origins (Vadillo et al., 2018). T-ALL emerges from a complex sequence of circumstances, involving the accumulation of genetic changes that collectively disrupt critical oncogenic, tumor suppressor, and developmental pathways governing the conventional regulation of cell growth, replication, viability, and differentiation throughout thymocyte development (Mullighan, 2009). T-ALL mutations can be categorized into two group, based on their reciprocal distribution and their effects when deregulated. One of them, lead to the overexpression of transcription factors crucial to T-cell development. These occurrences define specific subgroups, such as, NKX2-1/2-2, HOXA, TLX3 and TAL/LMO enabling the molecular categorization of about 70% of T-ALL occurrence, with distinctions observed between pediatric and adult populations. In contrast, the other one include abnormalities encompass genes coding for various protein families, including signaling pathway proteins ,tyrosine kinases, ribosomal proteins, and epigenetic factors.(Bardelli et al., 2021).The complex interaction among key regulators in the initial stages of T cell development and the signals leading to oncogenesis associated with T-ALL revolves significantly around NOTCH1. NOTCH1 serves as a pivotal factor in both T cell fate determination and thymocyte development. At least, 60% of T-ALL, this factor becomes stimulated through gain-of-function mutations. In tandem with these NOTCH1 mutations, Frequently, there is a concurrent deletion of the cyclin-dependent kinase inhibitor 2A locus, which encodes

the tumor suppressor genes p14ARF and p16INK4A. These occurrences often align with chromosomal rearrangements, culminating in the aberrant expression of various T cell-specific transcription factors that may acquire oncogenic functions.(Belver and Ferrando, 2016).

1.2.2. B-lineage ALL

As previously mentioned, ALL can manifest as either B or T cell phenotypic subtypes. B-cell acute lymphoblastic leukemia (B-ALL) represents a hematological malignancy typified by the unrestrained expansion of precursor B cells within the bone marrow (Safarzadeh Kozani et al., 2021) This disorder obstructs the development of B lymphoid cells, preventing their maturation at an immature stage, in the progenitor phase. Subsequently, it triggers an uncontrolled proliferation of leukemia blasts in the bone marrow, followed by their migration from the marrow to infiltrate various vital organs, including the liver, central nervous system, spleen, lymph nodes, and thymus. This dominance of the hematopoietic system by leukemia blasts also interferes with the generation of crucial blood cell types responsible for blood clotting and oxygen transport. Consequently, the patient's systems suffer significant deficiencies, ultimately leading to a fatal outcome. Early indications of this condition encompass symptoms like weariness, diminished appetite, bone discomfort, abdominal enlargement due to an enlarged liver and spleen and also swelling of lymph nodes. Acute leukemia follows a swift and aggressive disease progression, often taking mere weeks in contrast to the more gradual course of chronic leukemia, which unfolds over months (Malouf and Ottersbach, 2018). Yet in the adult population, the B-cell phenotype comprises more than two-thirds of all cases. ALL encompasses a broad age range, affecting all age groups with distinctive treatment results within each age bracket. Notably, more than half of recently discovered B-cell ALL cases emerge in the pediatric cases, while a secondary peak in incidence is observed in individuals aged over 60 years (Franquiz and Short, 2020). In pediatric patients diagnosed with B-ALL, contemporary chemotherapy protocols have demonstrated the ability to achieve prolonged overall survival rates ranging from 80% to 90%. Conversely, this level of success has not been replicated in adult patients. Despite an initial high rate of complete response to treatment, typically between 80% and 90%, a significant majority of adult individuals eventually experience relapse characterized by resistance

to chemotherapy. The long-term overall survival for adults diagnosed with B-ALL hovers within a range of 30% to 50%. The prognosis for individuals with relapsed or refractory ALL is even more discouraging, with a mere 5-year overall survival rate (Wei et al., 2017). B-ALL displays consistent and distinct chromosomal abnormalities that has a crucial effect in foreseeing how the disease progresses and personalizing treatment strategies. These genetic irregularities like non-random chromosomal rearrangements, gene deletions, amplifications, and aneuploidy frequently interfere with genes that oncogenes or cause essential proteins in the development of leukemia. Some of these specific genetic anomalies could be explored as hopeful targets for new treatment approaches (Reshmi et al., 2017). Genetic irregularities serve as crucial markers for diagnosis, prognosis, and treatment guidance, helping in the early identification of the disease, risk assessment, and therapeutic direction. Advances in technology, specifically the utilization of techniques like next-generation sequencing encompassing comprehensive approaches such as transcriptome sequencing, deletion-duplication analysis and whole exome sequencing, have facilitated the definition of twenty three distinct genetic subcategories of B-ALL (Gu et al., 2019). Some of these subtypes are seen more infrequently than abundant types. Hyperdiploidy can be given as an example of significant abnormalities. Hyperdiploidy can be categorized into two specific subgroups: high hyperdiploidy, defined by the existence of 51 to 65 chromosomes and low hyperdiploidy, defined by the range of 47 to 50 chromosomes (Lejman et al., 2022).High hyperdiploidy is regarded as a positive prognostic element, manifesting around 30% in children and 10% in adults individuals diagnosed with B-ALL. Chromosomal gain is predominantly viewed with chromosomes 4, 6, 10, 14, 17, 18, 21, and X, whereas chromosomes 1, 2, and 3 exhibit a lower frequency of such alterations. Generally, the comprehensive prognosis is brilliant. Despite that, the presence of additional copies of specific chromosomes carries distinct prognostic implications. An increase in the number of chromosomes 4, 6, 10, and 17 is indicative of a positive prognosis, while the presence of an extra chromosome 5 or isochromosome 17 is associated with a less favorable outlook within this cohort (Zhang et al., 2017). Mutations affecting genes responsible for modifying histones and those within the RTK-RAS pathway like KRAS and FLT3, are prevalent in individuals with high hyperdiploidy (Paulsson et al., 2015). Low hyperdiploidy represents an adverse prognostic indicator in the context of B-ALL, manifesting in around 10% of

pediatric cases and 15% of adult cases, with its prevalence increasing in older age groups. Research findings indicate that individuals with LHyper tend to experience diminished survival rate compared to normal karyotypes or various chromosomal abnormalities (Groeneveld-Krentz et al., 2019).

Hypodiploidy, an uncommon cytogenetic aberration in ALL, is the loss of one or more chromosomes. Children and adults with B-ALL have hypodiploid karyotypes that are less than 7% (Lejman et al., 2022). The condition can be subcategorized into distinct groups based on chromosomal content: high hypodiploidy, low hypodiploidy ,and near haploidy. As the number of chromosomes decreases, the patient's prognosis gradually worsens. (Harrison et al., 2004). Individuals with low hypodiploidy often exhibit deletions in the IKZF2 gene and frequent TP53 sequence mutations, which are often inherited. This subtype is notably rare among children, constituting less than 1% of cases, but its prevalence increases significantly with age. It is associated with an exceedingly unfavorable prognosis. Near-haploid ALL is characterized by the presence of Ras-activating mutations and alterations in the IKZF3 gene. It is relatively uncommon, comprising approximately 2% of childhood ALL cases, and even less frequent in adults, constituting less than 1% of cases in these age groups (Roberts, 2018).

The fusion gene known as ETV6-RUNX1 is one of the predominant genetic anomalies that trigger the development of B-cell lymphoblastic leukemia. This fusion arises from a concealed translocation event, denoted as t(12;21)(p13.2;q22.1), and has been documented in around 30% of cases in pediatric B-ALL and 4% of cases in adults. ETV6 acts as a transcriptional repressor and operates as a tumor suppressor. RUNX1 emerges as the most prevalent partner in B-ALL (Zhang et al., 2022). RUNX1 may become a transcriptional repressor when the ETV6-RUNX1 protein interferes with the expression of genes that are controlled by RUNX1. Erythropoietin receptor overexpression and JAK-STAT signaling activation are also brought on by ETV6-RUNX1(Mullighan, 2012).

A further subtype of B-ALL is ETV6-RUNX1 fusion-like B-ALL. While lacking the fusion gene, this subtype of ALL is very similar to ETV6-RUNX1 with immunophenotypic profiles. Children make up around 3% of ETV6-RUNX1-like instances, which account for more than 80% of pediatric B-ALL cases (Lilljebjörn et al., 2016).

More than 90 translocation partners have been found in the KMT2A gene, which is mutated in more than 80% of infant B-ALL and nearly 9% of adult B-ALL (Ghazavi et al., 2015). Translocations associated with leukemia that affect the 11q23 region result in KMT2A fusion with over 90 different partner genes. Among these partner genes, AFF1 is most commonly observed, particularly in cases with the KMT2A-AFF1 fusion, which is associated with a particularly lower overall survival (Lejman et al., 2022).

The genetic alteration TCF3-PBX1, is found in approximately 5% of pediatric cases and around 3 % of adults. Although previously categorized as a Although previously considered a high-risk subtype, it is currently linked to a positive response to contemporary ALL treatments. Conversely, the TCF3-HLF fusion gene defines an uncommon subtype of ALL occurring in less than 1% of cases across all age groups. This subtype typically leads to relapse and mortality within two years of diagnosis. Intriguingly, primary leukemic cells carrying Patients with the TCF3-HLF mutation have demonstrated responsiveness to the Bcl2 inhibitor, venetoclax, presenting a potential innovative treatment approach for this deadly type.(Roberts, 2018).

Ph-like ALL, a form of leukemia, exhibits gene expression patterns and characteristics resembling those of Ph+ ALL. However, it distinguishes itself by the absence of the BCR-ABL1 fusion gene. Its occurrence varies from approximately 12% in pediatric cases to 20-27% in adults. Ph-like ALL can manifest across different age groups and is consistently linked with an unfavorable prognosis. CRLF2 is rearranged in a significant portion of BCR-ABL1-like ALL cases, accounting for up to 50% (Zhang et al., 2022). However, until recently, the underlying factors responsible for activating kinases in the remaining cases remained unidentified. By employing advanced sequencing methods, including and whole genome sequencing and mRNA sequencing on BCR-ABL1-like ALL cases, researchers have detected various rearrangements, sequence mutations, and DNA copy number alterations that trigger kinase signaling in all these cases. These genetic alterations encompass rearrangements involving genes such as PDGFRB, ABL1, JAK2, and EPOR, in addition to deletions or mutations affecting SH2B3 and IL7R. Significantly, a number of these genetic changes have been demonstrated to activate downstream signaling pathways like JAK/STAT. Furthermore, experimental evidence has shown that the transformation of cells can be reduced with inhibitors targeting JAK or ABL1/PDGFRB (Mullighan, 2012).

Another significant subtype is BCR-ABL Fusion. Information on this specific subtype is provided in section 1.3.

All of the sup types of B-lineage ALL provided at figure 1 .(Lejman et al., 2022)

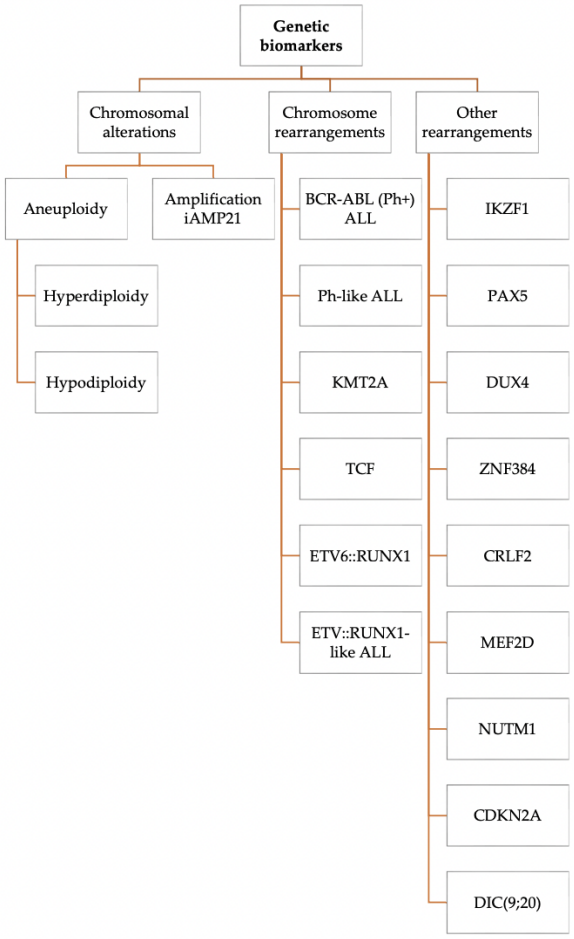

Figure 1. Illustrative representation genetic biomarkers associated with B-ALL.(Source: Lejman et al., 2022)

1.3. Philadelphia Chromosome

The Philadelphia (Ph) chromosome, denoted as a shortened chromosome 22, results from a reciprocal exchange of genetic material between chromosomes 9 and 22. This genetic event combines the Breakpoint Cluster Region (BCR) gene from chromosome 22 with the Abelson (ABL) gene on chromosome 9 (Figure 2). The resultant fusion gene, BCR-ABL, possesses an elevated tyrosine kinase activity, leading to the persistent activation of various downstream signaling pathways like AKT/mTOR,PI3K, RAS, NF-κB and JAK/STAT that promote cell proliferation and survival. Consequently, this genetic alteration is a key factor in the development of

leukemia. In adults diagnosed with ALL, the Ph chromosome stands as the most common cytogenetic abnormality, affecting approximately 20% to 30% of adult patients. However, its occurrence is less frequent in pediatric cases, found in about 5% of children with this condition. The likelihood of this genetic anomaly increases with age, and it is present in roughly 50% of patients who are older than 50 years (Ravandi and Kebriaei, 2009).In individuals with Ph+ ALL, the most prevalent simultaneous genetic anomalies involve the removal of specific genes, namely IKZF1, PAX5, and EBF1. These genetic alterations are detected in approximately 80%, 50%, and 14% of Ph+ ALL patients, respectively. Additionally, the deletion of CDKN2A/2B is also a recurring occurrence in this patient group, with an occurrence rate of roughly 50% (Lejman et al., 2022).BCR-ABL serves as a vital biomarker in Ph+ ALL diagnosis and is a target for tyrosine kinase inhibitors (TKIs). Nevertheless, it is widely recognized that this translocation has the potential to generate resistance to therapeutic drugs.(Leoni and Biondi, 2015).

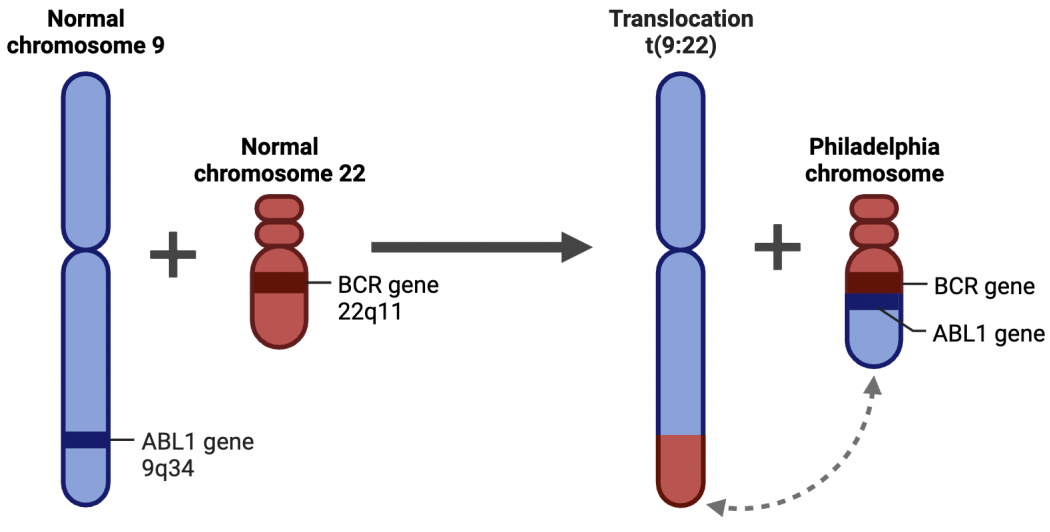

Figure 2. Formation of Philadelphia chromosome

1.4. Treatment Strategies for ALL and Ph (+) ALL

In contrast to the more than 90% cure rate typically achieved in pediatric ALL, the prognosis for adult ALL has historically been quite grim. Cure rates in adults have lingered at less than 40%, largely owing to the existence of high-risk disease characteristics within this age range and the considerable toxicity associated with chemotherapy. Among the cases of ALL, B-cell ALL, which approximately 75% of

instances, has traditionally exhibited inferior treatment outcomes when compared to T-cell ALL. More specifically, prior to the introduction of TKIs, Ph (+) ALL within the B-cell subset was notably associated with highly unfavorable prognoses (Samra et al., 2020). The understanding that ALL comprises diverse subtypes has influenced treatment strategies tailored to the specific characteristics of each patient, including the leukemia's phenotype, genotype, and associated risks. Consequently, mature B-cell ALL is the sole subtype managed with brief, aggressive chemotherapy regimens. In contrast, other patients follow distinct treatment protocols that consistently prioritize initial therapy to induce remission, subsequent intensification therapy, followed by continuous treatment to eliminate any remaining leukemia cells(Pui and Evans, 2006).

1.4.1. Treatment Strategies for ALL

Typically, the management of ALL in adult patients involves initiating a phase focused on achieving remission, which is then followed by consolidation or intensification phases. Subsequently, patients may receive ongoing maintenance therapy or undergo hematopoietic stem cell transplantation (HCT) (Ram et al., 2010).

Initial Phase

The initial phase of treatment, known as induction therapy for adult ALL, efforts to eliminate the disease burden and restore normal hematopoiesis. A chemotherapeutic cocktail used for induction commonly includes L-asparaginase, anthracyclines., glucocorticoids, L-asparaginase, and vincristine. Notably, there is a shift from prednisone to dexamethasone in response to pediatric research demonstrating reduced central nervous system relapse rates and improved overall survival. It's important to exercise caution when determining the dexamethasone dosage regimen, as sustained use of higher doses may result in long-term complications like avascular bone necrosis and an elevated risk of morbidity and mortality due to infections (Gökbuget and Hoelzer, 2006). The commonly utilized anthracycline is daunorubicin. One randomized study revealed a disease-free survival rate of 36% when DNR was used. In the majority of ongoing adult ALL investigations, asparaginase is incorporated into the induction therapy, although the cumulative doses administered are notably lower than those in pediatric trials. During induction, asparaginase is often administered in parallel with steroids to patients experiencing cytopenia, potentially inducing unforeseen complications like coagulation abnormalities and liver issues. These

adverse effects are challenging to predict. Consequently, the use of asparaginase may result in treatment delays and can impact the treatment intensity on an individual basis. Supportive care plays an increasingly vital role during the induction phase(Gökbuget and Hoelzer, 2006).

Consolidation Phase

Consolidation marks the second phase of the treatment plan, comprising a series of brief, consecutive chemotherapy courses spaced every two weeks. Typically, this involves the use of, asparaginase, high-dose methotrexate, cytarabine, glucocorticoids and vincristine, spanning a 12-week timeframe. Following this, a subsequent intensification phase, commonly known as reinduction therapy, is implemented, utilizing a comparable combination of drugs employed in the initial induction therapy. (Malard and Mohty, 2020).

Maintenance Therapy

Maintenance therapy involves the daily administration of mercaptopurine and weekly doses of methotrexate, which may or may not include vincristine, along with periodic glucocorticoid pulses occurring every 1 to 3 months. This maintenance regimen is typically continued for a period of 2 to 3 years following the initial induction phase, and no added benefits have been observed beyond this timeframe. While tioguanine, like mercaptopurine, obstructs the synthesis of new purines, it demonstrates higher lymphoblast cytotoxicity in vitro. As a result, mercaptopurine remains the established standard for maintenance therapy (Malard and Mohty, 2020).

Allogeneic hematopoietic stem cell transplantation

HCT remains an essential component of adult ALL therapy and is recommended as an integral part of the initial treatment for adults with high-risk ALL (Faderl et al., 2010). However, the definition of high-risk ALL that warrants early HCT has evolved beyond conventional clinical factors like patient age and initial white blood cell counts. It now encompasses factors related to molecular and genetic characteristics and minimal residual disease dynamics following the commencement of therapy, especially when employing pediatric-inspired treatment regimens. Most experts concur that allogeneic HCT is advisable for adults who have undergone adequate therapy and exhibit high-risk cytogenetic features (MLL gene rearrangements, complex karyotypes, Philadelphia chromosome-positive, hypodiploidy, particularly those with low hypodiploidy and near-haploidy), persistent MRD, and potentially high-risk molecular

traits like Ph-like ALL. Conversely, allogeneic HCT serves as the sole curative option for advanced ALL, encompassing cases of relapsed and refractory disease. Consequently, the evolution of transplantation in ALL has paralleled advancements in chemotherapy. New transplantation modalities have been developed to address prior challenges related to aspects like transplantation in elderly patients, donor selection, and transplantation for chemo-refractory ALL (Pui and Evans, 2006).

1.4.2. Treatment Strategies for Ph (+) ALL

The management of Ph (+) ALL can be divided into two distinct periods: the era predating the introduction of TKIs and the era subsequent to their incorporation.

Before the usage of TKIs, complete response was less common Ph (+) ALL cases compared to those with Ph (-) ALL. Complete response rates were below 70%, and long-term overall survival remained under 20%, with varying outcomes depending on the post-remission treatment. The most favorable results were observed in individuals who underwent HSCT, with long-term survival around 45% (Saleh et al., 2022). Patients with Ph (+) ALL exhibit a less favorable prognosis when treated exclusively with chemotherapy. Standard chemotherapy regimens yield complete remission in only about two-thirds of Ph (+) ALL patients. The 5-year overall survival rate is disappointingly low, typically around 10%. In a specific study involving 229 individuals newly diagnosed with ALL, induction therapy employing doxorubicin, vincristine, l-asparaginase, cyclophosphamide, and prednisone led to a complete response rate of 51% among Ph (+) ALL patients, in contrast to an 83% complete response rate in Ph (–) ALL patients. Consequently, the 6-year overall survival rate for Ph(+) ALL patients was significantly inferior, standing at 5%, compared to 39% for Ph– ALL patients (Yilmaz et al., 2018). The use of chemotherapy regimens, such as doxorubicin, vincristine, and dexamethasone showed promise by achieving a high complete response rate of 92% in a study. Nevertheless, due to a significant recurrence rate and fatalities related to treatment, the 5-year overall survival rate remained modest, standing at only 12%. This corresponds to survival rates documented in various clinical trials investigating different chemotherapy protocols.(Thomas and Heiblig, 2016a).

The incorporation of TKIs alongside chemotherapy has brought about a transformative shift in the treatment of individuals diagnosed with Ph (+) ALL and has become the

established standard for treatment. The primary objective in managing Ph (+) ALL is not solely to attain and sustain a complete clinical response but also to promptly achieve a comprehensive molecular response during the early phases of treatment (Samra et al., 2020).

TKIs are small oral substances that competitively hinder the interaction between ATP and the ATP-binding domain of BCR-ABL, thereby reducing downstream signal transduction pathways. Imatinib marked the advent of TKIs, paving the way for the subsequent emergence of second-generation TKIs which are bosutinib, nilotinib, and dasatinib and third-generation TKIs which is ponatinib, characterized by their heightened and expedited efficacy in antagonizing BCR-ABL. Second and third generation TKIs have demonstrated their prowess in circumventing various ABL mutations, pivotal in mediating resistance to treatment and relapse. Notably, contemporary advances have led to the inception of monoclonal antibodies such as blinatumomab, instigating the development of regimens devoid of chemotherapy. These innovations have yielded exceptionally promising outcomes, coupled with an impressive level of patient tolerability (Saleh et al., 2022). Each of the TKIs, including imatinib, Dasatinib, nilotinib, and ponatinib, exhibits clinical efficacy in the treatment of Ph (+) ALL. It is worth noting that a head-to-head comparison of these various TKIs has yet to be undertaken in a clinical trial. The selection of a specific TKI may be influenced by considerations such as toxicity profiles, dosing regimens, concomitant medical conditions, drug availability, and cost. However, the amalgamation of available data indicates that all these TKIs demonstrate activity in the context of Ph+ ALL, with distinctions between them that are generally minimal in nature (Horowitz and Rowe, 2019). The prevailing consensus within the academic community underscores the widespread recommendation for the incorporation of a TKI into the therapeutic strategy for all recently diagnosed Ph+ ALL patients. This integration is designed to accomplish several key objectives, including enhancing the rate of complete remission, extending the duration until relapse occurs, augmenting eligibility for HCT, and enhancing leukemia-free survival. Following the achievement of complete remission, it is considered advisable to sustain the TKI treatment course until the emergence of disease progression or the occurrence of HCT (Forghieri et al., 2015)

Given the thesis's primary emphasis on the use of imatinib in the treatment of Ph+ ALL, it was considered pertinent to provide a more in-depth elucidation of imatinib as one of the TKIs.

1.4.2.1. Imatinib

A prominent compound initially identified through a screen for inhibitors of protein kinase C underwent subsequent modifications, ultimately demonstrating robust inhibitory effects against a highly specific set of kinases in laboratory settings. Notably, these targeted kinases included ABL and the receptor tyrosine kinases KIT and PDGFR. Given the central role played by BCR-ABL kinase activity in the pathogenesis of CML, there was a concerted effort to delve deeper into the potential of the ABL kinase domain for its potential. This intensive focus on medicinal chemistry optimization culminated in the creation of STI-571, which was subsequently bestowed with the name "Imatinib" (Lamontanara et al., 2013). The remarkable tolerability and outstanding efficacy demonstrated during the phase I and II clinical trials led to the swift approval of Imatinib by the US Food and Drug Administration in 2001, followed by subsequent recognition from the European Medicines Agency. Consequently, imatinib marked the pioneering instance of a kinase inhibitor being routinely employed in cancer patients. Recently, imatinib has evolved into a paradigmatic treatment. Its introduction has profoundly transformed this once grimly prognosticated cancer into a manageable chronic condition, affording the majority of patients the potential to approach a normal lifespan and enjoy an enhanced quality of life. Today, imatinib serves as the primary therapeutic approach for patients with Ph(+) ALL, CML and also gastrointestinal stromal tumors, and a select range of other medical conditions (Ottmann and Pfeifer, 2009). Imatinib functions by occupying the nucleotide-binding pocket within the BCR-ABL protein, effectively obstructing ATP. This inhibition mechanism prevents tyrosine autophosphorylation and, consequently, associated substrates phosphorylation. As a result, downstream signaling pathways crucial for the promotion of leukemogenesis are deactivated. Imatinib's impact extends to the kinase activity of various other targets(Thomas and Heiblig, 2016b). Early preclinical investigations demonstrated that imatinib exerts robust inhibitory effects on the growth of Ph (+) leukemias, both in laboratory settings and in live subjects. These encouraging findings swiftly prompted the initiation of clinical trials. The

introduction of imatinib in combination with conventional chemotherapy regimens in the initial treatment phase marked the onset of a transformative era. This combination exhibited a generally favorable safety profile and yielded impressive complete remission rates ranging from around 95%. For instance, it attained a 50% overall 5-year survival rate, which was unparalleled. In a recently updated phase 2 trial conducted at a single institution, where imatinib was combined with Adriamycin, dexamethasone vincristine, hyperfractionated cyclophosphamide, and vincristine, chemotherapy, 54 older patients, were treated. The trial yielded a remarkable Complete remission rate of 93%, with a notable 45% achieving complete molecular remission within three months. Despite a relatively modest proportion of patients undergoing subsequent HCT during their first remission, the 5-year Overall survival reached 43%, a notably improved outcome compared to historical control groups (Abou Dalle et al., 2019). Usage Imatinib into the therapeutic approach for Ph+ ALL has heralded significant progress in the management of this formidable ailment. Nevertheless, despite the substantial therapeutic strides achieved, patients have, in some instances, developed resistance to imatinib. This resistance has underscored the imperative need to explore novel treatment modalities for Ph+ ALL, consequently driving the quest for the subsequent generation of TKIs (Abou Dalle et al., 2019). As a result of this situation, newer generation of TKI were generated.

1.5. Imatinib Resistance on Acute Lymphoblastic Leukemia

Imatinib resistance- in patients with Ph(+) ALL can occur due to acquired or intrinsic factors. Acquired resistance may be caused by BCR-ABL dependent factors, such as increased expression of BCR-ABL or point mutations within the kinase domains. It can also result from BCR-ABL independent factors, like changes in drug metabolism that reduce imatinib levels in Ph (+) cells. Furthermore, the initiation of alternative signaling pathways, like those associated with Src kinases, might play a role in developing resistance. (Ravandi and Kebriaei, 2009). Point mutations give rise to amino acid substitutions within the kinase domain of BCR-ABL, a phenomenon capable of conferring resistance to imatinib. These mutations exert their resistance by impeding imatinib's entry into the ATP-binding pocket of BCR-ABL, consequently thwarting its inhibitory effect. Initially, mutations were predominantly reported in cases of relapsing Ph(+)ALL. The two most prevalent mutations are T315I, which

blocks imatinib binding. The second common mutation type pertains to P-loop mutations in the phosphate-binding region (Thomas and Heiblig, 2016b). Certain mutations exhibit varying levels of resistance to drugs, with some causing only slight resistance. However, mutations like T315I indicate a very high level of resistance to both imatinib and second-generation TKIs. P-loop domain alterations cause the structural stability to be so upset that the kinase domain is unable to assume the inactive conformation which is necessary for the binding of Imatinib.(Eiring and Deininger, 2014). Researchers have recently discovered a new mechanism of resistance to TKIs in patients with Ph(+) ALL. This mechanism involves the expression of alternative spliced isoforms of IKAROS family zinc finger 1, which is an important regulator in the development of normal lymphocytes. One specific isoform, called Ik6, lacks four N-terminal zinc fingers responsible for DNA binding. Interestingly, this Ik6 isoform was found in 91% of Ph(+) ALL patients who exhibited resistance to Dasatinib or Imatinib. The Ik6 expression are also associated to the levels of BCR-ABL transcripts. These findings suggest that targeting and restoring the IKZF1 function could be a promising approach to addressing TKI resistance in the future (Lee et al., 2011).

1.6. Computational Approaches in Life Sciences

Over the past twenty years, technology has made remarkable strides, leading to an unprecedented increase in data related to biology. Gene and RNA sequencing, proteomics, metabolomics, lipidomics, and microbiome investigations have flourished alongside the- integration of clinical data through computational methods. Consequently, researchers have had to employ increasingly sophisticated analytical techniques to derive valuable insights. The adoption of systems biology methodologies now allows scientists to analyze vast datasets and conduct comprehensive studies that span both experimental and theoretical models (Joshi et al., 2021). Systems biology is a multidisciplinary approach that uses computational methods to critically analyze a wide range of biological phenomena, particularly those related to disease (Pandita et al., 2022). Medical sciences have great potential to influence the field rather than intellectually down to individual molecules alone, systems biology aims to unveil the interactions of many components of biological processes in order to achieve a comprehensive understanding (Turanli et al., 2021). In pharmacology, systems biology techniques are used to investigate the biomolecular interactions of drugs and their

targets in the cellular environment. Combined with wet lab experiments, systems chemistry can be computerized methods that have successfully quantified biological agents, prove valuablity for new drug discovery targets and therapeutic molecules, facilitating the design of effective therapies for patients. Furthermore, systems chemistry-based methods explore drug-target interactions, predict drug-target interactions or interactions, assess potential side effects of drugs, and enable rehabilitation opportunities (Zou et al., 2013)

1.6.1. System Biology

The heart of systems biology lies in the quest to fully grasp the complex web of interactions and connections between the molecular building blocks of a biological system, which ultimately give rise to its overall behavior (Sobie et al., 2011). A defining aspect of systems biology is its focus on exploring the interconnections among numerous components, going beyond the conventional method of examining singular molecular traits. With its diverse range of computational tools, systems biology plays a pivotal role in generating hypotheses that can be further tested through experiments. This method hinges on seamless collaboration between hands-on experiments that encompass the tracking of multiple cellular elements and sophisticated computational methods that can interpret a wide range of datasets. From this process, the generation of precise experimental data not only enhances but also refines the computational model, ultimately leading to a more accurate depiction of the biological system being studied (Zou et al., 2013).

Two main computational methods are used in systems biology: data-driven methods (top-down method) and hypothesis-driven methods (bottom-up approach). Bottom-up approach are often used in systems with less molecules. The main challenge with this approach is the lack of accurate quantitative information on these interactions. Consequently, it is necessary to formulate hypothetical equations that describe these relationships and then calculate the corresponding parameter values. Dynamic modeling, a basic method of hypothesis, is employed to clarify the connection between molecules and the resulting reactions resulting from interactions (Faratian et al., 2009). Each of these complements other data-driven methods that involve the acquisition of extensive omics datasets and are subsequently analyzed using mathematical modeling methods. In conventional data-driven methods, the use of network structures gains

prominence and provides valuable insight into complex interactions between many molecules, often hundreds or thousands (Zou et al., 2013). Technological advances since the human genome was cloned and sequenced have made it easier to obtain a wide variety of molecular data in tissues or cells. This new technology can be used to capture biological processes in biological systems with a broad overview and is widely known as "omics". Numerous realms of scientific inquiry fall under the omics umbrella. Instances include proteomics, epigenomics, genomics, lipidomics, metabolomics, and transcriptomics, each of comprehensive examinations of proteins, RNA, genes, metabolites, lipids, and methylated DNA respectively. Omics research is driven by various objectives, with one prevalent aim being the attainment of an exhaustive comprehension of the biological system under investigation (Micheel et al., 2012). Transcriptomics serves as a potent tool for elucidating the roles of significant genes and for comparing gene expression across diverse stress conditions. It achieves this by conducting high-throughput microarray analysis. In a distinct vein, metabolomics is defined as the investigation of alterations in endogenous metabolites within biological systems, encompassing, cells, tissues or biofluids in response to various stressors. In parallel, lipidomics stands as a subfield of metabolomics, with a specific focus on the study of lipids and their roles in these biological responses (Maan et al., 2023). Another frequent objective of omics investigations is the correlation of omics-derived molecular data with specific clinical outcomes of interest. The underlying rationale is that by harnessing omics-based measurements, there exists the potential to formulate a more precise predictive or prognostic model for a given condition or disease (Micheel et al., 2012).

1.6.2. Analyses Used in Systems Biology Studies

The distinctive and diverse gene expression patterns observed in ALL necessitate the application of non-conventional biomolecular techniques to unravel its pathogenesis. Among these approaches, gene expression profile chips emerge as an optimal method for investigating the molecular mechanisms at play in ALL, given their ability to gauge the expression levels of a multitude of genes. Over the past few years, there has been a growing supply of gene expression profile data, igniting a compelling wave of research exploring the use of bioinformatics for analysis.

In this particular thesis, the research adopts bioinformatics methodologies to analyze gene expression profile data to discern the genes whose expression differs significantly between ALL and normal B cells. This pursuit aims to provide fresh insights into the exploration of ALL's pathogenesis. To this end, a myriad of analyses was used during the study, the data for these was accessed from the NCBI Gene Expression Omnibus database (GEO) (Edgar et al., 2002). GEO functions as a public database for an extensive array of experimental data. This dataset encompasses various types of experiments, such as single and dual-channel microarray-based assessments measuring protein levels, genomic DNA and mRNA along with non-array techniques. Presently, GEO hosts an extensive collection, including almost 140,000 samples and above 3,000 distinct microarray platforms. GEO's organizational structure is built upon four fundamental components. The first three elements, namely Sample, Series and Platform,, are contributed by users, while the fourth component, the dataset, is compiled and curated by GEO personnel using the data submitted by users.This platform files offer insights into the layout and contents of microarrays, while GEO samples provide information about the actual outcomes of individual hybridizations. The complete experiment, including information on all hybridizations and their respective platform descriptions, is available as a GEO series. Subsequently, The data within GEO is accessible in a proprietary format termed SOFT (Davis and Meltzer, 2007).

Once the relative or absolute expression levels of all transcripts have been evaluated, the subsequent phase involves the examination of statistical hypotheses. These hypotheses generally revolve around distinctions between two biological conditions, such as healthy versus diseased tissues or modified versus unaltered cells. A primary objective of these tests is to pinpoint the genes that predominantly contribute to the variation between the studied biological states, commonly referred to as differentially expressed genes (DEG) (Clark et al., 2014). Genes don't operate in solitariness; they're integral components of a complex network with regulatory and functional interconnections which often result in significant correlations between their expression. One of the most accepted differential expression analysis method is the Linear Models for Microarray Data (limma) , Significance Analysis of Microarrays (Tusher et al., 2001), and Welsh's t-test, (Smyth, 2004) (Clark et al., 2014).

The limma package plays a central role in Bioconductor, an open-source software development project for statistical genomics based on the R programming language. It has gained widespread popularity for analyzing data derived from various experimental platforms, including polymerase chain reaction, microarrays and arrays, and others. One of its notable features is its adaptability, allowing for a consistent analysis workflow across diverse technologies after initial data preprocessing and normalization (Ritchie et al., 2015). With its use of advanced computational techniques, the software provides a complete solution for data analysis and guarantees reliable performance even with large datasets. It improves user-friendliness and data handling by using object-oriented principles to describe expressive data and simplify the user interface.

Subsequently, determining DEGs the next step is Gene Set Enrichments Analysis (GSEA). However, before applying this analysis the prob names came form limma function should be uploaded into an annotation tool such as DAVID tool (Jiao et al., 2012).

Enrichment analysis is a systematic and statistically sound approach for examining and elucidating extensive gene lists by drawing upon pre-existing knowledge. It evaluates whether there is an excessive or insufficient occurrence of a defined set of genes within the given gene list. If a statistically significant proportion of genes from this predefined set is found in the list, it can suggest the involvement of the associated biological pathway in the studied biological condition. This analytical process is replicated for numerous available gene sets, which could encompass a vast number (Merico et al., 2010). To this end, an enrichment analysis tool called Metascape (Zhou et al., 2019) selected.

Metascape is specifically developed for researchers, enabling them to leverage robust computational analysis pipelines for the examination and comprehension of extensive datasets. To ensure that the information it offers remains up-to-date, a novel pipeline for knowledgebase synchronization has been implemented. Metascape combines gene membership analysis, gene annotation and multi-gene-list meta-analysis. Researchers can directly assess their data to uncover new mechanisms of action, therapeutic targets or deeper insights into diseases. In summary, Metascape stands as an user-friendly web tool designed to streamline the analysis and interpretation of multi-platform OMICs data for the research community (Zhou et al., 2019).

Furthermore, the subsequent stage involves the establishment of a protein-protein interaction (PPI) network involving the proteins encoded by the DEGs. PPIs has significance in many biological processes, including cell-cell communication, as well as in the regulation of metabolic and developmental pathways. In systems biology, proteins and protein interaction studies have emerged as a major focus. These interactions are based on noncovalent interactions between amino acid residues in the side chains, which are key driving forces for protein folding, aggregation, and the establishment of protein-protein interactions and other mechanisms (Rao et al., 2014). Consequently, PPI networks allows for a deeper understanding of disease mechanisms, disease-related genes or proteins, and their associations. Employing network science, characterized by nodes (components) and edges (interactions), offers a systematic approach to addressing complex biological issues. This network-centric perspective plays a significant role in elucidating the functions of proteins within cells. By leveraging PPI networks to unravel the underpinnings of disease mechanisms associated with biological processes, it becomes possible to identify drug targets and biomarkers for these diseases (Fiscon et al., 2018).In this regard, BioGRID database (Chatr-Aryamontri et al., 2017) was used. The BioGRID is an openly available database that contains protein and genetic interactions from various species.This valuable resource contains approximately 1.93 million meticulously curated interactions, offering the opportunity to construct intricate networks that can significantly support discoveries in biomedicine, particularly concerning human health and diseases (Oughtred et al., 2021).

Subsequently, it is essential to visualize protein-protein interaction (PPI) networks and compute various topological characteristics, including local and global measures. For this purpose, this thesis employed Cytoscape(Shannon et al., 2003) in conjunction with the CytoHubba plug-in (Chin et al., 2014). Cytoscape is a free, open-source software used to visualization of molecular interaction networks originating from the analysis of high-throughput data. It merges biological pathways with gene annotations, expression profiles, and information extracted from literature, aiming to offer comprehensive insights into system changes(Shannon et al., 2003). Within Cytoscape, proteins or genes are represented as nodes, and their pairwise interactions are denoted by edges. Both nodes and edges can be linked with data attributes that define the characteristics of the proteins or interactions. Remarkably, Cytoscape enables the

customization of visual elements for nodes and edges.This attribute-to-visual mapping empowers biologists to simultaneously visualize diverse data types within a network framework (Cline et al., 2007). Furthermore, users can enhance Cytoscape's functionality by developing or downloading supplementary software modules referred to as 'plugins' such as CytoHubba plug-in. The Cytoscape plugin known as cytoHubba is employed for the prioritization of nodes within a network according to their network-related characteristics. cytoHubba offers a comprehensive selection of 11 topological analysis techniques (Chin et al., 2014). In this thesis, Degree and Betweenness, were used.

1.6.3. Drug Repurposing

The biopharmaceutical industry encounters significant challenges in the process of research and development for drug discovery. The process of drug development typically spans approximately 13 years. This extended period encompasses various stages, including drug design, and production, as well as the essential evaluation of the drug's potential toxicity, effectiveness, also pharmacokinetic and pharmacodynamic characteristics through in vitro and animal studies. Importantly, the journey of introducing a new drug from laboratory research to practical clinical application is not only lengthy but also costly, with estimated expenses ranging from USD 2 to 3 billion for bringing a new chemical entity to market (Zhang et al., 2020). A mandatory stage in drug development involves assessing the drug effectiveness and safety in the human body through a series of clinical trials, typically consisting of four phases. Phase I, mark the initial testing of the new drug in a small group of individuals usually up to 80, primarily to evaluate its safety to use. Subsequently, in Phase II, the intervention is studied among a wider population , usually involving several hundred participants, to assess both its effectiveness and further examine its safety profile. Phase III studies then focus on evaluating effectiveness in even larger groups, ranging from hundred to thousand individuals. These trials also closely monitor adverse effects and gather additional data to ensure the safe use of the intervention. Following the marketing of the drug, Phase IV studies come into play (Zhang et al., 2020). This type of researches conduct to observe the intervention's effectiveness on the people and gather adverse effects that may arise during widespread, extended usage. Generally, if the drug proves to be effective in Phase III trials, it secures FDA approval. FDA approval is a relatively

rare outcome, with only about one in 5,000 to 10,000 potential anticancer agents successfully obtaining this status (Paul et al., 2010). This process is characterized by its time-consuming, resource-intensive nature and is associated with inherent risks related to the efficacy and safety of new drug candidates. The pharmaceutical sector is grappling with productivity issues attributed to escalating costs, competition from generic drugs, and stringent regulatory requirements. As a result of these existing circumstances, drug developers have been compelled to seek innovative approaches for identifying new therapeutic applications for existing drugs. This innovative concept is commonly referred to as drug repurposing. It presents numerous benefits, especially for drug candidates with well-established formulations, comprehensive pharmacokinetic data, toxicity profiles, clinical trial histories, and post-marketing surveillance safety records (Turanli et al., 2021). Over the past decade, the concept of drug repositioning has gained significant therapeutic importance, attracting attention not only within academic research but also in the biopharmaceutical industry. Up to the present, numerous instances of drugs successfully repurposed have come to light. The first and most renowned example of drug repositioning was serendipitous in nature. Sildenafil, generated for treating a coronary disease, encountered setbacks during phase 2 trials. However, its side effect of inducing penile erections led to its redirection for the treatment of erectile dysfunction. Several other drugs, such as minoxidil, everolimus, thalidomide, nelfinavir, and much more, have also demonstrated efficacy in treating conditions different from their originally intended indications (Turanli et al., 2018). Additionally, many of these initiatives have harnessed in silico drug repositioning methods to generate hypotheses (Hodos et al., 2016). Examples of repurposing studies applied to leukemia are also available in the literature. For instance, Niclosamide that's been approved by the FDA for treating tapeworm infections. Interestingly, it has shown potential in the fight against cancer. In cancer cells, Niclosamide appears to block certain signaling pathways, like NF-kB, and even induces a process called apoptosis by generating something called reactive oxygen species. In particular, it seems to slow down the growth of leukemia cells by interfering with CREB-dependent pathways. Its is remarkable because CREB is often overactive in leukemia and linked to a poor prognosis. In preclinical studies, Niclosamide extended the survival of AML patient-derived xenograft mice. It also appears to work well in combination with other chemotherapy drugs like cytarabine

and daunorubicin. These promising findings position Niclosamide as a strong candidate for early-phase clinical trials (Hamdoun et al., 2017). Another anthelmintic named Mebendazole is a drug commonly used to treat intestinal worm infections by interfering with tubulin, a protein involved in microtubule assembly. But, in the context of AML, it shows a different side. In AML models, mebendazole throws a wrench in the works of the heat shock protein 70 chaperone system, which results in the breakdown of a crucial transcription factor called c-MYB in AML cells. In laboratory tests, mebendazole not only reduced the viability of human cells but also extended the lifespan of mice with MLL-AF9 xenografts. The potential of mebendazole isn't limited to AML. There are currently six studies registered with the National Institutes of Health's Clinicaltrials.gov, exploring mebendazole as a treatment for various cancers, including colorectal and glioma (Guerini et al., 2019). Furthermore, Verteporfin received FDA approval for photodynamic therapy, specifically for eliminating abnormal blood vessels associated with macular degeneration. Beyond this primary use, its potential extends to the field of ALL. Researchers have examined its anti-leukemic properties while assessing its minimal impact on normal hematopoiesis. In a study by Xiu et al., verteporfin was employed to treat AML cells. Their findings showed that it effectively inhibited cell growth in laboratory conditions and delayed the progression of the disease in vivo, underlining its promise as a therapeutic agent for AML (Xiu et al., 2018). Another example of repurposed drug for leukemia is Fidaxomicin, a medication primarily employed for managing diarrhea associated with Clostridium difficile infection, which demonstrated notable effects in the context of MLL-rearranged HSC cells. When utilized in vitro, fidaxomicin effectively inhibited cell growth. The remarkable synergy between fidaxomicin and conventional chemotherapy in reducing tumor burden within the animal models suggests the potential of repurposing fidaxomicin to target ABCC3 in leukemia. This approach can enhance the efficacy of standard chemotherapy and address chemoresistance concerns in MLL-rearranged leukemia (Zeisig et al., 2021). Based on a recent study from Zazuli et al., claimed that chlorprothixene, sirolimus, dihydroergocristine, papaverine, and tamoxifen could be candidates for possible repurposing for ALL (Zazuli et al., 2022). Moreover, as reported by Bonnet et al., three candidates, which are bioactive molecules authorized by the FDA, namely alpha-estradiol, nordihydroguaiaretic acid, and prochlorperazine dimaleate, have exhibited

the induction of apoptotic cell death across a spectrum of T-ALL cell lines. These candidates have also been found to trigger a response related to DNA damage and impede the persistent activation of mTORC1 as well as the expression of c-MYC.In light of these findings, researchers posited that these molecules might be well-suited for repurposing studies (Bonnet et al., 2020). As can be seen, studies in this field have attracted attention, especially in recent years. However, there remains a notable scarcity of drug repositioning studies focusing on acute lymphoblastic leukemias within the existing literature.

The primary challenge in drug repositioning revolves around identifying new associations between drugs and diseases. To tackle this challenge, an array of methods has been created, encompassing computational techniques, biological experiments, and hybrid methodologies. Novel applications for a drug candidate may arise by chance or can be pursued through systematic and logic-driven methods. Hypothesis driven methods for drug repositioning encompass both computational and experimental approaches, offering significant potential for gaining deeper insights into the mechanisms and pathways implicated in disease development (Parvathaneni et al., 2019). Experimental repositioning methods consist of binding assays and phenotypic screening techniques. These methods help uncover interactions between ligands and assay components, as well as identify promising lead compounds from extensive compound libraries (Pushpakom et al., 2019). Computational strategies can be classified into various categories, such as knowledge-based, target based and signature-based etc. These approaches are cost-effective and hold great promise for the discovery of new therapeutic agents. Importantly, computational methods enhance drug discovery by effectively harnessing the fields of bioinformatics, and systems biology and network biology, (Jin and Wong, 2014).

Target-based involves the investigation of a drug using a biological target, such as a receptor or protein, to assess its impact on a biological reaction. This identifies novel applications for a drug by establishing connections between the drug and a specific disease, primarily based on the drug's interactions with protein targets (Sawada et al., 2015). The identification of novel uses for a drug can stem from its primary target as well as its interactions with off-target proteins. Target repositioning occurs when a drug is newly applied to interact with the same target protein identified beforehand.

Remarkably, around 80 percent of drug repurposing initiatives have been driven by target-based method(Parvathaneni et al., 2019).

Knowledge-based techniques use bioinformatics methods to integrate a wide range of data, including details about drugs, and its interactions, formulations of drugs etc. Also includes clinical trials. However, the information contained in blind and target-based methods may sometimes be insufficient to unveil novel mechanisms that extend beyond the established drug targets. In contrast, knowledge-based methods incorporate existing information to forecast previously unidentified mechanisms, such as emerging drug targets, subtle similarities between drugs, and new disease biomarkers. By infusing substantial existing knowledge into the drug repositioning process, these methods aim to enhance the accuracy of their predictions (Kulkarni et al., 2023).

Utilizing target-based and cell-based methods constitutes a signature-based approach in the realm of drug repositioning studies (Iorio et al., 2013). Approaches to drug repurposing based on signatures hinge on utilizing genes extracted from omics data associated with diseases, both with and without treatment. These methods aim to unveil undiscovered off-targets or unidentified disease mechanisms. With the progression of next-generation sequencing technologies and microarray there is a substantial accumulation of genomics data relevant to drug repurposing studies. This wealth of data can be leveraged to identify gene signatures, particularly from databases like NCBI-GEO, facilitating the exploration of previously unknown disease-altering pathways (Jin and Wong, 2014). While signature-based approaches involve challenges such as cost, time, labor, and dependence on specialized equipment, they offer several advantages. These include their efficacy when creating intricate diagrams illustrating the links between diseases and the actions of drugs. Consequently, the biological significance of signature-based drug data extends beyond the discovery of new candidates to the experimental evaluation of candidates predicted through computational methods (Turanli et al., 2021). As the effectiveness of a drug is influenced by individual gene signatures, the utilization of a gene signature database proves beneficial in the drug repurposing process through computational means. Methods based on signatures uncover previously unknown mechanisms of drug action, including altered gene and protein expression. Techniques like Connectivity Map (CMap) (Subramanian et al., 2017), and Library of Integrated Network-Based Cellular

Signatures (LINCS) and weighted gene co-expression network analysis (Langfelder and Horvath, 2008) are employed in this context (Parvathaneni et al., 2019).

In the systems biology, networks play a crucial role by furnishing a comprehensive framework to amalgamate both quantitative and qualitative and connections among biological entities, encompassing gene expressions, their correlations, and the existence of interactions. Molecular networks, for drug disease and target combinations, and co-expression signaling, transcriptional regulatory, and metabolic and, protein-protein interactions, find diverse usage in the field of systems pharmacology(Azuaje, 2013). Network-based models have been employed to discern elucidate molecular mechanisms and pinpoint diagnostic biomarkers in a range of diseases, spanning metabolic disorders to cancers. Despite being in the early stages in pharmacology, network modeling is already shedding light on drug targets, interactions, and potential drug candidates for treating numerous diseases, along with predicting drug side effects. Additionally, network modeling serves as a primary approach in computational drug repositioning, commonly employed to construct a disease,gene and drug triangle, where nodes represent drugs, diseases, or gene products, and edges signify the interactions between them(Turanli et al., 2021).

Specifically, transcriptomic and clinical genomic data have been subjected to a comprehensive and systematic network study for in silico drug repositioning, utilizing gene expression data that is accessible to the public Additionally, the development of bioinformatics tools has facilitated researchers in efficiently conducting drug repositioning studies, with examples like geneXpharma (Turanli et al., 2017), PROMISCUOUS (von Eichborn et al., 2011), PharmDB (Lee et al., 2012), DrugMAP central (Fu et al., 2013) and others. This approach, for instance, aids in identifying and prioritizing novel drug targets. These networks aid in the discovery of potential therapeutic targets as well as the repurposing of drug candidates and evaluation of their effects on cell models (Turanli et al., 2021).

In this thesis, a network-based approach was applied for repurposing analyses. For this purpose, LINCS and genexpharma systems were used as the last step of bioinformatics analysis, after the establishment of protein-protein interactions.

LINCS, funded by the NIH Common Fund, aims to create an extensive repository of response signatures. This involves employing a variety of array of disturbances such as genetic, disease and chemical states. Also includes model systems like variety of

cell lines. Moreover, involves types of assay including epigenetic modification, protein and gene expression and also imaging (Stathias et al., 2020). An economical genome-wide transcriptomics assay named L1000, utilizing Luminex bead technology, has been developed. Data from LINCS-L1000 is accessible, providing information on the reactions of approximately 50 human cells to around 20,000 molecules at various concentrations, leading to more than one million experiments. The computational extraction of RNA expression data, like LINCS-L1000 data, can be achieved through diverse statistical approaches. Presently, signatures derived from LINCS-L1000 data are computed utilizing the regulated Z-score method (Duan et al., 2016). Recent research indicates that employing the characteristic direction method for processing L1000 data, through distinct intrinsic and extrinsic benchmarking schemes, significantly enhances signal-to-noise in comparison to the currently utilized Z-score method for computing L1000 signatures. In light of this, the characteristic direction processed L1000 signatures are made available through an advanced L1000CDS2 is an online search engine application. Thousands of small chemical signatures and their paired combinations can be prioritized with this tool, which also predicts the likelihood that they will either imitate or reverse an input gene expression signature using two different approaches. Additionally, for all small compounds profiled by the processed L1000 assay, the L1000CDS2 program predicts drug targets. (Duan et al., 2016).

Furthermore, another pharmaceutical search tool developed by Turanlı et al. called GeneXpharma was utilized for drug repurposing. GeneXpharma offers potential drug candidates for 48 diseases derived from repositioning analyses based on gene expression. The analyses leverage extensive drug-gene association data sourced from the Drug Gene Interaction Database, which encompasses 15 different databases. The process incorporates 118 gene expression profiling datasets specific to 48 diseases, and it includes statistical assessments for both drug-disease connections and gene-disease (Turanli et al., 2017). GeneXpharma showcases 50,304 interactions between drugs and genes, encompassing 4,344 genes and 11,939 drugs in total (Rahman et al., 2019).

2. The Aim of Study

In light of all the aforementioned information about both leukemia and its treatment options, the primary aim of this thesis is to investigate the repositioning of FDA-

approved drugs to address diverse medical conditions. The focus is on establishing their potential as therapeutic agents across various scenarios characterized by low treatment efficacy. Furthermore, attention is directed towards Ph+ ALL, the predominant clinically encountered subtype identified as a high-risk group. The objective is to discover alternative treatment options for addressing the challenge of imatinib resistance. Through this methodology, the ultimate goal is to enhance treatment effectiveness and propose a new therapeutic approach for a leukemia subtype with a notably weak clinical response. Additionally, important objectives involve implementing more comprehensive projects using the acquired data and eventually subjecting the project outcomes to clinical testing through a translational approach.

CHAPTER 2: METHODS

2.1. Computational Studies

2.1.1. Obtaining transcriptome (gene expression) data sets

Selected transcriptomic datasets were chosen in accordance with the objectives of the study emphasizing the presence of gene expression data from healthy individuals alongside diseased samples or samples categorized based on the presence or absence of drug resistance. Furthermore, considering qualitative differences that contribute to heterogeneity, such as disease subtype, sample type, cancer stage, etc., the samples will be classified. Adult mRNA gene expression datasets for ALL and Ph+ ALL were acquired from GEO. Differentially expressed genes analysis was performed on eight datasets for ALL (GSE26530, GSE12995, GSE635, GSE26865, GSE66004, GSE79533, GSE56449, and GSE66002) and four datasets for Ph+ ALL (GSE66004, GSE79533, GSE66792, and GSE66002). In the absence of control samples in seven datasets for ALL and four datasets for Ph+ ALL, control samples from the GSE26725 and GSE22529 datasets were chosen based on their experimental platform. The details of the selected GEO datasets are provided in Table 2.

Table 2. The table comprises GEO datasets utilized within the study's framework, encompassing ALL, Ph+ ALL, B-CLL, and CLL

Disease	Accession No	Platform	Sample Size		Pubmed ID
			Disease (n)	Control (n)	
ALL	GSE26530	GPL9115	28	8	22173241(Nordlund et al., 2012)
ALL	GSE12995	GPL96	175	-	19129520(Mullighan, Su, et al., 2009)
ALL	GSE635	GPL96	173	-	15295046(Holleman et al., 2004)

Table 2. (Continued) The table comprises GEO datasets utilized within the study's framework, encompassing ALL, Ph+ ALL, B-CLL , and CLL

ALL	GSE26865	GPL570	12	-	22173241(Nordlund et al., 2012)
ALL	GSE66004	GPL96	109	-	27561722(Herold et al., 2017)
ALL	GSE79533	GPL570	229	-	27634205(Hirabayashi et al., 2017)
ALL	GSE56449	GPL570	32	-	25515960(Schinnerl et al., 2015)
ALL	GSE66002	GPL570	98	-	27561722(Herold et al., 2017)
Ph+ ALL	GSE66004	GPL96	42	-	27561722(Herold et al., 2017)
Ph+ ALL	GSE79533	GPL570	17	-	27634205(Hirabayashi et al., 2017)
Ph+ ALL	GSE66792	GPL19883	15	-	25775523(McClellan et al., 2015)
Ph+ ALL	GSE66002	GPL570	30	-	27561722(Herold et al., 2017)
B-CLL	GSE26725	GPL570	-	5	21296997(Vargova et al., 2011)
CLL	GSE22529	GPL96	-	11	20595513(Gutierrez et al., 2010)

2.1.2. Identifying Differentially Expressed Genes at the mRNA Level

Each dataset for both ALL and its Philadelphia-positive subtype underwent independent analysis to identify DEGs, employing the principle of comparing gene expression levels between disease and healthy samples. In datasets lacking a control group, specifically GSE56449, GSE79533, GSE66002, GSE66792, and GSE26865,

analyses utilized control samples from GSE26725, while GSE12995, GSE635, and GSE66004 datasets were analyzed with control samples from GSE22529. Raw data underwent normalization using the Robust Multiarray Average (RMA)(Bolstad et al., 2003), and gene expressions were subjected to statistical comparison using the LIMMA(Ritchie et al., 2015) method under the R/Bioconductor platform(version Rx64 4.2.1)(Gentleman et al., 2004) for DEG analysis. Correction of p-values in multiple hypothesis tests employed the False Discovery Rate (FDR) method. Statistical significance was assessed on dual criteria: a p-value < 0.05 and 2-fold changes (FC). Furthermore, RRA analysis was done by using R/Robustrankaggreg. The direction of DEGs was ascertained as up-regulated if FC > 2 or down-regulated if FC < 2. Gene nomenclature was organized using the bioDBnet platform(Mudunuri et al., 2009). Given the analysis of multiple datasets for both ALL and Ph+ ALL, the mean fold changes of DEGs were statistically calculated using the R/Robustrankaggreg platform(Kolde et al., 2012) with a p-value < 0.05 criteria.

2.1.3. Functional Enrichment of Gene Sets

GSEA were undertaken to elucidate the functional roles of the identified DEGs. Metascape(Zhou et al., 2019), a bioinformatics tool, was employed to determine the involvement of DEGs in biological processes, molecular pathways, intracellular localizations, and associated diseases.In these analyses, information was extracted for the relevant genes using KEGG(Kanehisa, 2019) and Gene Ontology (GO) (Thomas et al., 2022) resources. In the GSEA analyses, significance was attributed to p-values below 0.01.

2.1.4. Establishing Protein-Protein Interaction Networks

The BioGRID database (version 3.5.184) (Chatr-Aryamontri et al., 2017) , encompassing 44,219 PPIs involving 14,373 distinct proteins, was utilized to discern physical associations among proteins associated with DEGs in ALL and Ph+ ALL. Cytoscape software 3.10.0(Shannon et al., 2003), along with the CytoHubba plug-in(Chin et al., 2014), was employed for the visualization of PPI networks and the computation of both local and global topological features, including degree and betweenness.

2.1.5. Drug Repositioning for Candidate Drug Identification

The L1000CDS2 platform (Duan et al., 2016) houses a repository containing 30,000 drug expression profiles sourced from the Library of Integrated Network-based Cellular Signatures (LINCS)-L1000 dataset (Campillos et al., 2008). Its primary purpose is to facilitate the identification of potential drug candidates for repositioning by analyzing the expression patterns of up-regulated and down-regulated DEGs specific to a given disease. Additionally, a network-centric approach was incorporated through the genexpharma tool (Turanli et al., 2017), utilizing hub proteins as drug targets. This tool encompasses an extensive compendium of 50,304 documented drug-gene interactions. This comprehensive approach augments the accuracy and thoroughness of drug repositioning initiatives, consequently elevating the likelihood of uncovering innovative therapeutic interventions.

2.2. Cell Culture

In order to assess the in vitro efficacy of drugs determined in vivo, human cell lines were employed. Within the thesis scope, drugs were identified for the treatment of both ALL and its subtype, Ph(+) ALL. Consequently, cell lines specific to these types were utilized for testing the identified drugs for both ALL variants. Towards this objective, the Jurkat cell line was employed for ALL, while the SUP-B15 cell line was used for Ph(+) ALL.In the course of these experiments, drugs found efficacious in Ph(+) and Ph(-) ALL cell lines will undergo testing on HUVEC cells, serving as the healthy control cell line. This process aims to identify drugs that exhibit minimal impact on healthy cells.

Jurkat cells were cultured, in accordance with the literature, in RPMI-1640 supplemented with 10% Fatal Bovine Serum (FBS) and 1% penicillin/streptomycin (Guo et al., 2019). Also, SUP-B15 cells were cultured in again RPMI-1640 supplemented with 1% penicillin/streptomycin however for these cells the ratio of FBS supplement was determined as 20 % for better proliferation (Wang et al., 2014). Furthermore, a healthy cell line, HUVEC, was cultured in DMEM supplemented with 10% Fatal Bovine Serum (FBS) and 1% penicillin/streptomycin(Chiew et al., 2015).

2.2.1. Thawing Frozen Cells

After obtaining the cell lines Jurkat, SUP-B15, and HUVEC, the cells were thawed in a 37°C water bath and promptly moved into 5 ml of pre-warmed media for centrifugation. Afterwards, SUP-B15 cells underwent centrifugation at 300 g for 5 minutes, Jurkat cells at 900 rpm for the same duration and finally, HUVEC cells at 500g for the same duration to remove the supernatant containing DMSO. The resulting pellet was reconstituted in fresh pre-warmed required media and then transferred into T25 culture flasks for SUP-B15 and Jurkat, T75 culture flasks for HUVEC.

2.2.2. Subculturing of Cells

Prior to commencing cell passage, cellular vitality and confluency were scrutinized through microscopic observation (Olympus, CKX53SE). Subsequently, the cells were transferred to Falcon tubes and subjected to centrifugation (400 g for SUPB15, 900 RPM for JURKAT). Following centrifugation, supernatants were carefully decanted, and the resultant pellets were dissolved in 3 ml of required culture media. Further, a dilution to a 1/3 ratio was performed, nearly 5 X 10^5 cell/mL viable cells were then seeded into T25 flasks. Subsequently, the passaged cells were incubated in an incubator at 37 degrees and 5% CO2 in air atmosphere, and this process was repeated every 3 days for SUPB15 cells and every 2 days for Jurkat cells. For HUVEC cell, Firstly media was removed from the flasks then cells were washed with PBS twice then 3 ml of trypsin was added to cells to unadhere the cells. Then cells were incubated for 5 minutes. Afterwards, 5 ml of media was added to stop the activity of trypsin. Then, cells were collected in a falcon tube and subject to centrifugation (500 g,5 minutes) Further, a dilution to a 1/2 ratio was performed, nearly 1 X 10^6 cell/mL viable cells were then seeded into T75 flasks.

2.2.3. Freezing Cells

Earlier in the experiments, cells were frozen for subsequent use in further studies. Approximately 2x10^6 cells were gathered through centrifugation, and the resulting pellet was reconstituted with 1.5 ml of freezing media comprising 70% FBS and RPMI 1640 media with 10% DMSO. Thorough mixing of the cells and freezing media occurred, and 1.5 ml of the cell suspension was dispensed into individual cryogenic

vials, followed by incubation at -80°C. This freezing step was repeated every 3-4 weeks.

2.2.4. Cell Counting

The number of cultured cells was determined using a hemocytometer to maintain uniform cell quantities for each procedure and also passage. The cells were gathered in Falcon tubes and subsequently centrifuged for 5 minutes at varied g or rpm settings based on the cell types. The supernatant was carefully decanted from the centrifuged Falcon tube. The resulting pellet was reconstituted in 3 mL of medium, and 1 mL of cells was aliquoted into an Eppendorf tube. Subsequently, 30 µL of cells were transferred from this primary Eppendorf to a secondary Eppendorf tube. Afterwards, cells were diluted 1:1 (v/v) with 0.4% Trypan Blue staining solution. Live cells, possessing an intact membrane, exhibited a bright white appearance and did not uptake the blue dye. Count the number of viable (seen as bright cells) cells in 4 squares and calculate the total number of cells via the formula below (1)

$$Number\ of\ Cell/mL = \frac{(Number\ of\ counted\ cells)}{4}\ x\ Dilution\ Factor\ x\ 10^4 \quad (1)$$

2.2.5. Establishing an Imatinib-Resistant Cell Line Ph (+) ALL

There are several ways to generate a resistant cell line. In this thesis, a gradually increasing method was used to develop drug resistance. The generation of the Imatinib-resistant cell line involved exposing the sensitive SUP-B15 cell line to gradually increasing concentrations of imatinib. Imatinib exposure began at 0.2 µM, with increments of 0.2 µM every 7 days, contingent on viability exceeding 70% in culture, as determined by the trypan blue exclusion method. If viability fell between 30% and 70%, the imatinib concentration remained unchanged; however, if viability dropped to 30% or less, imatinib was withdrawn, a process termed rescue. The duration of rescue periods depended on recovery times. Imatinib was reintroduced at 50% of the last attained level when viability reached 90% in the culture. The Imatinib-resistant cell line SUP-B15/RI was harvested and evaluated when the imatinib concentration reached up to 4 µM (Xing et al., 2012). After achieving the ability to grow in the presence of 4 µM imatinib, the cells were designated as SUPB15/R, and the drug concentration was maintained at a constant level of 4 µM throughout the research. At

each dosage administration, the resistant cell group from the preceding step and the corresponding controls of that group were frozen at -80°C and archived as backups.

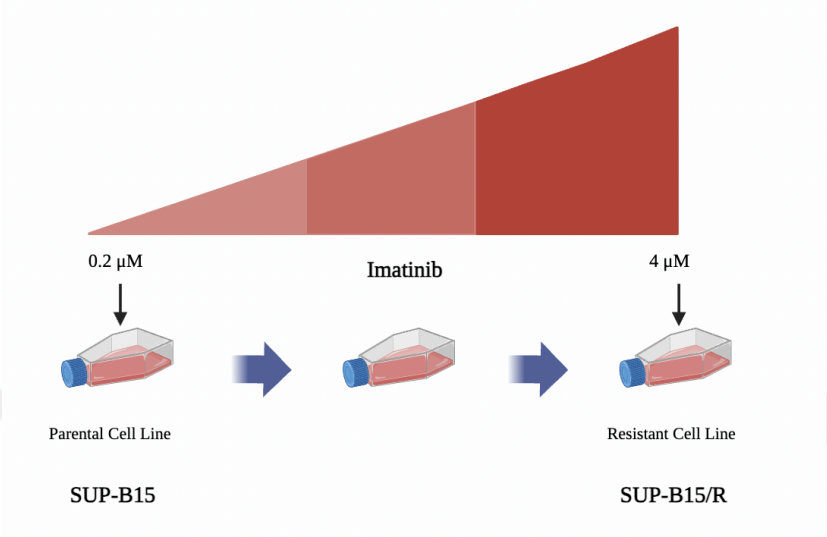

Figure 3. Generation of Imatinib resistant SUP-B15/R cell line by gradually exposing the cells to increasing concentrations of Imatinib over an extended period.

2.2.6. Validating Imatinib Resistance with MTT Assay

The examination of resistance development in SUPB15/R cells, exposed to a progressively escalating drug regimen, was carried out using the Thiazolyl blue tetrazolium bromide (MTT) assay. Following one passage without exposure to the drug, the cells underwent centrifugation at 400 g for 5 minutes to eliminate the drug. Upon confirming the viability and count of the collected cells using trypan blue, they were seeded in a 96-well plate at a density of $1x10^4$ cells per well in 100 µL of RPMI media and exposed to imatinib for 72h. Following that, 15 µl of MTT solution (5 µg/ml) was introduced into the wells and allowed to incubate for 4 hours at 37°C in a CO_2 incubator. Subsequently, the cells were pelleted through centrifugation at 250 g for 10 minutes, and the medium was aspirated from each well. Then, 100 µl of DMSO was added and incubated for 30 minutes on a light-protected shaker. Measurements were conducted using a spectrophotometer at a wavelength of 570 nm.

2.2.7. Validating Imatinib Resistance with Growth Curve

To demonstrate the development of resistance, both SUP-B15 and SUP-B15/R cells were cultured in two different 6-well plates at a density of 500,000 cells per ml in 3

ml volumes. Three wells served as controls, while the remaining three were exposed to an IC50 drug concentration. Trypan blue cell counting was performed at 48 and 72 hours on both control and treated wells, with the results being documented. Upon completion of the experiment at the 72nd hour, a growth curve was constructed based on the obtained data.

2.2.8. Validating Imatinib Resistance with Flow Cytometry

To assess drug resistance via flow cytometry, both SUPB15 and SUPB15/R cells were cultured in 6-well plates and exposed to imatinib for 48h and 72h. Subsequently, 1x 10^6 cells were collected, PBS-washed twice, and re-suspended in 100 µl of binding buffer. Following this, 5 µl of Annexin V-FITC was introduced, and after a 10-minute interval, 10 µl of PI was added. The cells were then incubated in darkness at room temperature for 15 minutes, followed by the addition of 400 µl of binding buffer. The stained cells were subjected to analysis using a flow cytometer.

2.3. Evaluating the Cytotoxic Activity of Drug Candidates for Ph (-) ALL on Jurkat Cell Line

2.3.1. Determination of Anti-Proliferative Effects of Drugs on Ph (-) ALL Cells with MTT Assay

Maytansine and Isoprenaline were identified as the chosen drug candidates for Ph (-) ALL. Additionally, Doxorubicin was employed as a positive control for these drugs. To assess their cytotoxic potential on the Jurkat cell line, an MTT assay was executed. Initially, Jurkat cells underwent centrifugation at 900 rpm for 5 minutes. Subsequent to this, their count and viability were determined using Trypan Blue. Following the enumeration, Jurkat cells were seeded onto a 96-well plate at a density of 2x 10^4, and individual treatments with Maytansine (0-2nM) and Isoprenaline (0-50 µM) were administered. Following a 48-hour incubation period, 15 µL of MTT solution was introduced to the wells, and the plate was incubated for an additional 4 hours without exposure to light. Upon removal of the media from the wells, 100 µL of DMSO was added, and the plate was incubated for 30 minutes on a light-protected shaker.

2.3.2. Assessment of Cytotoxic Effects of Drugs Possessing Established Anti-Proliferative Properties on Ph (-) ALL Cells with Trypan Blue Assay

To substantiate the cytotoxic efficacy of Maytansine and Isoprenaline, the Trypan Blue Assay was employed. For this purpose, Jurkat cells were seeded at a density of $5x10^5$ across two distinct 6-well plates, where one plate was designated for Maytansine, and the other for Isoprenaline. Wells were categorized into control, IC50, and IC80 concentrations of the respective drugs. Cell counts were performed using trypan blue at both 24, 48, and 72. hours for each well. The data obtained from the counts were utilized to construct a growth curve.

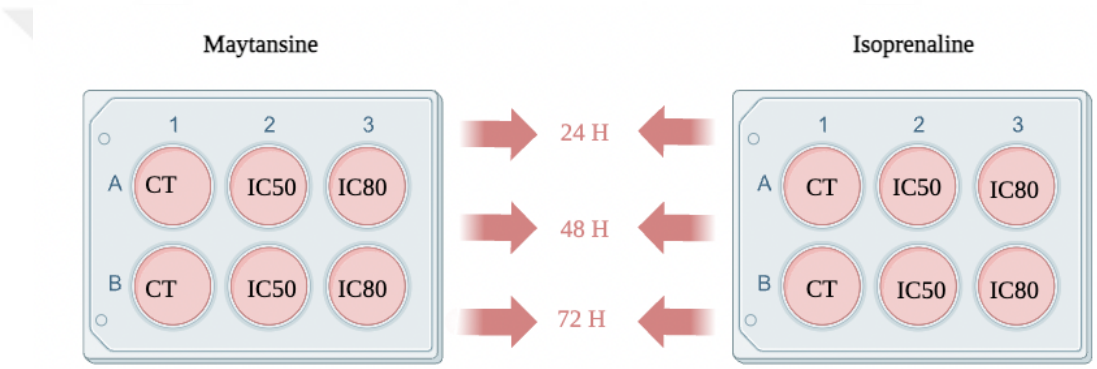

Figure 4. Schematic representation of the 6-well plate arrangement for the Trypan Blue experiment.

2.4. Estimation of the Cytotoxic Effects of Drugs, Both Individually and in Combination with Imatinib, on Imatinib-Sensitive and Resistant Ph+ ALL Cells.

2.4.1. Determination of Cytotoxic Effects of Drugs on Both Sensitive and Imatinib Resistant Ph (+) ALL Cells with MTT Assay

Desipramine and Glipizide were selected as the preferred drug candidates for Ph (+) ALL. To evaluate their cytotoxic potential on the SUP-B15 and SUP-B15/R cell lines, an MTT assay was conducted. Initially, cells were centrifuged at 400 g for 5 minutes. Subsequently, their count and viability were assessed using Trypan Blue. After enumeration, both cell lines were seeded onto a 96-well plate at a density of $2x10^4$, and individual treatments with Desipramine (0-25 µM) and Glipizide (0-80 µM) were

administered. After a 72-hour incubation period, 15 µL of MTT solution was added to the wells, and the plate was incubated for an additional 4 hours without exposure to light. Following the aspiration of media from the wells, 100 µL of DMSO was added, and the plate was incubated for 30 minutes on a light-protected shaker.

2.4.2. Determination of the Cytotoxic Effect of Drugs Given in Combination with Imatinib by MTT Assay.

To comprehend the additive, synergistic & antagonistic effects of imatinib and Ph (+) drugs, a combined MTT assay was employed on imatinib-resistant SUP-B15/R cells. The experimental design included wells treated with only imatinib IC20, only the drug (Desipramine or Glipizide), and a combination of both. In the combination wells, imatinib concentration remained stable at IC20, while the required drug concentration was increased. This experiment was repeated separately for both Desipramine and Glipizide.

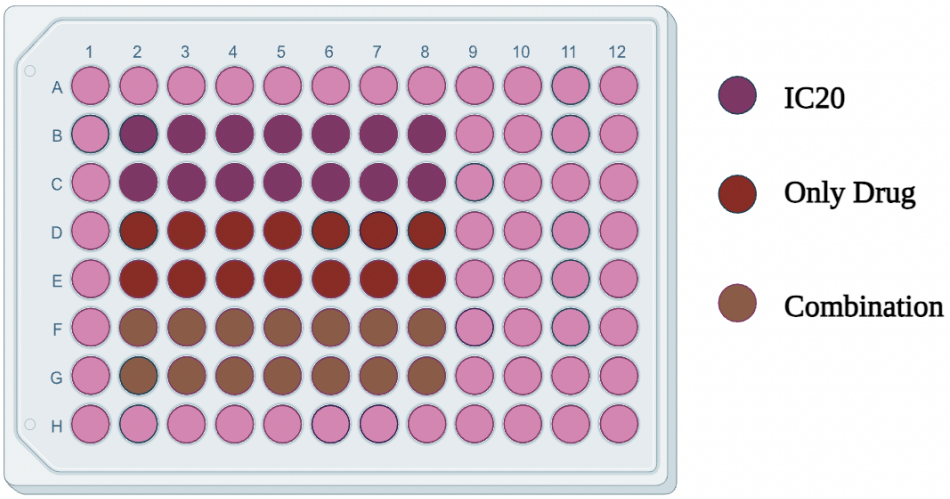

Figure 5. Representation of combination MTT assays with selected drugs on a 96-well plate.

2.4.3. Confirmation of Cytotoxic Activity of Selected Synergistic Doses Using Trypan Blue Exclusion Assay

Upon identification of synergistic doses using computational tools, a trypan blue staining assay was employed to validate the impact of these dosages. In pursuit of this,

SUP-B15 and SUP-B15/R cells were harvested and seeded onto 6-well plates, where the determined synergistic dosages were administered to the respective wells, alongside a control well. Cell counting was conducted at 48 hours and 72 hours, and the acquired data were utilized to construct a growth curve.

2.5. Assessment of the Apoptotic Effects of Synergic Doses of the Selected Drugs Determined to Have Potent Cytotoxic Effects on the Cells.

2.5.1. Determination of Apoptotic Cell Population via Annexin/FITC dual staining

The apoptotic effects of two drugs, which have been determined to exhibit strong cytotoxic activity among the tested drugs, will be assessed on cells using the Annexin/FITC dual staining method. Based on flow cytometry analyses resulting from Annexin and FITC staining, cells with dual positivity will be classified as "late apoptotic/dead," Annexin-positive and FITC-negative cells as "early apoptotic," Annexin-negative and FITC-positive cells as "necrotic," and cells negative for both Annexin and FITC as "healthy." Furthermore, apoptotic activations will be determined in Ph (-) Jurkat cells exposed to IC20 and IC50 concentrations, calculated based on MTT assay results, during the specified combination or individual applications of drugs for 48 and 72 hours, as well as in Ph (+) imatinib-sensitive SUP-B15 cells and imatinib-resistant SUP-B15/R cells. Jurkat, SUPB15, and SUPB15/R cells were cultured in 6-well plates and treated with required dosages of drugs for 48h and 72h. Subsequently, $1x10^6$ cells were harvested, washed twice with PBS, and re-suspended in 100 µl of binding buffer. Following this, 5 µl of Annexin V-FITC was added, and after a 10-minute incubation, 10 µl of PI was introduced. The cells were then incubated in darkness at room temperature for 15 minutes, followed by the addition of 400 µl of binding buffer. The stained cells underwent analysis using a flow cytometer.

2.6.1. Confirmation of Cytotoxic Activity of Selected Drugs on HUVEC Cells Using Trypan Blue Exclusion Assay

HUVECs were seeded in 6-well plates at a concentration of $5 x10^4$. After 24 hours of adhesion, the media was removed from the 6-well plates. Then, the drugs were added to the 6-well plates with fresh media at the IC50 dose that was determined. After 48

hours of incubation, the cells were counted using trypan blue, and the cytotoxic effect of the drugs on the HUVEC cell line was determined.

CHAPTER 3: RESULTS

3.1. Determination of the Drugs to be Repositioned

The identification of DEGs in eight datasets related to ALL and four datasets related to Ph+ ALL was performed using the LIMMA R package. Figures 6A and 6B present the counts of DEGs, up-regulated DEGs, and down-regulated DEGs for both diseases. R/Robustrankaggreg, a statistical approach combining data from multiple datasets, was employed to enhance the statistical robustness of the DEGs. This method assigned a ranking to each gene in each dataset and computed the mean FC with a significance threshold of p-value <0.05. The analysis revealed a total of 799 DEGs in ALL, with 386 up-regulated genes and 413 down-regulated genes. For Ph(+) ALL, 295 DEGs were identified, consisting of 132 up-regulated and 163 down-regulated genes. Among the top 20 up-regulated and down-regulated DEGs based on their FC illustrated in Figure 7, ADA and HBD were notably highlighted as up-regulated DEGs in the top 20 DEGs for ALL, while these genes did not exhibit differential expression in Ph+ ALL. Conversely, SPATS2L was identified as an up-regulated DEG in Ph(+) ALL but did not show significant differential expression in ALL.

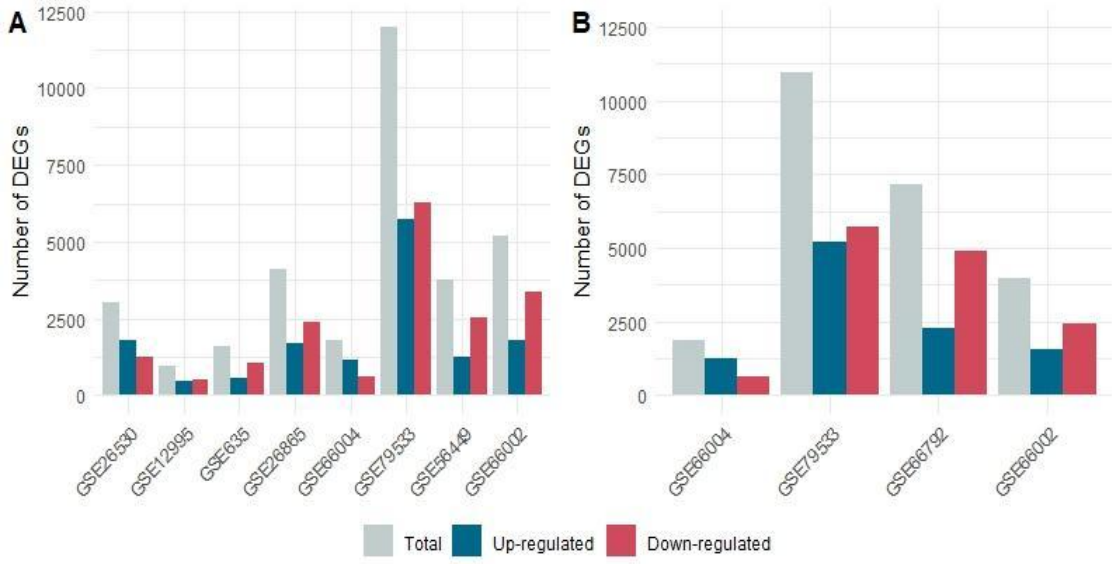

Figure 6. Number of DEGs in the result of DEG analysis of each dataset A) in ALL and B) in Ph+ ALL.

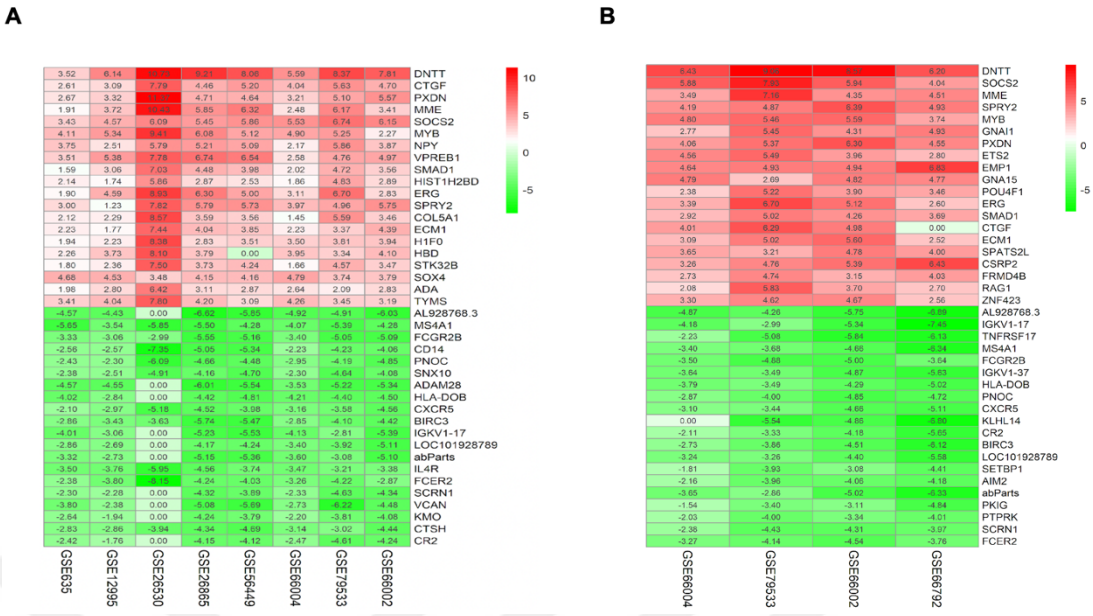

Figure 7. Representation of R/Robustrankaggreg analysis results with heatmap diagram of fold changes (logFC) of the top 20 genes with increased and decreased expression in the ALL (A) and Ph (+) ALL data sets (B).

3.1.1. Identification of HUB Proteins

In the course of the investigation, a total of 3031 PPIs associated with protein coding DEGs were identified in cases of ALL, whereas 519 PPIs were recognized in Ph+ ALL. Following this, an analysis of the top 20 proteins, considering both degree and betweenness centrality, was conducted using the CytoHubba package for both disease categories. The hub proteins for each respective condition were designated as the set union of proteins identified as top-degree and top-betweenness.

As a result, in ALL, a total of 24 hub proteins were determined, encompassing AGR2, CBX5, CDC42, CDC5L, CDK1, CDKN1A, EGFR, EZH2, HSP90AA1, HSP90AB1, HSPD1, JUN, MYC, PCNA, PIK3R1, RAC1, RANBP9, SMARCA4, SNCA, TNFAIP3, TRAF3, YWHAB, YWHAE, and ZBTB16. Moreover, 33 hub proteins were identified for Ph (+) ALL, including ATM, ATP2B1, BIRC3, CCND2, CDK6, CDKN2A, CDKN2C, CTBP2, DSP, GNAI1, GRB10, HDAC6, HIPK2, IL6ST, INSR, IQGAP1, KIAA1429, KRAS, LCK, LEF1, LGALS3BP, LYN, MYB, MYH10, RAI14, RANBP9, SAP30, SMAD1, SYK, SYNCRIP, TRAF5, TRAPPC10, and YES1.

Remarkably, an overlap was noted where 16 hub proteins were identified as common in both ALL and 7 hub proteins were shared in the case of Ph (+) ALL found by degree and betweenness to depict the interactions among these hub proteins visually, a network visualization was created using Cytoscape (Figure 8).

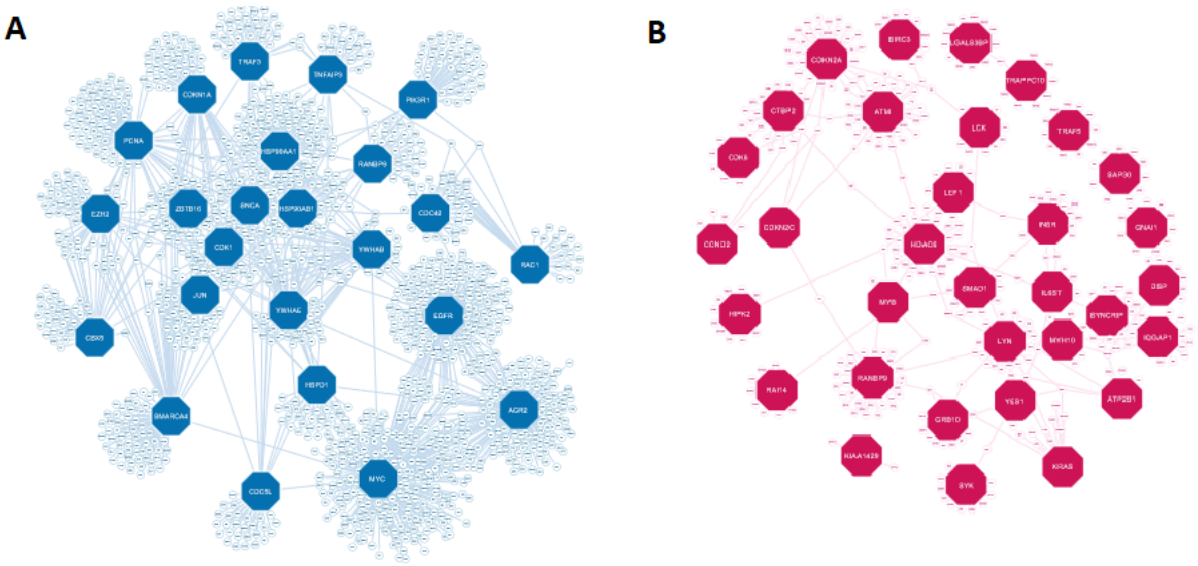

Figure 8. A) The interaction network illustrating the connections of hub proteins (depicted by blue octagons) with other proteins in ALL. B) The interaction network showcasing the links of hub proteins (depicted by red octagons) with other proteins in Ph+ ALL.

3.1.2. Gene Enrichment Analysis

Through comparative gene set enrichment analysis, it was determined that 11 pathways were shared between both diseases out of the 20 significant pathways associated with DEGs. These pathways included cellular response to cytokine stimulus, hematopoietic cell lineage, hemostasis, inflammatory response, negative regulation of cell activation, negative regulation of the immune system process, positive regulation of cell death, positive regulation of cytokine production, positive regulation of the immune response, regulation of immune effector process, and response to bacterium. In addition to these, cell cycle, cytokine signaling in the immune system, neutrophil degranulation, regulation of B cell activation, signaling by Rho GTPases, Miro GTPases, and RHOBTB3 were notable pathways observed in

ALL. B cell activation, enzyme-linked receptor protein signaling pathway, and regulation of the MAPK cascade pathways were also significant pathways in Ph+ ALL.

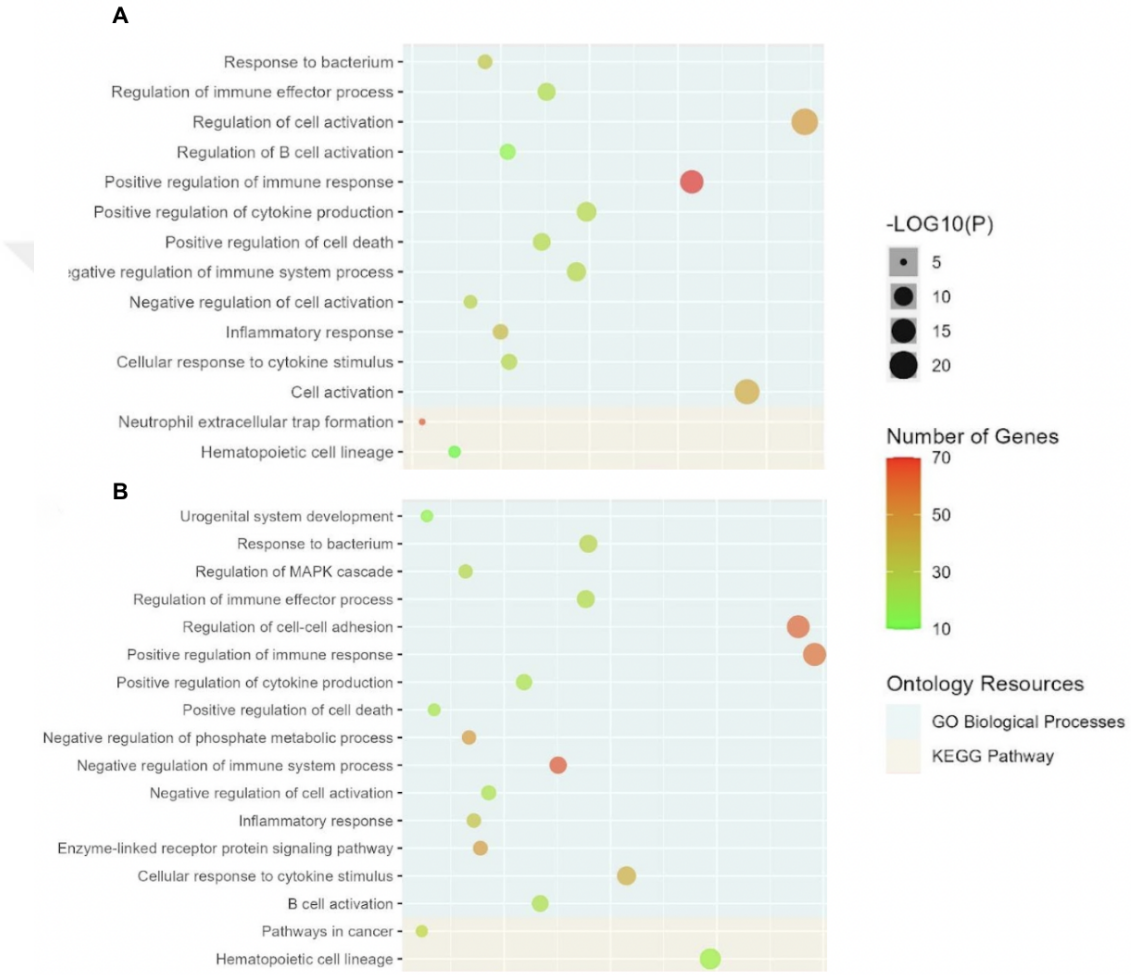

Figure 9. Pathways/biological processes activated by genes exhibiting differential gene expression in ALL (A). Pathways/biological processes activated by genes exhibiting differential gene expression in Ph-positive ALL (B).

3.1.3. Selected Repositioned Drugs

Two different approaches were used in the research to investigate drug repositioning techniques for ALL and its Ph+ subtype: the discovery of DEGs as viable drug targets

that have the ability to reverse gene expression patterns, and the targeting of hub proteins as potential drug targets. Using L1000CDS2, a medication repositioning technique, it was possible to find 39 distinct drugs for Ph+ ALL and 40 distinct drugs for up-regulated and down-regulated DEGs in ALL. notably, a subset of six medications Dasatinib, NVP-BGT226, Parthenolide, Selamectin, Selumetinib, and Tyrphostin AG 1478 that are shared by both disorders were discovered. Dasatinib is currently used as a first-line treatment for Ph+ ALL in adult patients(Wieduwilt, 2022). Selamectin, on the other hand, is an antiparasitic drug that interacts with various targets, including multidrug resistance protein, Akt/mTOR, and WNT-TCF pathway(Juarez et al., 2018). Tyrphostin, tested in mice, is an active EGFR inhibitor recommended for individuals with mutations in human pre-B acute lymphoblastic leukemia. When these drugs are examined, drugs such as Dasatinib, already prioritized in the clinic for ALL treatment, or drugs recommended for ALL treatment, such as Parthenolide and Tyrphostin AG 1478, have been identified(Lee and Rhee, 2017). The presence of drugs from the literature that is already used in the clinic or have therapeutic effects in our study is also evidence that the gene sets used in the study accurately reflect the disease. From the 24 core proteins identified for ALL, 13 of them have formed a network with a total of 123 interactions involving 99 drugs. In the case of Ph+ ALL, 19 out of 33 core proteins have constituted a network with a total of 289 interactions involving 203 drugs. Conclusively, within the scope of the thesis, the drugs that could be effective from many data sets were compiled as the first two drugs for each of the two diseases using different methods. These include Maytansine and Isoprenaline for ALL and Desipramine and Glipizide for Ph (+) ALL.

Table 3. The first two drugs targeting core proteins in ALL disease

Name of Drug	p-value	Target Hub Protein	Information of Drug
MAYTANSINE	0.000227	HSP90AA1	Maytansine is a cytotoxic agent that binds to the rhizoxin-binding site, preventing the assembly of microtubules by binding to tubulin.
ISOPRENALINE	0.000247	PIK3R1	Isoprenaline is a medication used for the treatment of bradycardia, heart block, and occasionally asthma.

Table 4. The first two drugs targeting core proteins in Ph (+) ALL disease

Name of Drug	p-value	Target Hub Protein	Information of Drug
DESIPRAMINE	3.65995E-08	KRAS	Desipramine is a tricyclic antidepressant used in the treatment of depression.
GLIPIZIDE	0.000131224	CDKN2A,GRB10,CDKN2A	Glipizide is an anti-diabetic medication belonging to the sulfonylurea class, used in the treatment of type 2 diabetes.

3.2. Generation of Imatinib Resistant Cell Line

3.2.1. Results of MTT assays

Within the framework of this thesis, a central objective was the examination of cytotoxic effects induced by repurposed drugs on imatinib-resistant SUP-B15 cell lines. Emphasis was placed on meticulous observation of the mechanisms through

which these drugs could potentially mitigate imatinib resistance. To this end, increasing dosages of Imatinib were given to parental cells for 6 months. This process was continued to reach 4 µM of resistance. To confirm the resistance in developed imatinib-resistant SUP-B15/R cells, an MTT assay was conducted, wherein cells were exposed to increasing doses of imatinib and cell viability was measured after 72 hours using the MTT test. The results of the MTT assays indicated that while the IC50 value for imatinib in sensitive parental SUP-B15 cells was approximately 2.8 µM, the IC50 value for the developed imatinib-resistant SUP-B15/R cells was observed almost 20 µM. Thus, it was determined that the resistant cells exhibited resistance to imatinib of 7-fold compared to the sensitive parental cells (Figure 10).

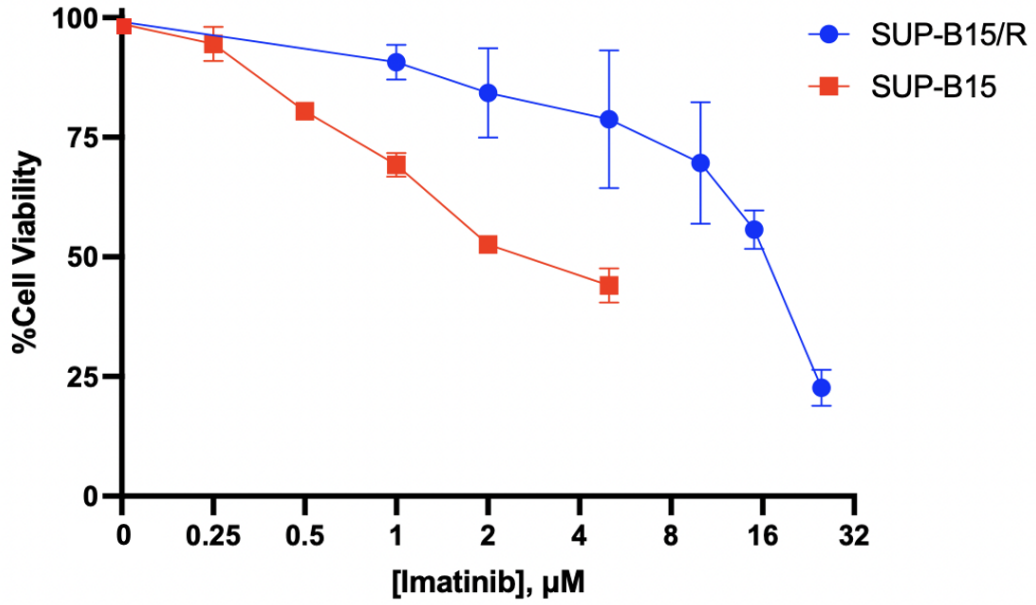

Figure 10. Determination of the viability of SUP-B15 and SUP-B15/R cells with imatinib treatment. Imatinib application was carried out for 72 hours, and viability analysis was performed using the MTT test. The experiments were repeated three times. Error bars indicate the standard deviation.

3.2.2. Representation of Growth Curve for Validating Imatinib Resistance

After performing MTT analysis, a growth curve analysis was executed to assess imatinib resistance in SUP-B15/R cells. Utilizing parental and imatinib-resistant cells from two different 6-well plates, in each 6-well plate, three wells functioned as controls, while the remaining three were subjected to a 4µM drug concentration.

Trypan blue cell counting occurred at 48 and 72 hours for both control and treated wells. Consequently, the variance in proliferation between parental cells and imatinib-resistant cells was observed. As observed in Figure 11, the untreated parental cell line and untreated SUP-B15/R exhibited similar proliferation, whereas a notable difference was evident between the proliferation of the parental cell line treated with 4μM imatinib and the SUP-B15/R treated with the same concentration. While significant cell death was observed in the drug-treated parental cell line, the resistant group displayed a proliferation similar to its untreated state under 4μM drug exposure.

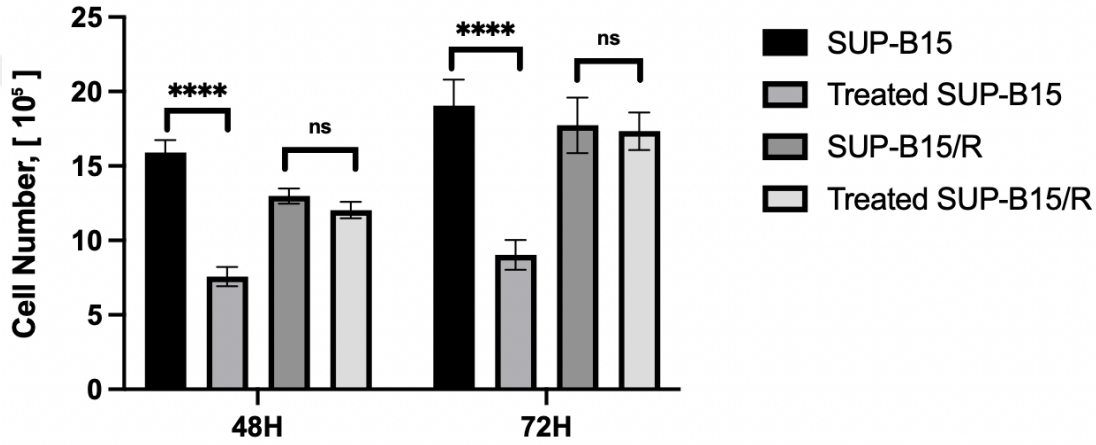

Figure 11. Representative growth curve created with data obtained from the trypan blue experiment on SUP-B15 and SUP-B15/R. Imatinib application was carried out for 72 hours, and viability analysis was performed using the MTT test. The experiments were repeated three times. Error bars indicate the standard deviation.

3.2.3. Flow cytometry for determining resistance

To demonstrate the developed Imatinib resistance in SUP-B15/R cells, Imatinib treatment was applied to both SUP-B15 and SUP-B15/R cells, and apoptotic cells were detected using the Annexin/PI staining method. The experiment lasted for 72 hours, with measurements taken at 48 and 72 hours using flow cytometry, and graphs were generated accordingly. According to the results of the Annexin/PI staining, the apoptotic cell count observed in Imatinib-resistant SUP-B15/R cells remained unchanged following the application of the IC50 Imatinib dose (Figure 12). In contrast, a significant increase in apoptotic cell count, particularly at 72 hours, was evident in Imatinib-sensitive SUP-B15 cells treated with the IC50 Imatinib dose. Cells that did

not receive treatment did not exhibit a notable change in apoptotic cell count. Consequently, the resistance of SUP-B15/R cells to Imatinib, as confirmed by both MTT tests and trypan blue staining applications, has been reaffirmed.

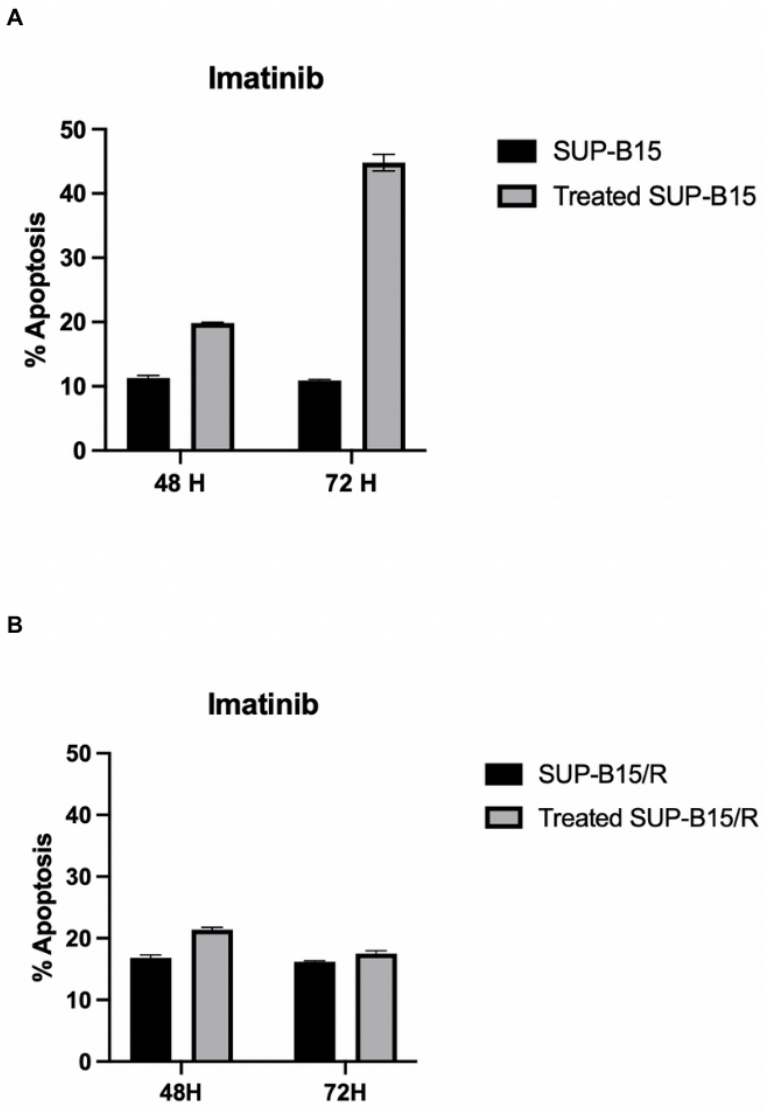

Figure 12. Representation of apoptotic cells identified in SUP-B15 and SUP-B15/R cells treated with IC50 Imatinib dose using Annexin/PI staining. Imatinib application was carried out for 72 hours, and viability analysis was performed using the MTT test. The experiments were repeated three times. Error bars indicate the standard deviation

3.3. Cytotoxic Effects of Maytansine and Isoprenaline on Ph (-) ALL cell line

3.3.1. Ascertainment of Anti-Proliferative Effects of Maytansine and Isoprenaline With MTT Assay

To assess the cytotoxic effects of the two drugs, Maytansine and Isoprenaline, identified through bioinformatic analyses for Ph (-) ALL, separate MTT assays were conducted on JURKAT cell lines, a cell line representative of ALL. Additionally, Doxorubicin was employed as a positive control for these drugs. In the Jurkat cell line, the IC50, IC20, and IC10 doses for Maytansine were determined to be 439 pM, 200 pM, and 120 pM, respectively (Figure 13A). The results of the MTT assay indicated that the Jurkat cell line exhibited high sensitivity to Maytansine, with potent cytotoxic effects observed even at picomolar concentrations. Furthermore, IC50, IC20, and IC10 doses for Isoprenaline were found to be 15.33 µM, 7.92 µM and 5.21 µM respectively. (Figure 13B).

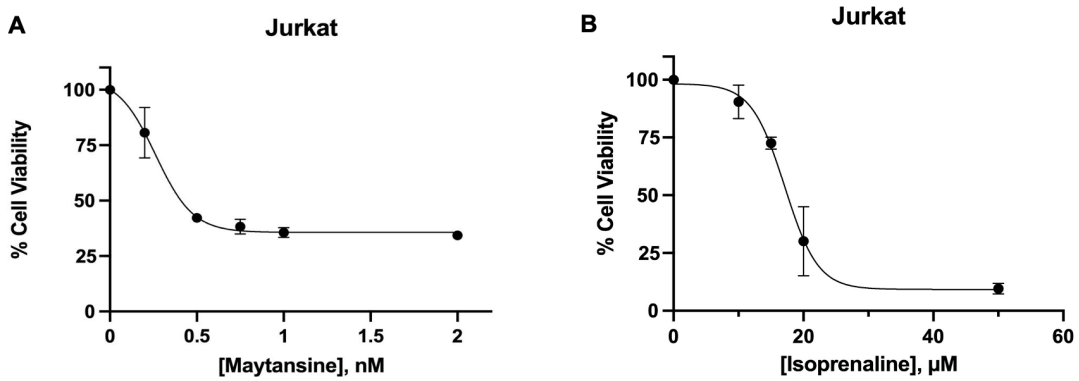

Figure 13. Determination of the viability of Jurkat cells treated with Maytansine (A) and Isoprenaline (B). Both treatment was conducted for 48 hours, and viability analysis was performed using the MTT test. The experiments were repeated three times. Error bars indicate standard deviation.

Additionally, the MTT assay test results revealed that in the Jurkat cell line, the IC50, IC20, and IC10 values for Doxorubicin hydrochloride were determined as 27.88 nM, 13.16 nM, and 12.2 nM, respectively (figure 14). Upon examination of the MTT results for Doxorubicin hydrochloride used as a control, as well as Maytansine and

Isoprenaline identified through analyses, it was discerned that the Jurkat cell line exhibits significantly greater sensitivity to Maytansine.

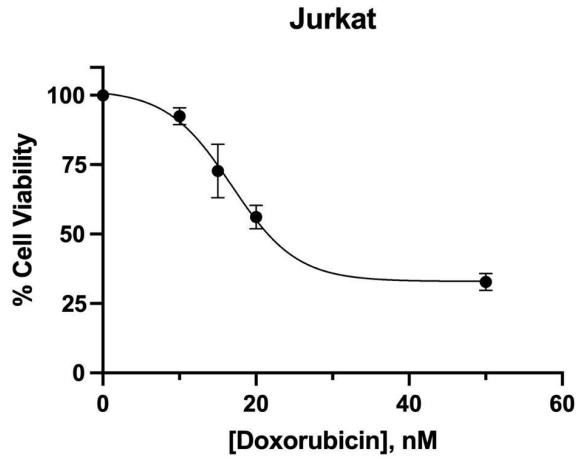

Figure 14. Determination of the viability of Jurkat cells treated with Doxorubicin. treatment was conducted for 48 hours, and viability analysis was performed using the MTT test. The experiments were repeated three times. Error bars indicate standard deviation.

3.3.2. Results of Trypan Blue Staining on Ph (-) ALL cell line after Drug Administrations

The trypan blue staining method was employed to determine the cytotoxic effects of drugs with identified anti-proliferative activity on Ph (-) ALL cells. Cell counts were conducted at 24, 48 and 72. hours were used to construct a proliferation graph based on the obtained data.

As a result of this experiment, the cytotoxic effects of Maytansine and Isoprenaline on Jurkat cell line have been confirmed. While the group without drug treatment and used as control exhibited a linear increase over the course of 3 days, the proliferation in the group treated with the IC50 dose was significantly slower compared to the control. At the IC80 dose, a linear decrease was observed, leading to a substantial reduction in the number of viable cells on the third day (Figure 15).

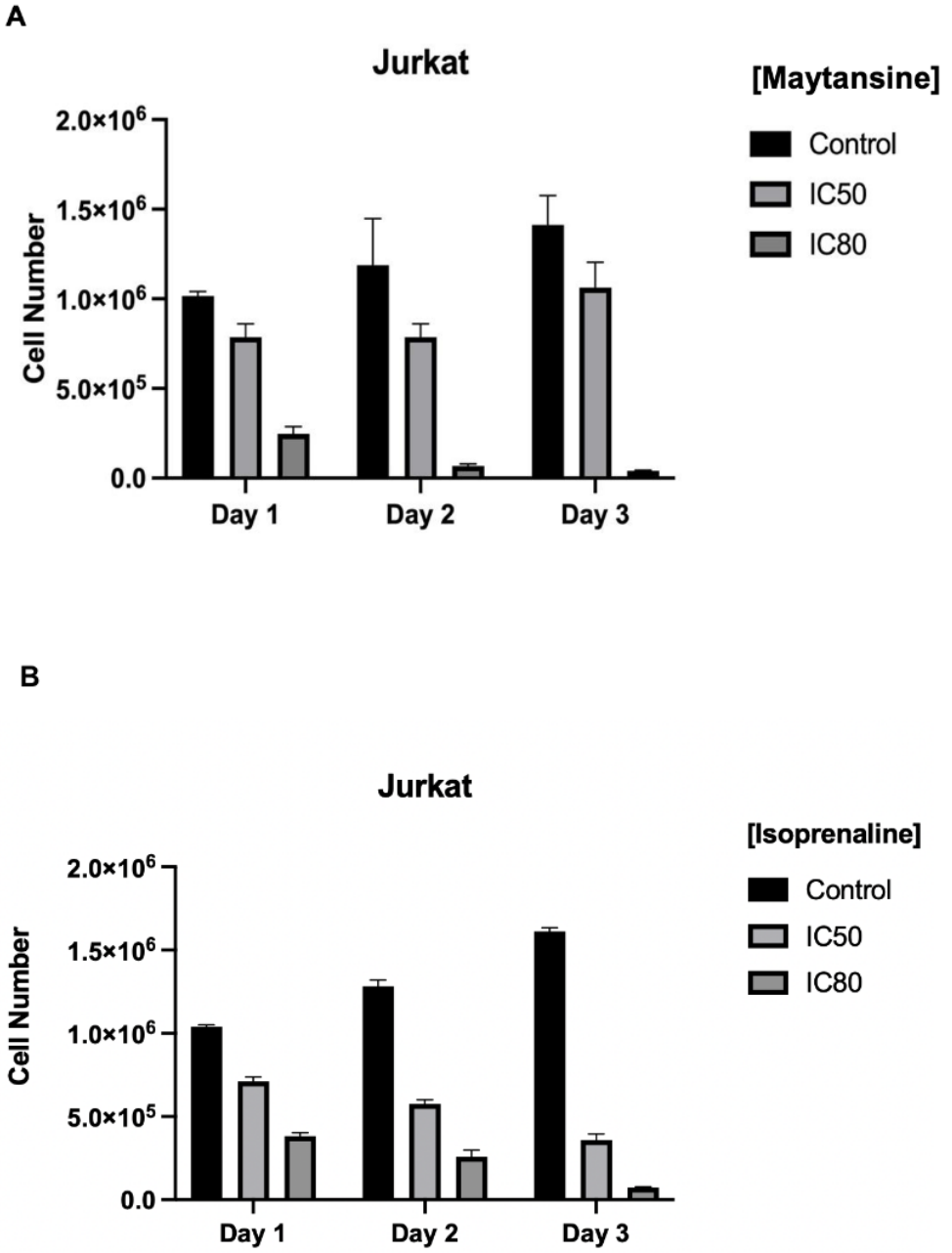

Figure 15. Determination of the cytotoxic effects of Maytansine (A) and Isoprenaline (B) on Jurkat cells based on the trypan blue staining results obtained from the assessment of their anti-proliferative activity. The experiment was repeated three times. Error bars indicate standard deviation.

3.4. Assessment of the Cytotoxic Impact of Glipizide and Desipramine, Both Individually and in Conjunction with Imatinib, on Ph (+) ALL Cells

3.4.1. MTT Assay Results for Antiproliferative Effects Induced by Glipizide and Desipramine in Ph (+) ALL Cells

Desipramine and Glipizide, identified as effective drugs for Ph (+) ALL through bioinformatic analyses, were individually subjected to MTT analyses to determine their cytotoxic effects on both parental SUP-B15 and Imatinib-resistant SUP-B15 cell lines. The MTT assay was established, taking into account a duplication period of 72 hours. According to the MTT results, the IC50, IC20, and IC10 values for Desipramine in parental SUP-B15 cells were determined to be 22.04 µM, 9.27 µM, and 8.89 µM, respectively (Figure 16). For Imatinib-resistant SUP-B15/R, the IC50 dose was found to be the same as Imatinib-sensitive SUP-B15. Despite SUP-B15/R cells being 7 times more resistant to Imatinib compared to SUP-B15, Imatinib resistance did not alter the IC50 dose for Desipramine. From this result, it is evident that Imatinib resistance does not lead to any decrease in the anti-proliferative effect of Desipramine.

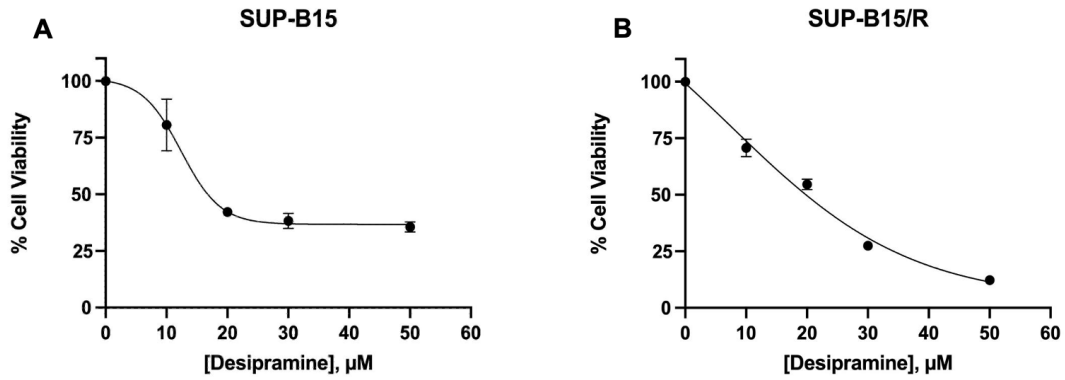

Figure 16. Determination of the viability of SUP-B15 (A) and SUP-B15/R (B) cells treated with Desipramine. Desipramine treatment was carried out for 72 hours, and viability analysis was conducted using the MTT test. The experiments were repeated three times. Error bars indicate standard deviation.

In addition, the second identified drug, Glipizide, exhibited IC50, IC20, and IC10 doses of 68.02 µM, 25.2 µM, and 12.68 µM, respectively, in parental SUP-B15 cells. For Imatinib-resistant SUP-B15/R cells, the IC50, IC20, and IC10 doses were determined to be 116.93 µM, 30.38 µM, and 25.15 µM, respectively (Figure 17). When comparing the IC50 values of Imatinib-resistant SUP-B15/R and Imatinib-sensitive

SUP-B15, it is evident that the IC50 value of the resistant group is approximately 2 times higher than the drug-sensitive group. This result clearly indicates that Imatinib resistance has led to a reduction of approximately 2 times in the anti-proliferative effect of Glipizide. In other words, cells showing resistance to Imatinib have developed cross-resistance to the drug Glipizide.

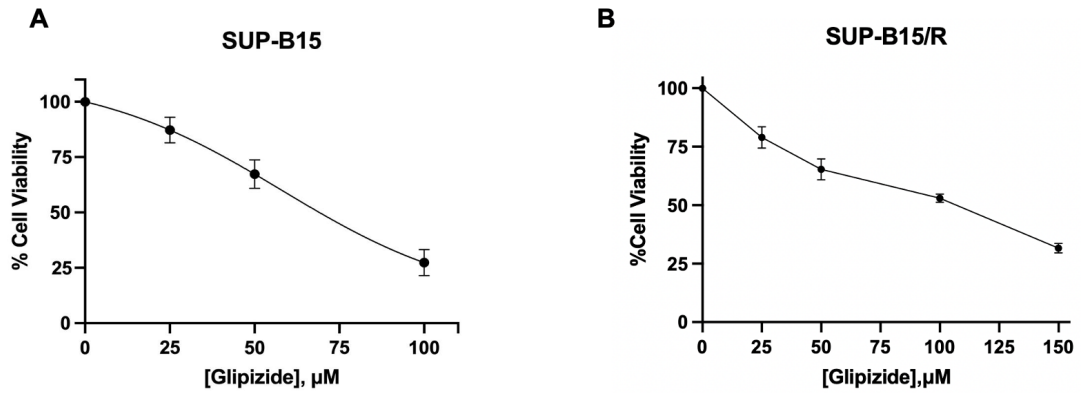

Figure 17. Determination of the viability of SUP-B15 (A) and SUP-B15/R (B) cells treated with Glipizide. Glipizide treatment was carried out for 72 hours, and viability analysis was conducted using the MTT test. The experiments were repeated three times. Error bars indicate standard deviation.

In addition to all of these, Dasatinib was used as a positive control for SUP-B15 and SUP-B15/R cells. According to MTT results IC50, IC20 and IC10 dosages of Dasatinib on SUP-B15 cells were 15.96 nM, 2.02 nM, and 1.01 nM respectively. Additionally, SUP-B15/R cells have demonstrated similar values (Figure 18). According to these results, SUP-B15 and SUP-B15/R were more sensitive to Dasatinib compared to Desipramine and Glipizide.

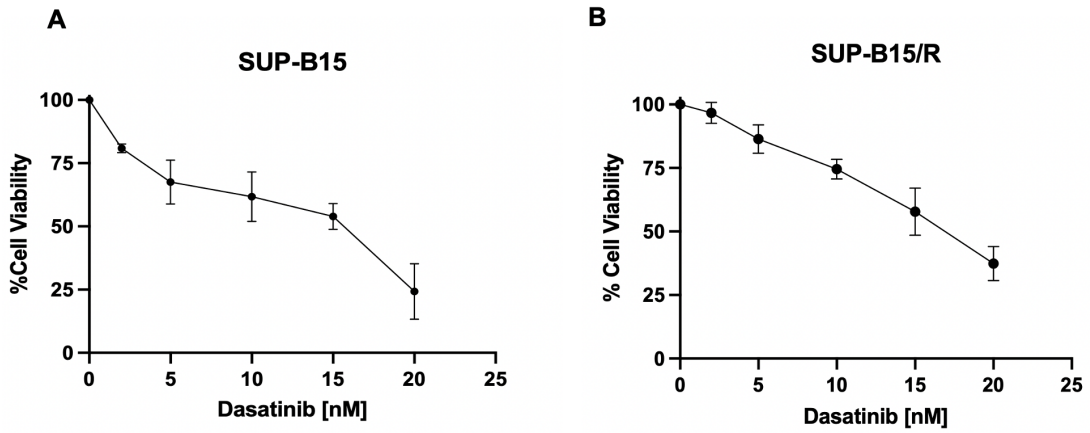

Figure 18. Determination of the viability of SUP-B15 (A) and SUP-B15/R (B) cells treated with Dasatinib. Dasatinib treatment was carried out for 72 hours, and viability analysis was conducted using the MTT test. The experiments were repeated three times. Error bars indicate standard deviation.

3.4.2. MTT Assay outcomes obtained with Glipizide and Desipramine combinations in conjunction with Imatinib administration on Ph (+) ALL Cells Respectively

The drugs with identified efficacy were applied in combination with Imatinib to both sensitive SUP-B15 and resistant SUP-B15/R cells. This allowed for the testing of the impact of repositioned drugs on the effectiveness of Imatinib. Experimental groups for determining the anti-proliferative effect were established as follows: control; Imatinib alone; drug alone; Imatinib and drug combination. During these combination treatments, the concentration of Imatinib was kept constant at IC20, while the identified drugs were applied in escalating doses. According to the results of the MTT assay applied to SUP-B15 and SUP-B15/R cells for the combination of Desipramine and Imatinib, the IC50 value of the drug Desipramine on SUP-B15 cells, which is 22.04 μM, was determined to be 15.41 μM when combined with IC20 Imatinib. Additionally, the IC50 dose of Desipramine on SUP-B15/R is quite similar to that on SUP-B15 cells (Figure 19).

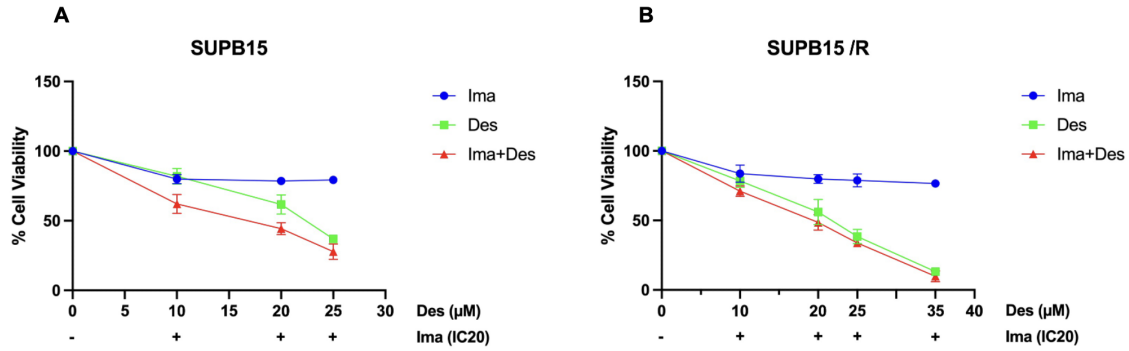

Figure 19. Determination of the viability of SUP-B15 (A) and SUP-B15/R (B) cells treated with Imatinib (IC20), Desipramine, and Imatinib (IC20) plus Desipramine combination. All treatments were carried out for 72 hours, and viability analysis was conducted using the MTT test. The experiments were repeated three times. Error bars indicate standard deviation.

Furthermore, in the investigation conducted using the Compusyn system to determine potential synergistic, additive, or antagonist relationships between the drugs, a synergistic effect was observed in combination doses of Desipramine at 10µM, 20µM, and 25µM with Imatinib in parental SUP-B15 cells. However, it was determined that only the dose of Desipramine at 35µM shows a synergistic relationship with Imatinib in SUP-B15/R cells. (Figure 19)

Moreover, for another Ph (+) ALL drug, Glipizide, a combination experiment was set up on both parental SUP-B15 and Imatinib-resistant SUP-B15/R cells. While keeping Imatinib at a constant IC20 dose, Glipizide was administered in increasing doses. In light of the MTT assay results conducted on SUP-B15 and SUP-B15/R cells to assess the combination of Glipizide and Imatinib, the IC50 value of Glipizide for SUP-B15 cells, which is 68.02 µM, determined to be 53 µM when combined with IC20 Imatinib. Additionally, the IC50 dose of Glipizide on SUP-B15/R which is 116.93 µM, was determined to be 56.17 µM when combined with IC20 Imatinib. Moreover, the inquiry utilizing the Compusyn system to discern potential synergistic, additive, or antagonistic interactions among the drugs revealed a synergistic effect at combination doses of Glipizide at 10 µM, 25 µM,50 µM and 80 µM with Imatinib in parental SUP-B15 cells. Moreover, the synergistic effect at combination doses of Glipizide at 10 µM, 50 µM, 80 µM and 100 µM with Imatinib in SUP-B15/R cells.

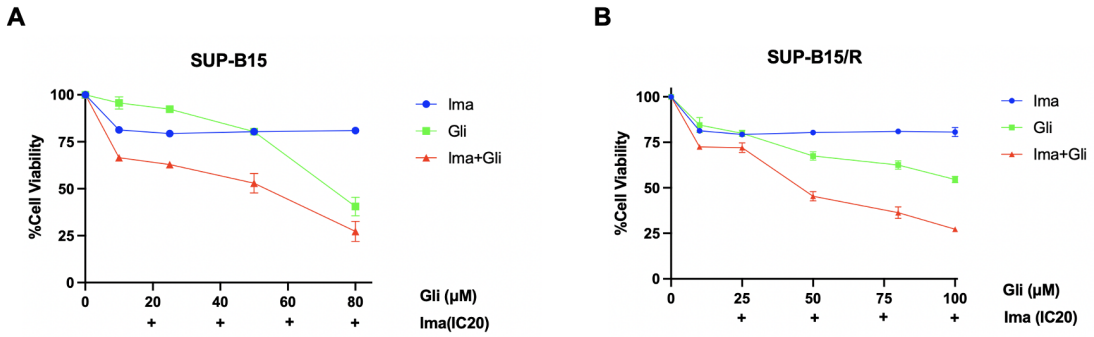

Figure 20. Determination of the viability of SUP-B15 (A) and SUP-B15/R (B) cells treated with Imatinib (IC20), Glipizide and Imatinib (IC20) plus Glipizide combination. All treatments were carried out for 72 hours, and viability analysis was conducted using the MTT test. The experiments were repeated three times. Error bars indicate standard deviation.

3.4.3. Findings from Trypan Blue Staining at the Selected Synergistic Doses on Ph(+) ALL Cells

The cytotoxic impacts of synergic drug doses of Imatinib, Desipramine and Glipizide on SUP-B15 and SUP-B15/R cells were assessed using the trypan blue staining method. Proliferation graphs were constructed based on cell counts performed at 48 and 72 hours using the collected data. As a result of the experiment, the cytotoxic activities of selected combination dose of Desipramine and Imatinib, which were 10 µM, have been determined on SUP-B15 cell line. The statistical analyses performed for both the Desipramine 10µM and the combination group of Desipramine 10µM with Imatinib IC20 revealed a noteworthy and statistically significant difference between these groups at both 48 and 72 hours. Moreover, this significant difference was observed to further intensify at the 72-hour time point. Additionally, when the cell death rates are examined, it has been demonstrated that the combination group of Desipramine 10 µM and IC20 Imatinib dose creates more antiproliferative effect than the sum of these doses in the cell. (Figure 21)

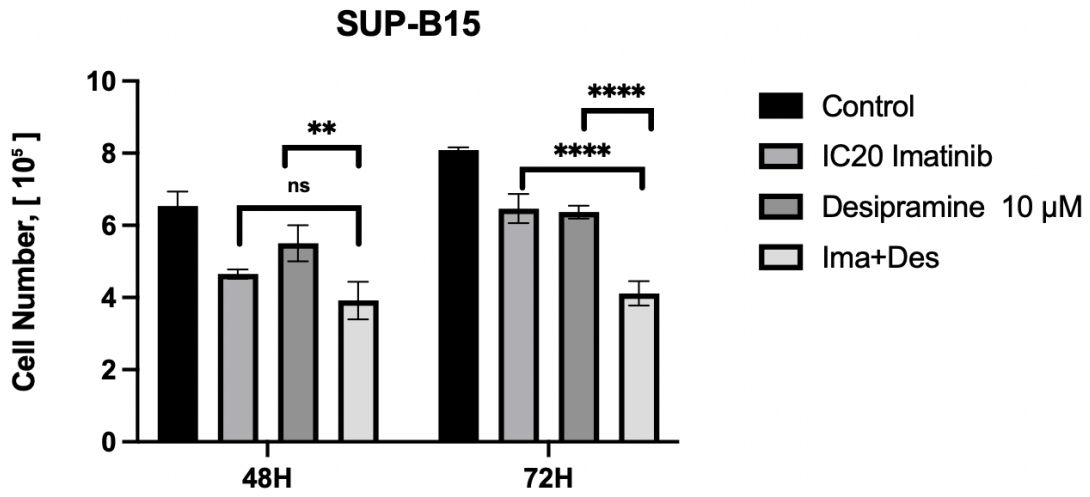

Figure 21. Determination of the cytotoxic effects of IC20 Imatinib, Desipramine 10 µM, and their combinations on SUP-B15 cells based on the trypan blue staining results obtained from the assessment of their anti-proliferative activity. The experiment was repeated three times. Error bars indicate standard deviation.

Furthermore, Glipizide and Imatinib, which were 10 µM and 80 µM, have been confirmed on SUP-B15 cell line. The statistical analyses conducted for the Glipizide 10µM and Glipizide 10µM with Imatinib IC20 combination groups indicated a statistically significant difference between these groups at both 48 and 72 hours. This significant difference further increased at 72 hours (Figure 22).

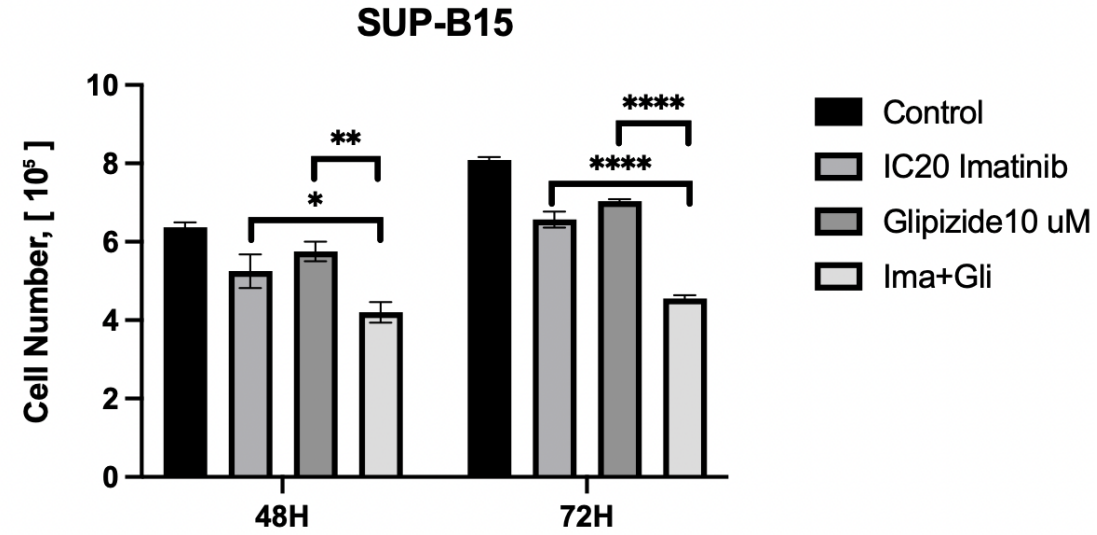

Figure 22. Determination of the cytotoxic effects of IC20 Imatinib, Glipizide 10 µM, and their combinations on SUP-B15 cells based on the trypan blue staining results obtained from the assessment of their anti-proliferative activity. The experiment was repeated three times. Error bars indicate standard deviation.

Additionally, the same analyses were repeated for the Glipizide 80μM and Glipizide 80μM plus Imatinib 20 combination. Accordingly, a statistically significant difference was again found between these groups at both 48 and 72 hours. However, in this case, the significance does not increase over time. (Figure 23)

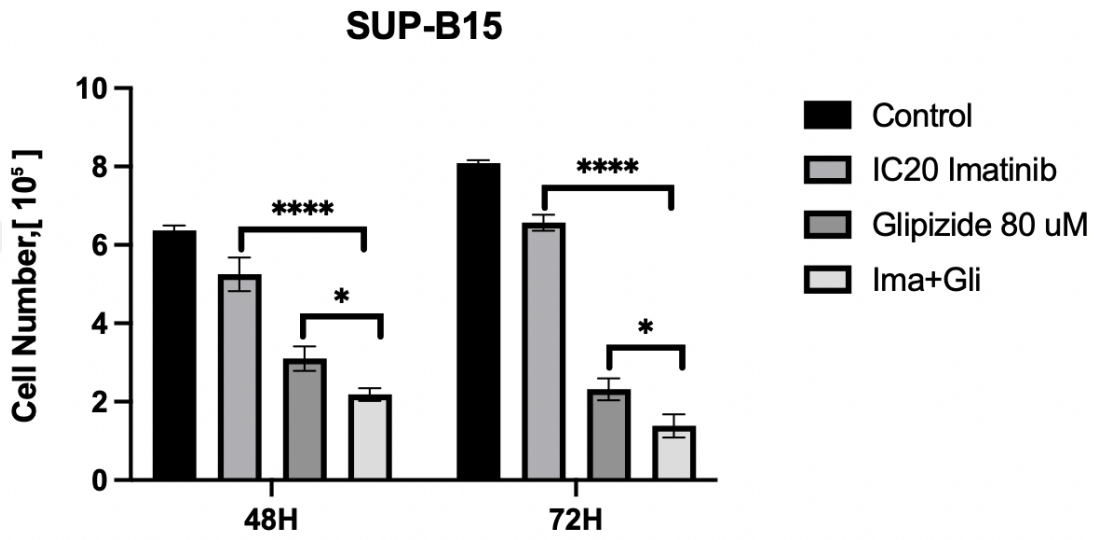

Figure 23. Determination of the cytotoxic effects of IC20 Imatinib, Glipizide 80 μM, and their combinations on SUP-B15 cells based on the trypan blue staining results obtained from the assessment of their anti-proliferative activity. The experiment was repeated three times. Error bars indicate standard deviation.

Furthermore, same combination analyses were conducted on SUP-B15/R cells to understand the cytotoxic activity of synergistic dosages on Imatinib resistance. Following the experiment, the cytotoxic effects of specific combined doses, namely 50 μM, of Glipizide and Imatinib were evaluated on the SUP-B15/R cell line. Statistical analyses conducted on both the Glipizide 50 μM group and the combined Glipizide 50 μM with Imatinib IC10 group demonstrated a significant and notable difference between these sets at the 72-hour mark (Figure 24).

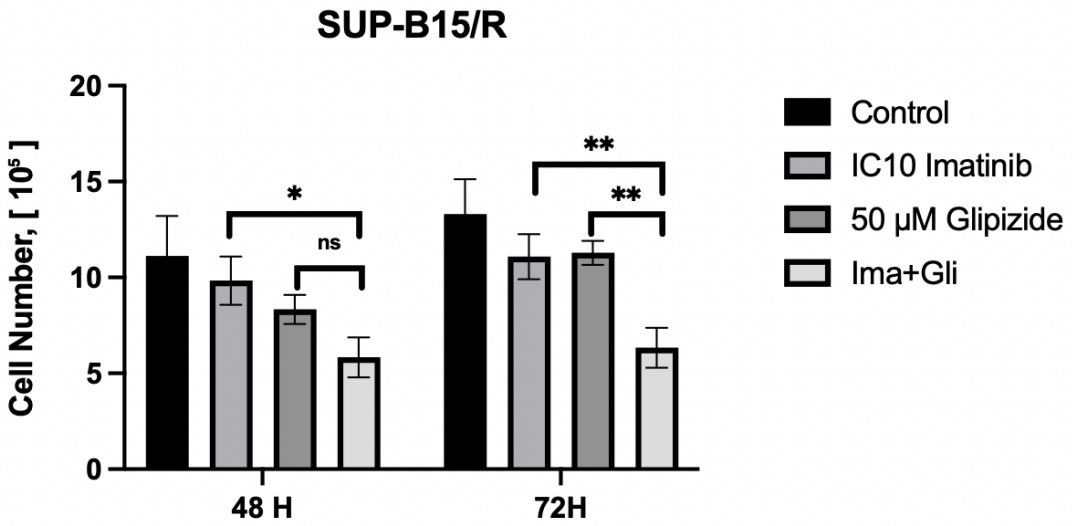

Figure 24. Determination of the cytotoxic effects of IC10 Imatinib, Glipizide 50µM, and their combinations on SUP-B15/R cells based on the trypan blue staining results obtained from the assessment of their anti-proliferative activity. The experiment was repeated three times. Error bars indicate standard deviation.

3.5. Evaluation of Apoptotic Effects of Selected Drugs on ALL Cells.

3.5.1 Determination of Apoptotic Effects of Maytansine and Isoprenaline on Jurkat Cells

The Annexin/PI staining method was employed to determine the apoptotic effects of the selected drugs, Maytansine and Isoprenaline, on Jurkat, a Ph(-) ALL cell line. The experiment lasted a total of 48 hours, and measurements were taken every 24 hours using a flow cytometry device. During the experiment, Jurkat cells were treated with the IC20 and IC50 doses of Maytansine and Isoprenaline separately at the specified time intervals. Based on Annexin/PI staining, the IC20 and IC50 doses of Maytansine and Isoprenaline (Figure 25) have led to progressively increasing apoptosis. Furthermore, these experimental results have substantiated the accuracy of the doses obtained from the MTT assay.

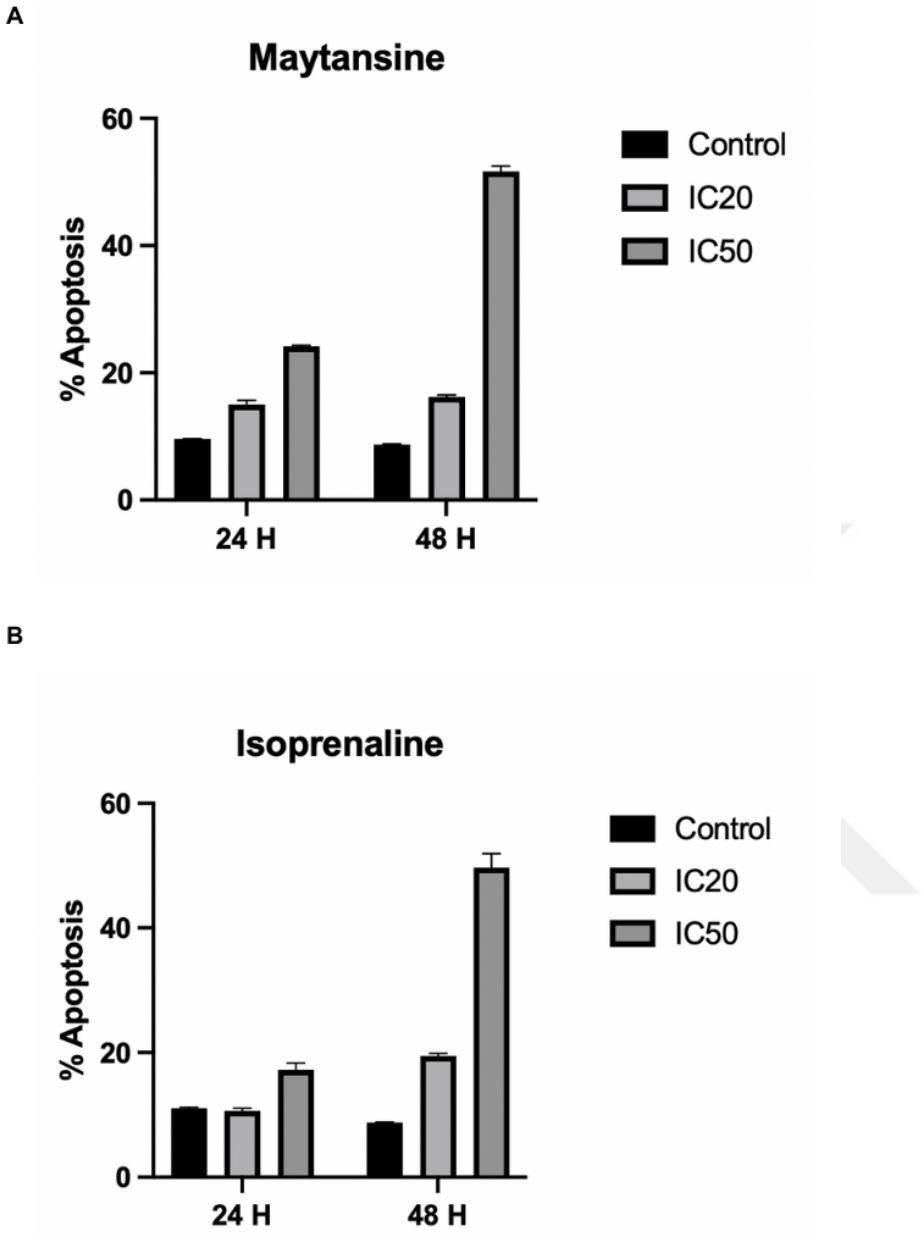

Figure 25. Determination of Apoptotic effects of Maytansine (A) and Isoprenaline (B) on Jurkat cell line based on the Annexin/PI double staining results. The experiment was repeated three times. Error bars indicate standard deviation.

3.5.2. Determination of Apoptotic Effects of Glipizide and Desipramine on SUP-15 and SUP-B15/R cells

The apoptotic effects of combined doses of Imatinib, Glipizide, and Desipramine on SUP-B15 and SUP-B15/R cells were evaluated through Annexin/PI staining. Apoptotic cell graphs were generated to illustrate the apoptotic cell population at both

48 and 72 hours. The experiment confirmed the apoptotic effects of the selected combination doses of Glipizide (10 and 80μM) (Figure 26), Desipramine (10μM) (Figure 27) and Imatinib on the SUP-B15 cell line. For Desipramine the acquired apoptosis level is near synergistic. For Glipizide a higher level of apoptosis has been observed in the synergistic combination doses of the drugs compared to their individual administration.

A

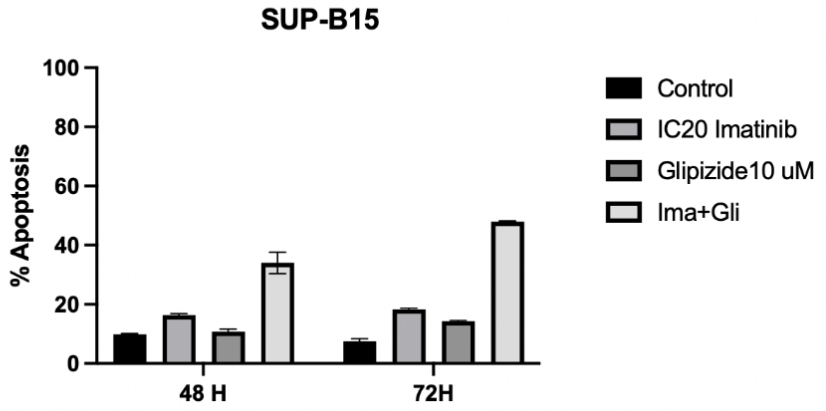

B

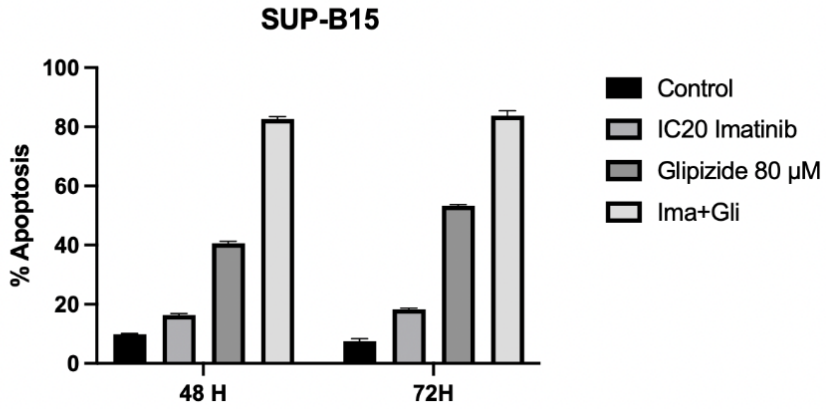

Figure 26. Determination of the Apoptotic effects of IC20 Imatinib, Glipizide 10 μM and their combinations (A) and IC20 Imatinib, Glipizide 80 μM and their combinations (B) on SUP-B15 cells based on the Annexin/PI double staining experiment. The experiment was repeated three times. Error bars indicate standard deviation.

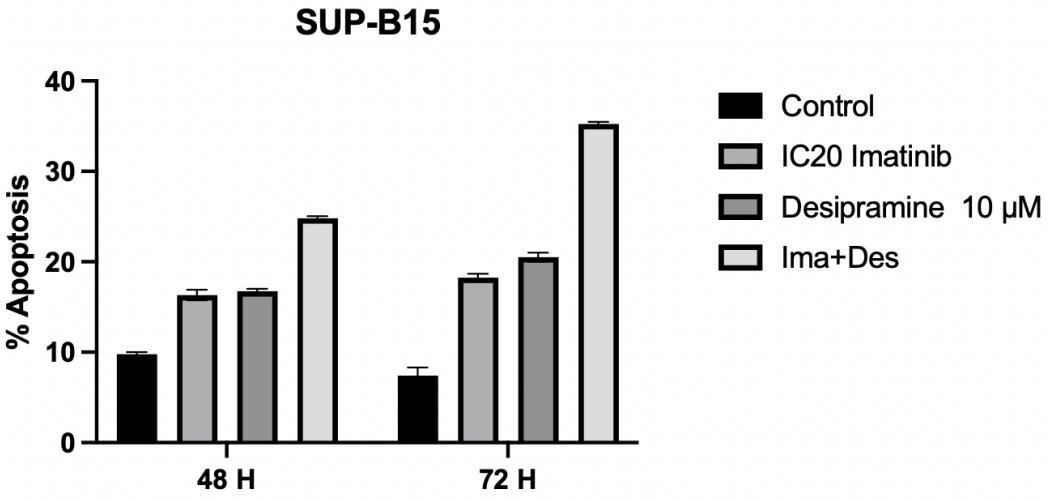

Figure 27. Determination of the Apoptotic effects of IC20 Imatinib, Desipramine 10 µM and their combinations on SUP-B15 cells based on the Annexin/PI double staining experiment. The experiment was repeated three times. Error bars indicate standard deviation.

Furthermore, the same combination experiment was performed for SUP-B15/R cells with the selected doses of Glipizide (50 µM) (Figure 28) and Desipramine (10 µM) (Figure 29) and IC10 Imatinib on the SUP-B15/R cells to understand the combination effects on Imatinib resistance. According to results, synergistic doses of both Glipizide and Desipramine have potentially significant apoptotic effects on Imatinib resistant SUP-B15/R cells.

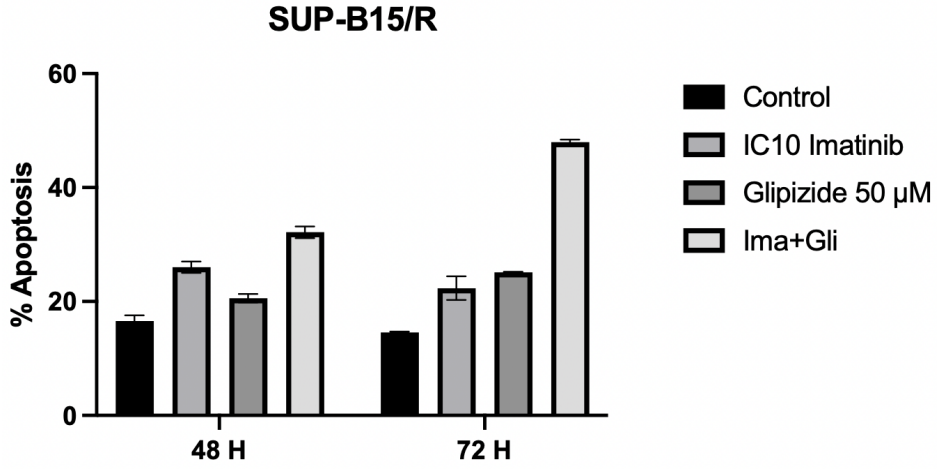

Figure 28. Determination of the Apoptotic effects of IC10 Imatinib, Glipizide 50 µM and their combinations on SUP-B15/R cells based on the Annexin/PI double staining

experiment. The experiment was repeated three times. Error bars indicate standard deviation.

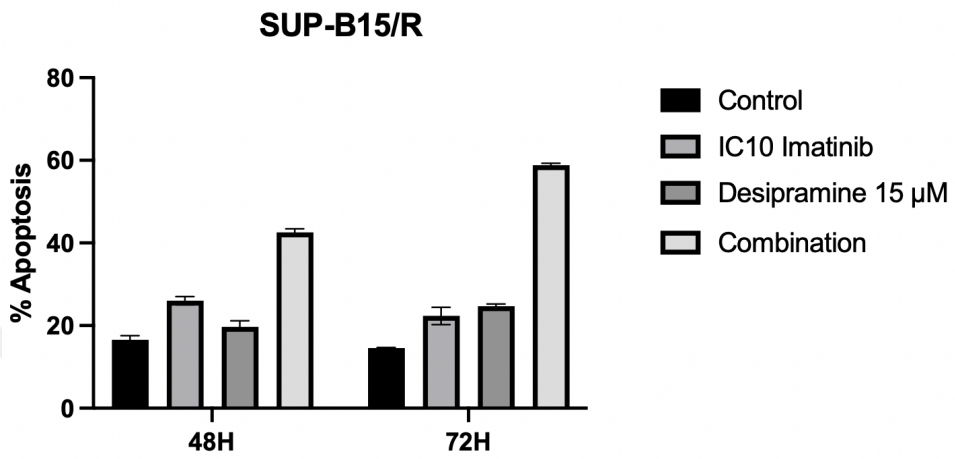

Figure 29. Determination of the Apoptotic effects of IC10 Imatinib, Desipramine 15 µM and their combinations on SUP-B15/R cells based on the Annexin/PI double staining experiment. The experiment was repeated three times. Error bars indicate standard deviation.

3.6. Findings from Trypan Blue Staining at the Selected Drugs on HUVEC Cells

The trypan blue staining method was employed to determine the cytotoxic effects of drugs with identified anti-proliferative activity on Ph (-) ALL and Ph (+) cells. Cell counts were conducted at 48 hours were used to construct a cytotoxic effect graph based on the obtained data.

As a result of this experiment, the cytotoxic effects of Maytansine, Isoprenaline (Figure 30), Glipizide and Desipramine (Figure 31) on HUVEC cell line have been confirmed. According to the results of the experiment, the cytotoxic effects of the drugs on the relevant cell lines and HUVECs were compared. It was concluded that the cytotoxic effect of the drugs on the healthy control HUVEC cell line was lower than that on the relevant cell lines.

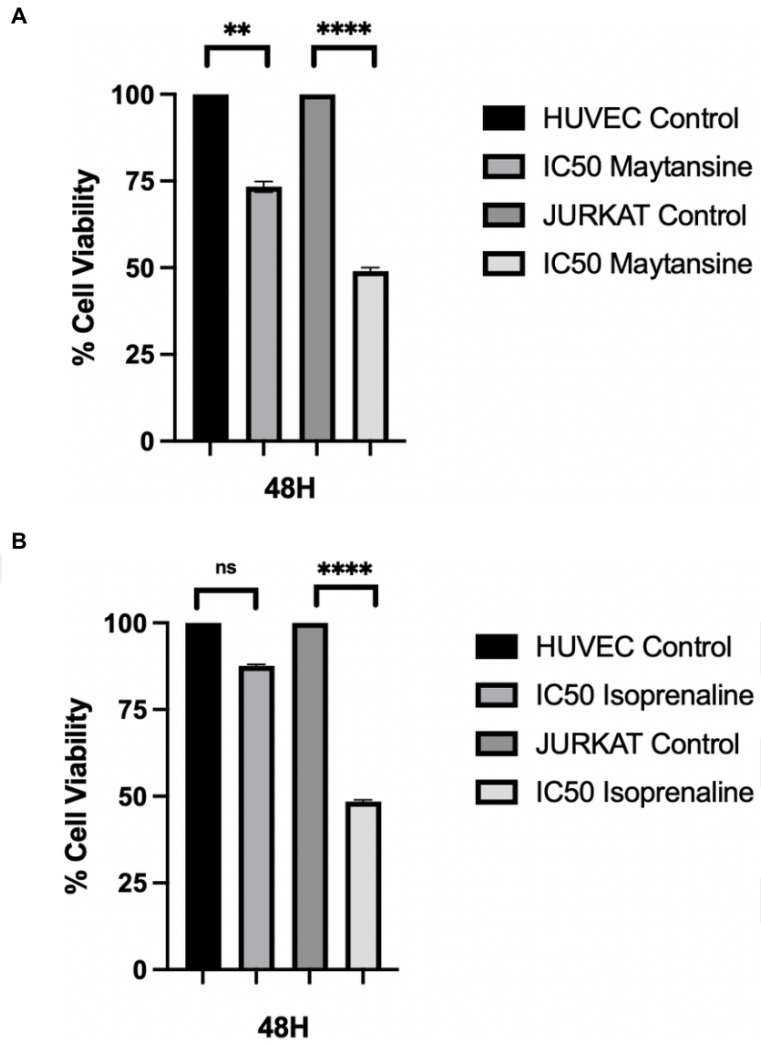

Figure 30. Determination of the cytotoxic effects of Maytansine (A) and Isoprenaline (B) on HUVEC and Jurkat cells based on the trypan blue staining results obtained from the assessment of their anti-proliferative activity. The experiment was repeated three times. Error bars indicate standard deviation.

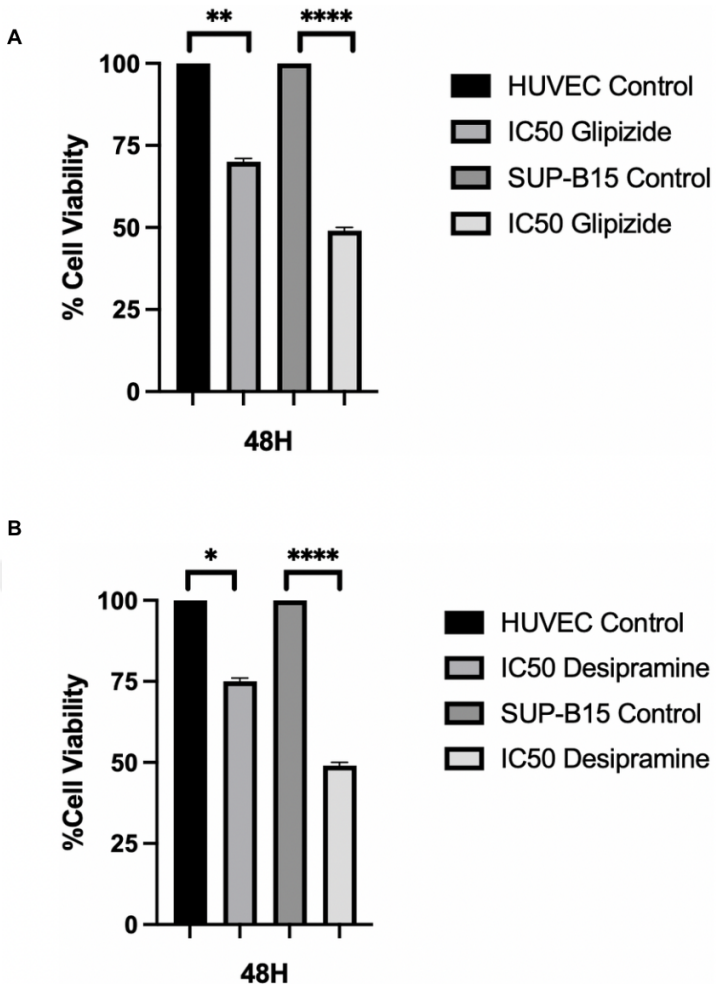

Figure 31. Determination of the cytotoxic effects of Glipizide (A) and Desipramine (B) on HUVEC and SUP-B15 cells based on the trypan blue staining results obtained from the assessment of their anti-proliferative activity. The experiment was repeated three times. Error bars indicate standard deviation.

CHAPTER 4: DISCUSSION

This thesis conducts a thorough comparative evaluation of ALL and Ph (+) ALL at various molecular levels, encompassing transcriptomics, proteomics, and metabolomics. Despite the significant diversity observed in ALL, its origin involves a range of distinct genetic abnormalities. The most prevalent among these is the Ph+ ALL subtype, characterized by the BCR/ABL translocation, which stands out as the most aggressive and high-risk variant within the spectrum of ALL subtypes. Notably, the presence of drug resistance, particularly imatinib resistance, in Ph (+) ALL poses a significant challenge, creating a formidable obstacle in its therapeutic management. In addressing these challenges, this research aims to provide a new avenue for optimism in treating these conditions through the application of drug repositioning. It's worth noting that, to the best of our knowledge, no previous studies have undertaken a comparative transcriptomic analysis between ALL and Ph+ ALL. Furthermore, this study pioneers the use of the robust rank aggregation method to identify DEGs associated with diseases related to ALL. Differentially expressed transcripts associated with diseases were identified through the analysis of 8 ALL and 4 Ph+ ALL datasets. A total of 799 DEGs for ALL and 295 DEGs for Ph+ ALL were found to be statistically significant. Commonly, 154 down-regulated DEGs and 110 up-regulated DEGs were observed in both diseases, with down-regulated genes outnumbering up-regulated genes in ALL diseases. The PPI network of both ALL and Ph+ ALL was reconstructed. Hub proteins were determined based on the union of the top 20 proteins according to degree, indicating the number of interactions of a protein, and betweenness, signifying the number of connections that a protein establishes with other proteins in the shortest path, and were accepted as such. The role of disease-associated genes in various pathways aids in unraveling the molecular mechanisms underlying diseases. In ALL, statistically significant pathways predominantly involve immune-related pathways (such as positive regulation of immune response and regulation of immune effector process) and cell cycle-related pathways (such as cellular response to cytokine stimulus, positive regulation of cell death, and regulation of B cell activation). Additionally, signaling pathways like signaling by Rho GTPases, Miro GTPases, RHOBTB3, and cytokine signaling are present. The development of Ph+ ALL also involves immune response and cellular response pathways, including pathways like

the adaptive immune system and regulation of cell-cell adhesion, which differ from those observed in ALL. Hub proteins in ALL are mainly associated with MAPK family signaling cascades, gastrin signaling pathway, cellular response to oxidative stress, kinase maturation complex 1, NOD-like receptor signaling pathway, etc. Similarly, hub proteins in Ph (+) ALL are primarily enriched in pathways such as DNA damage response, response to growth factor, signaling by receptor tyrosine kinases, FoxO signaling pathway, etc.

The identification of potential drugs for the treatment of ALL and Ph (+) ALL was facilitated using L1000CDS2 and genexpharma tools. Upon examining the drugs identified through these two analyses, 39 and 99 drugs were recommended for ALL, and 40 and 203 drugs were recommended for Ph (+) ALL by L1000CDS2 and genexpharma, respectively. The original indications for in vitro testing of these drugs were then investigated. The consideration included determining whether these drugs were utilized for hematologic cancers or other diseases. Notably, drugs utilized for solid tumors, hematologic cancers, neurodegenerative, and psychiatric diseases emerged as prominent candidates. In the process of determining drugs for in vitro testing, priority was given to selecting drugs not employed as cancer medications and those previously used in treating other human diseases but not tested for ALL or Ph (+) ALL. Subsequently, the decision was made to conduct in vitro testing on 2 drugs which were Maytansine and Isoprenaline for ALL and 2 drugs which were Desipramine and Glipizide for Ph (+) ALL. Maytansine is recognized as a heterocyclic organic compound with the ability to bind to the rhizoxin binding sites of tubulin, thereby impeding the assembly of microtubules, leading to their disassembly and subsequent inhibition of cell division (mitosis). Additionally, its cytotoxic properties have been observed against various cancer cell lines, effectively hindering the growth and proliferation of cancer in vivo. However, during human clinical trials for cancer treatment, Maytansine exhibited a limited therapeutic window due to its toxic side effects on the gastrointestinal tract and nervous system(Zafar et al., 2023). To address this challenge, an antibody-drug conjugate has been formulated, aiming to enhance Maytansine's therapeutic potential while minimizing its toxic side effects through selective targeting and destruction of cancer cells. In this targeted delivery approach, Maytansine, serving as a cytotoxic payload, is attached to an antibody with specificity for a particular cancer cell antigen, connected by a chemical linker molecule. Upon

binding to its specific receptor, the conjugate enters the cell via endocytosis, where the Maytansine payload is cleaved from the antibody, and the free Maytansine alters the microtubule dynamics(Bauzon et al., 2019). Beyond its cytotoxic effects in cancer cells, Maytansine sourced from plants and microbes also exhibits antimicrobial properties(Newman and Cragg, 2020). In the scope of this thesis, Maytansine targets the HSP90AA1 hub protein, which was found to be overexpressed in ALL compared to healthy samples. HSP90 is likely the most well recognized group of heat shock proteins implicated into leukemia types(Cabaud-Gibouin et al., 2023). To this end, despite its toxic side effects, through the application of recently developed techniques, the prospect for utilizing Maytansine as a therapeutic agent in ALL appears promising. The second drug for ALL was Isoprenaline. Isoprenaline, a β-agonist, is employed to induce cardiomyopathy, a condition that can be mitigated by reducing the expression of proinflammatory cytokines (IL-6, IL-10, and TNFα) and apoptotic markers (caspase-3 and Bax), while increasing the levels of the anti-apoptotic protein Bcl2. Phenylephrine and clonidine are recognized as α1 and α2 adrenergic receptor agonists with known effects on blood pressure, leading to an increase or decrease, respectively(Uchida et al., 2019). However, a recent investigation reported that Isoprenaline induced the secretion of vascular endothelial growth factor (VEGF) in gastric cancer cells. These results imply that isoprenaline induces the secretion of VEGF, leading to the subsequent upregulation of plexin-A1 and VEGFR2 expression in gastric cancer cells. This positive impact contributes to the promotion of tumor angiogenesis (Lu et al., 2017). In the context of this research, Isoprenaline focuses on the elevated hub protein PIK3R1 in ALL compared to healthy samples.PIK3R1 is responsible for producing the p85 regulatory protein in the PI3K/AKT pathway, a crucial pathway for cellular migration, proliferation and apoptosis(Bhattacharya et al., 2023). In light of this, although Isoprenaline targets the hub protein mentioned in the study, the findings highlighted in the gastric cancer research (Lu et al., 2017) cast a shadow on the potential utility of Isoprenaline, particularly in metastatic ALL. As a result of the repurposing study conducted for ALL, these two drugs (Maytansine and Isoprenaline) obtained were used in in vitro experiments. MTT tests, Trypan blue staining for determining cytotoxicity, and Annexin/PI staining applications for identifying apoptotic cells were performed on Ph (-) ALL cells, specifically Jurkat cells. After analyzing the MTT results for selected drugs, including Doxorubicin

hydrochloride as a positive control, it was observed that the Jurkat cell line demonstrates significantly higher sensitivity to Maytansine. This effect was further confirmed through trypan blue staining. Finally, Annexin/PI staining conducted to observe apoptotic effects indicated that the IC20 and IC50 doses determined by MTT for the drugs yielded results consistent with both MTT and trypan blue staining in Jurkat cells. Considering the wet lab experiments conducted, among the identified drugs for ALL, Maytansine stands out due to both its demonstrated cytotoxic effect and the potential for in vivo testing facilitated by newly developed techniques. However, this doesn't necessarily imply that the potential use of Isoprenaline cannot be realized. With appropriate patient selection and metastasis examination, it is believed that Isoprenaline could also be effective in the context of ALL. Furthermore, For Ph (+) ALL Desipramine and Glipizide were determined for further in vitro analysis. Desipramine, an antidepressant medication, is clinically utilized as a supplementary treatment for cancer patients. A pathological examination revealed its ability to inhibit the proliferation of HCC Hep3B cells through the induction of apoptosis, activation of MAPK signaling, and elevation of intracellular Ca2+ levels(Yang and Kim, 2017). Additionally, desipramine induced autophagy in glioma cells through PI3K-Akt-mTOR(Ma et al., 2013). Depending on the type of human colon carcinoma cell, desipramine induced cell death and apoptosis through both the mitochondrial and non-mitochondrial(Arimochi and Morita, 2008). Furthermore, it triggered apoptosis in human prostate cancer PC3 cells by activating the JNK kinase and caspase-3 pathways and increasing Ca2+ concentration(Chang et al., 2008). Evidence also suggests that desipramine augmented apoptosis induced by TRAIL, in lung cancer cells by upregulating TRAIL receptor-2 expression and inhibiting autophagic flux(Song et al., 2022). In this thesis, Desipramine targets the KRAS hub protein for Ph+ ALL. KRAS is a protein, which is a part of the RAS/MAPK pathway and intriguingly, the effects of Desipramine on MAPK signaling were previously determined, enforcing our hypothesis of Desipramine as a KRAS inhibitor. As seen in the literature, the use of desipramine as an anticancer agent is established on various cancer cell lines; however, this effect has not been previously observed in Ph(+) ALL. Therefore, testing this drug on Ph (+) ALL cells, as obtained from bioinformatic analyses, has not only contributed to the literature but also revealed the potential use of desipramine as a therapeutic agent for Ph(+) ALL. The second drug for Ph (+) ALL

was Glipizide. Glipizide, developed in the 1950s as a second-generation oral hypoglycemic drug for treating type II diabetes, stands out for its ability to selectively stimulate insulin secretion from β-cells. Recent investigations have unveiled an intriguing connection between diabetes and an elevated risk of various types of tumors. Notably, epidemiological studies have suggested that the prolonged use of certain anti-diabetic medications, including glipizide, might mitigate the risk of cancer development (Qi et al., 2014). A recent investigation discovered that glipizide has the potential to trigger TRAIL-mediated apoptotic cell death in human lung adenocarcinoma cells. Pretreatment with glipizide resulted in decreased levels of p-Akt and p-mTOR at various concentrations. Glipizide treatment also significantly reduced p62 expression levels in a dose-dependent manner. These observations suggest that glipizide induces autophagy flux in human lung cancer cells. Consequently, these findings propose that glipizide, by inhibiting Akt/mTOR, enhances TRAIL-induced tumor cell death through the activation of autophagy flux. Moreover, it suggests that glipizide might serve as a potential combined therapeutic target with TRAIL protein, especially in TRAIL-resistant cancer cells (Nazim et al., 2017). In the scope of this study, Glipizide targets CDKN2A and GRB10 hub proteins in Ph+ ALL. CDKN2A is already a crucial protein in Ph (+) ALL. To this end, targeting this hub gene with Glipizide can have significant potential to be used as an anticancer agent for ALL. Furthermore, the other hub gene targeted by Glipizide was GRB10, particularly noteworthy is that Glipizide, which has known effects on m/TOR signaling, further supports our hypothesis of its role as a GRB10 inhibitor, given its involvement in the mTOR pathway. As evident from the provided examples in the articles, the utilization of Glipizide as an anticancer agent has been proposed before. However, there is no existing research of this nature for Ph (+) ALL, similar to Desipramine. After the repurposing studies for Ph (+) ALL, the identified drugs (Desipramine and Glipizide) were employed in in vitro experiments. MTT tests, Trypan blue staining to determine cytotoxicity, and Annexin/PI staining applications to identify apoptotic cells were conducted on Ph (+) ALL cells, specifically SUP-B15 cells. Additionally, the drugs were tested on Imatinib-resistant SUP-B15 cells to observe their impact on a significant issue for Ph (+) ALL, which is Imatinib resistance. In line with this goal, Imatinib resistance was initially developed in parental SUP-B15 cells. To assess the developed resistance, MTT assay, growth curve analysis,

and Annexin/PI staining were employed. As depicted in Figure 10, the IC50 value of resistant cells is significantly higher compared to parental cells. Furthermore, the growth curve analysis (Figure 11) revealed that the drug-treated SUP-B15 cells exhibited much lower proliferation than drug-treated SUP-B15/R cells. Additionally, this growth curve analysis showed a relatively modest growth rate difference between the untreated control and SUP-B15/R cells. This observation was also evident in the Annexin/PI staining, where this difference decreased to a minimum with increasing hours. It is speculated that the disparity in growth rates may be attributed to the differences in passage numbers. In conclusion, these tests provide evidence that parental cells demonstrate resistance to Imatinib. Afterward, among the two drugs tested in both SUP-B15 and SUP-B15/R cell lines, Desipramine exhibited a higher antiproliferative effect at lower doses compared to Glipizide. However, the antiproliferative effect of Dasatinib used as a positive control, was higher at low doses than both selected drugs. Another crucial point is the observed cross-resistance phenomenon in the Imatinib-resistant SUP-B15/R cell line. The IC50 values demonstrated by Glipizide in SUP-B15 and SUP-B15/R are strikingly different from each other (Figure 17). When examining the IC50 values between Imatinib-resistant SUP-B15/R and Imatinib-sensitive SUP-B15, it becomes apparent that the IC50 value in the resistant group is roughly 2 times greater than that of the drug-sensitive group. This finding unequivocally suggests that the development of Imatinib resistance has resulted in an approximately 2 -fold reduction in the anti-proliferative impact of Glipizide. In simpler terms, cells exhibiting resistance to Imatinib have concurrently acquired resistance to the drug Glipizide. However, such an effect has not been observed with Desipramine. Moreover, the drugs were tested on both SUP-B15 and Imatinib-resistant SUP-B15/R cells to determine the combined effect they would exhibit when administered in conjunction with Imatinib. In the combination experiments conducted, the goal was to identify doses of Desipramine and Glipizide that synergistically work with Imatinib in both SUP-B15 and SUP-B15/R cells. According to the experiment results, doses were discovered where both Desipramine and Glipizide synergistically work with Imatinib. Subsequently, to validate these doses, trypan blue experiments were conducted, growth curves were created, and thus, synergistic cytotoxic effects were demonstrated. Finally, Annexin/PI staining was performed for the selected synergistic doses, comparing the effects of individual and

combined drugs on apoptotic cells. The results obtained from all these experiments showed that the combination of 10 μM Desipramine with IC20 Imatinib increased cytotoxic effects and apoptotic cells in SUP-B15 cells. Furthermore, combination of 10 μM and 80 μM of Glipizide with IC20 Imatinib showed same effects on SUP-B15 cells. Moreover, same experiments were conducted to SUP-B15/R to evaluate the effects of the synergistic dosages on Imatinib resistance. According to results, combination of 15 uM Desipramine with IC10 Imatinib increased cytotoxic effects and apoptotic cells. Also, combination of 50 μM of Glipizide and IC10 Imatinib showed the same effect on SUP-B15/R cells. Experimental results show that the combination of these drugs can achieve promising results on both non-resistant and Imatinib resistant cells in the clinic. Furthermore, all of the selected drugs were tested on healthy cell line, which was HUVEC, to evaluate their cytotoxic effects on non-cancerous cells. The results were showed that all drugs have significantly lower cytotoxic effects on HUVEC compared to relative cell lines (Figure 30 and Figure 31). This suggests that the drugs could be safe for use in clinics, as they are not as likely to damage healthy cells. In this respect, the repurposing of all selected drugs in the clinic may be promising.

CHAPTER 5: CONCLUSION

This thesis can be fundamentally divided into two separate components: the first involves computational studies, while the second entails laboratory experiments conducted to determine the effects of the drugs obtained from these studies.

In the first part, datasets for both ALL and Ph (+) were obtained using the GEO database. Subsequently, these datasets were analyzed for differential expression levels using the Limma package, revealing 799 diseases related DEGs for ALL and 295 for Ph+ ALL. BioGRID database was then utilized to establish protein-protein interactions among these DEGs. Cytoscape software, along with the CytoHubba plug-in, was employed to visualize PPI networks and compute local and global topological features such as degree and betweenness. This analysis identified 24 hub proteins for ALL and 33 for Ph (+) ALL. To elucidate the functional roles of the identified DEGs, functional enrichment analysis was conducted using the Metascape tool. According to this analysis, hub proteins of ALL were primarily involved in MAPK family signaling cascades, gastrin signaling pathway, cellular response to oxidative stress, kinase maturation complex 1, and NOD-like receptor signaling pathway. Additionally, for Ph+ ALL, the enriched pathways included DNA damage response, response to growth factor, signaling by receptor tyrosine kinases, and FoxO signaling pathway.

The final step of this part involved drug repurposing using The L1000CDS2 platform and genexpharma tool. The study revealed that, out of the 24 core proteins identified for ALL, 13 formed a network with a total of 123 interactions involving 99 drugs. Moreover, in the case of Ph+ ALL, 19 out of 33 core proteins constituted a network with a total of 289 interactions involving 203 drugs. As a result, considering various criteria, the drugs named for Maytansine and Isoprenaline for ALL and Desipramine and Glipizide for Ph (+) ALL, were determined, which will move to the second stage in this thesis.

In the second part of the thesis, the drugs identified in the first part were tested for their cytotoxic and apoptotic effects on relevant cells. For this purpose, the cytotoxic effects of Maytansine and Isoprenaline were initially determined using MTT and trypan blue staining methods, and both drugs showed cytotoxic effects on Jurkat cell line. Additionally, the apoptotic effect of the drugs was assessed using the Annexin/PI double staining method, and it was observed that the drugs induced apoptotic effects

in Jurkat cell line. The drugs identified for Ph (+) ALL, Glipizide and Desipramine, were tested on both parental SUP-B15 and Imatinib-resistant SUP-B15/R cells to observe their effects on Imatinib-resistant cells. For this purpose, an Imatinib-resistant cell line was developed, and the resistance was confirmed through both MTT tests and trypan blue staining methods. Furthermore, to confirm the developed resistance, the apoptotic cell ratio was determined by adding Imatinib treatment at the determined IC50 dose to both parental SUP-B15 and Imatinib-resistant SUP-B15/R cells, using Annexin/PI staining. The results of this experiment confirm the developed Imatinib resistance. Afterward, the cytotoxic effects of Desipramine and Glipizide were tested on both SUP-B15 and SUP-B15/R cells using the MTT test, and IC50, IC20, and IC10 doses were determined. Subsequently, the apoptotic effects of the selected drugs were also confirmed using the Annexin/PI test. Finally, to observe the combined effects of the identified drugs in combination with Imatinib on SUP-B15 and SUP-B15/R cells, drugs were administered to cells in combination with the IC20 Imatinib dose for SUP-B15, IC10 Imatinib dose for SUP-B15/R . The MTT assay was again used for cytotoxic effects. The results obtained from the tests were examined using the CompuSyn program to determine the synergistic, additive, or antagonistic relationships between the drugs. Then, growth curves were obtained using the trypan blue method to determine the cytotoxic effects of the identified synergistic doses. Additionally, the apoptotic effects of these selected synergistic doses were determined using Annexin/PI. Furthermore, HUVEC cells were included in the study as a healthy control to evaluate cytotoxic effects of the selected drugs. Results indicate that, Maytansine, Isoprenaline, Glipizide and Desipramine showed lower cytotoxic activity on healthy cells compared to relevant cell lines.

In conclusion, based on both computational results and the anti-proliferative effects in cell lines, this thesis suggests that Maytansine and Isoprenaline could be potential to repositioned for ALL treatment. For Ph (+) ALL, considering the anti-proliferative effects in parental SUP-B15 cells, as well as the synergistic doses identified to work in combination with Imatinib, Glipizide, and Desipramine, it is believed that the repositioning of both drugs could have a positive impact on ALL treatment. Moreover, using both Desipramine and Glipizide in Imatinib resistant SUP-B15/R cell line is promising due to the synergistic effects they exhibited.

REFERENCES

Abou Dalle, I., Jabbour, E., Short, N. J., and Ravandi, F. (2019). *Treatment of Philadelphia Chromosome-Positive Acute Lymphoblastic Leukemia.* Current Treatment Options in Oncology, Vol. 20(1), pp. 4.

Arimochi, H., and Morita, K. (2008). *Desipramine induces apoptotic cell death through nonmitochondrial and mitochondrial pathways in different types of human colon carcinoma cells.* Pharmacology, Vol. 81(2), pp.164–172.

Azuaje, F. (2013). *Drug interaction networks: an introduction to translational and clinical applications.* Cardiovascular Research, Vol. 97(4), pp. 631–641.

Bardelli, V., Arniani, S., Pierini, V., Di Giacomo, D., Pierini, T., Gorello, P., Mecucci, C., and La Starza, R. (2021). *T-Cell Acute Lymphoblastic Leukemia: Biomarkers and Their Clinical Usefulness.* Genes, Vol. 12(8), pp.1118.

Bauzon, M., Drake, P. M., Barfield, R. M., Cornali, B. M., Rupniewski, I., and Rabuka, D. (2019*). Maytansine-bearing antibody-drug conjugates induce in vitro hallmarks of immunogenic cell death selectively in antigen-positive target cells.* Oncoimmunology, Vol. 8(4), pp. e1565859.

Belver, L., and Ferrando, A. (2016). *The genetics and mechanisms of T cell acute lymphoblastic leukaemia.* Nature Reviews. Cancer, Vol. 16(8), pp. 494–507.

Bhattacharya, S., Basu, S., Sheng, E., Murphy, C., Wei, J., Kersh, A. E., Nelson, C. A., Bryer, J. S., Ashchyan, H. A., Steele, K., Forrestel, A., Seykora, J. T., Micheletti, R. G., James, W. D., Rosenbach, M., and Leung, T. H. (2023). *Identification of a neutrophil specific PIK3R1 mutation facilitates targeted treatment in a patient with Sweet syndrome.* The Journal of Clinical Investigation, Vol. 133(1), pp. e162137.

Bolstad, B. M., Irizarry, R. A., Astrand, M., and Speed, T. P. (2003). *A comparison of normalization methods for high density oligonucleotide array data based on variance and bias.* Bioinformatics , Vol. 19(2), pp.185–193.

Bonnet, R., Nebout, M., Brousse, C., Reinier, F., Imbert, V., Rohrlich, P. S., and Peyron, J.-F. (2020). *New Drug Repositioning Candidates for T-ALL Identified Via Human/Murine Gene Signature Comparison.* Frontiers in Oncology, Vol. 10, pp.

557643.

Cabaud-Gibouin, V., Durand, M., Quéré, R., Girodon, F., Garrido, C., and Jego, G. (2023). *Heat-Shock Proteins in Leukemia and Lymphoma: Multitargets for Innovative Therapeutic Approaches.* Cancers, Vol. 15(3), pp.984.

Campillos, M., Kuhn, M., Gavin, A.-C., Jensen, L. J., and Bork, P. (2008). *Drug target identification using side-effect similarity.* Science, Vol. 321(5886), pp. 263–266.

Chang, H.-C., Huang, C.-C., Huang, C.-J., Cheng, J.-S., Liu, S.-I., Tsai, J.-Y., Chang, H.-T., Huang, J.-K., Chou, C.-T., and Jan, C.-R. (2008). *Desipramine-induced apoptosis in human PC3 prostate cancer cells: activation of JNK kinase and caspase-3 pathways and a protective role of [Ca2+] elevation.* Toxicology, Vol. 250(1), pp. 9–14.

Chatr-Aryamontri, A., Oughtred, R., Boucher, L., Rust, J., Chang, C., Kolas, N. K., O'Donnell, L., Oster, S., Theesfeld, C., Sellam, A., Stark, C., Breitkreutz, B.-J., Dolinski, K., and Tyers, M. (2017). *The BioGRID interaction database: 2017 update.* Nucleic Acids Research, Vol. 45(1), pp. 369–379.

Chiew, G. G. Y., Fu, A., Perng Low, K., and Qian Luo, K. (2015). *Physical supports from liver cancer cells are essential for differentiation and remodeling of endothelial cells in a HepG2-HUVEC co-culture model.* Scientific Reports, Vol. 5, pp. 10801.

Chin, C.-H., Chen, S.-H., Wu, H.-H., Ho, C.-W., Ko, M.-T., and Lin, C.-Y. (2014). cytoHubba: *Identifying hub objects and sub-networks from complex interactome. BMC Systems Biology,* Vol. 8, pp.11.

Clark, N. R., Hu, K. S., Feldmann, A. S., Kou, Y., Chen, E. Y., Duan, Q., and Ma'ayan, A. (2014). *The characteristic direction: a geometrical approach to identify differentially expressed genes*. BMC Bioinformatics, Vol.15, pp. 79.

Cline, M. S., Smoot, M., Cerami, E., Kuchinsky, A., Landys, N., Workman, C., Christmas, R., Avila-Campilo, I., Creech, M., Gross, B., Hanspers, K., Isserlin, R., Kelley, R., Killcoyne, S., Lotia, S., Maere, S., Morris, J., Ono, K., Pavlovic, V., … Bader, G. D. (2007). *Integration of biological networks and gene expression data using Cytoscape.* Nature Protocols, Vol. 2(10), pp. 2366–2382.

Davis, S., and Meltzer, P. S. (2007*). GEOquery: a bridge between the Gene Expression Omnibus (GEO) and BioConductor.* Bioinformatics, Vol. 23(14), pp. 1846–1847.

DeAngelo, D. J., Jabbour, E., and Advani, A. (2020). *Recent Advances in Managing Acute Lymphoblastic Leukemia. American Society of Clinical Oncology Educational Book.* American Society of Clinical Oncology. Annual Meeting, Vol. 40, pp. 330–342.

Duan, Q., Reid, S. P., Clark, N. R., Wang, Z., Fernandez, N. F., Rouillard, A. D., Readhead, B., Tritsch, S. R., Hodos, R., Hafner, M., Niepel, M., Sorger, P. K., Dudley, J. T., Bavari, S., Panchal, R. G., and Ma'ayan, A. (2016). *L1000CDS2: LINCS L1000 characteristic direction signatures search engine.* NPJ Systems Biology and Applications, Vol. 2, pp. 16015-16018.

Edgar, R., Domrachev, M., and Lash, A. E. (2002). *Gene Expression Omnibus: NCBI gene expression and hybridization array data repository.* Nucleic Acids Research, Vol. 30(1), pp. 207–210.

Eiring, A. M., and Deininger, M. W. (2014). *Individualizing kinase-targeted cancer therapy: the paradigm of chronic myeloid leukemia.* Genome Biology, Vol. 15(9), pp. 461.

Faderl, S., O'Brien, S., Pui, C.-H., Stock, W., Wetzler, M., Hoelzer, D., and Kantarjian, H. M. (2010). *Adult acute lymphoblastic leukemia: concepts and strategies.* Cancer, Vol. 116(5), pp. 1165–1176.

Faratian, D., Clyde, R. G., Crawford, J. W., and Harrison, D. J. (2009). *Systems pathology-taking molecular pathology into a new dimension.* Nature Reviews. Clinical Oncology, Vol. 6(8), pp. 455–464.

Fiscon, G., Conte, F., Farina, L., and Paci, P. (2018). *Network-Based Approaches to Explore Complex Biological Systems towards Network Medicine.* Genes, Vol. 9(9), pp. 437.

Forghieri, F., Luppi, M., and Potenza, L. (2015). *Philadelphia chromosome-positive Acute Lymphoblastic Leukemia.* Hematology, Vol. 20(10), pp. 618–619.

Franquiz, M. J., and Short, N. J. (2020). *Blinatumomab for the Treatment of Adult B-*

Cell Acute Lymphoblastic Leukemia: Toward a New Era of Targeted Immunotherapy. Biologics: Targets & Therapy, Vol. 14, pp. 23–34.

Fu, C., Jin, G., Gao, J., Zhu, R., Ballesteros-Villagrana, E., and Wong, S. T. C. (2013). *DrugMap Central: an on-line query and visualization tool to facilitate drug repositioning studies.* Bioinformatics, Vol. 29(14), pp. 1834–1836.

Gentleman, R. C., Carey, V. J., Bates, D. M., Bolstad, B., Dettling, M., Dudoit, S., Ellis, B., Gautier, L., Ge, Y., Gentry, J., Hornik, K., Hothorn, T., Huber, W., Iacus, S., Irizarry, R., Leisch, F., Li, C., Maechler, M., Rossini, A. J., Zhang, J. (2004). *Bioconductor: open software development for computational biology and bioinformatics.* Genome Biology, Vol. 5(10), pp. 80.

Ghazavi, F., Lammens, T., Van Roy, N., Poppe, B., Speleman, F., Benoit, Y., Van Vlierberghe, P., and De Moerloose, B. (2015). *Molecular basis and clinical*

significance of genetic aberrations in B-cell precursor acute lymphoblastic leukemia. Experimental Hematology, Vol.43(8), pp. 640–653.

Gökbuget, N., and Hoelzer, D. (2006). *Treatment of adult acute lymphoblastic leukemia. Hematology / the Education Program of the American Society of Hematology.* American Society of Hematology. Education Program, pp.133–141.

Groeneveld-Krentz, S., Schroeder, M. P., Reiter, M., Pogodzinski, M. J., Pimentel-Gutiérrez, H. J., Vagkopoulou, R., Hof, J., Chen-Santel, C., Nebral, K., Bradtke, J., Türkmen, S., Baldus, C. D., Gattenlöhner, S., Haas, O. A., von Stackelberg, A., Karawajew, L., Eckert, C., and Kirschner-Schwabe, R. (2019). *Aneuploidy in children with relapsed B-cell precursor acute lymphoblastic leukaemia: clinical importance of detecting a hypodiploid origin of relapse.* British Journal of Haematology, Vol. 185(2), pp. 266–283.

Guerini, A. E., Triggiani, L., Maddalo, M., Bonù, M. L., Frassine, F., Baiguini, A., Alghisi, A., Tomasini, D., Borghetti, P., Pasinetti, N., Bresciani, R., Magrini, S. M., and Buglione, M. (2019). *Mebendazole as a Candidate for Drug Repurposing in Oncology: An Extensive Review of Current Literature*. Cancers, Vol. 11(9), pp. 1284.

Guo, J., Zhao, C., Yao, R., Sui, A., Sun, L., Liu, X., Wu, S., Su, Z., Li, T., Liu, S.,

Gao, Y., Liu, J., Feng, X., Wang, W., Zhao, H., Cui, Z., Li, G., and Meng, F. (2019). *3D culture enhances chemoresistance of ALL Jurkat cell line by increasing DDR1 expression.* Experimental and Therapeutic Medicine, Vol. 17(3), pp. 1593–1600.

Guo, Y., Wang, W., and Sun, H. (2022). *A systematic review and meta-analysis on the risk factors of acute myeloid leukemia.* Translational Cancer Research, Vol 11(4), pp. 796–804.

Gu, Z., Churchman, M. L., Roberts, K. G., Moore, I., Zhou, X., Nakitandwe, J., Hagiwara, K., Pelletier, S., Gingras, S., Berns, H., Payne-Turner, D., Hill, A., Iacobucci, I., Shi, L., Pounds, S., Cheng, C., Pei, D., Qu, C., Newman, S.,Mullighan, C. G. (2019). *PAX5-driven subtypes of B-progenitor acute lymphoblastic leukemia.* Nature Genetics, Vol. 51(2), pp. 296–307.

Hamdoun, S., Jung, P., and Efferth, T. (2017). *Drug Repurposing of the Anthelmintic Niclosamide to Treat Multidrug-Resistant Leukemia.* Frontiers in Pharmacology,Vol. 8, pp. 110.

Harrison, C. J., Moorman, A. V., Broadfield, Z. J., Cheung, K. L., Harris, R. L., Reza Jalali, G., Robinson, H. M., Barber, K. E., Richards, S. M., Mitchell, C. D., Eden, T. O. B., Hann, I. M., Hill, F. G. H., Kinsey, S. E., Gibson, B. E. S., Lilleyman, J., Vora, A., Goldstone, A. H., Franklin, I. M., Childhood and Adult Leukaemia Working Parties. (2004). *Three distinct subgroups of hypodiploidy in acute lymphoblastic leukaemia.* British Journal of Haematology, Vol. 125(5), pp. 552–559.

Hodos, R. A., Kidd, B. A., Shameer, K., Readhead, B. P., and Dudley, J. T. (2016). *In silico methods for drug repurposing and pharmacology.* Wiley Interdisciplinary Reviews. Systems Biology and Medicine, Vol. 8(3), pp. 186–210.

Horowitz, N. A., and Rowe, J. M. (2019). *Advances in BCR/ABL positive ALL.* Advances in Cell and Gene Therapy, Vol. 2(3), pp. 60.

Iorio, F., Rittman, T., Ge, H., Menden, M., and Saez-Rodriguez, J. (2013). *Transcriptional data: a new gateway to drug repositioning.* Drug Discovery Today, Vol. 18(7-8), pp. 350–357.

Jacobson, S., Tedder, M., and Eggert, J. (2016). *Adult Acute Lymphoblastic Leukemia:*

A Genetic Overview and Application to Clinical Practice. Clinical Journal of Oncology Nursing, Vol. 20(6), pp. 147–154.

Jiao, X., Sherman, B. T., Huang, D. W., Stephens, R., Baseler, M. W., Lane, H. C., and Lempicki, R. A. (2012). *DAVID-WS: a stateful web service to facilitate gene/protein list analysis.* Bioinformatics, Vol. 28(13), pp. 1805–1806.

Jin, G., and Wong, S. T. C. (2014). *Toward better drug repositioning: prioritizing and integrating existing methods into efficient pipelines.* Drug Discovery Today, Vol.19(5), pp. 637–644.

Joshi, A., Rienks, M., Theofilatos, K., and Mayr, M. (2021). *Systems biology in cardiovascular disease: a multiomics approach.* Nature Reviews. Cardiology, Vol. 18(5), pp. 313–330.

Juarez, M., Schcolnik-Cabrera, A., and Dueñas-Gonzalez, A. (2018). *The multitargeted drug ivermectin: from an antiparasitic agent to a repositioned cancer drug.* American Journal of Cancer Research, Vol. 8(2), pp. 317–331.

Juliusson, G., and Hough, R. (2016). *Leukemia.* Progress in Tumor Research, Vol. 43, pp. 87–100.

Kanehisa, M. (2019). Toward understanding the origin and evolution of cellular organisms. Protein Science: A Publication of the Protein Society, 28(11), 1947–1951.

Kolde, R., Laur, S., Adler, P., and Vilo, J. (2012). *Robust rank aggregation for gene list integration and meta-analysis.* Bioinformatics, Vol. 28(4), pp. 573–580.

Kulkarni, V. S., Alagarsamy, V., Solomon, V. R., Jose, P. A., and Murugesan, S. (2023). *Drug Repurposing: An Effective Tool in Modern Drug Discovery.* Russian Journal of Bioorganic Chemistry, Vol. 49(2), pp. 157–166.

Lamontanara, A. J., Gencer, E. B., Kuzyk, O., and Hantschel, O. (2013). *Mechanisms of resistance to BCR-ABL and other kinase inhibitors.* Biochimica et Biophysica Acta, Vol. 1834(7), pp. 1449–1459.

Langfelder, P., and Horvath, S. (2008). *WGCNA: an R package for weighted correlation network analysis.* BMC Bioinformatics, Vol. 9, pp. 559.

Lee, H. J., Thompson, J. E., Wang, E. S., and Wetzler, M. (2011). *Philadelphia chromosome-positive acute lymphoblastic leukemia: current treatment and future perspectives.* Cancer, Vol. 117(8), pp. 1583–1594.

Lee, H. S., Bae, T., Lee, J.-H., Kim, D. G., Oh, Y. S., Jang, Y., Kim, J.-T., Lee, J.-J., Innocenti, A., Supuran, C. T., Chen, L., Rho, K., and Kim, S. (2012). *Rational drug repositioning guided by an integrated pharmacological network of protein, disease and drug.* BMC Systems Biology, Vol. 6, pp. 80.

Lee, M., and Rhee, I. (2017). *Cytokine Signaling in Tumor Progression.* Immune Network, Vol. 17(4), pp. 214–227.

Lejman, M., Chałupnik, A., Chilimoniuk, Z., and Dobosz, M. (2022). *Genetic Biomarkers and Their Clinical Implications in B-Cell Acute Lymphoblastic Leukemia in Children.* International Journal of Molecular Sciences, Vol. 23(5), pp. 2755

Leoni, V., and Biondi, A. (2015). *Tyrosine kinase inhibitors in BCR-ABL positive acute lymphoblastic leukemia.* Haematologica, Vol. 100(3), pp. 295–299.

Lightfoot, T., Smith, A., and Roman, E. (2017). *Leukemia.* In S. R. Quah (Ed.), International Encyclopedia of Public Health, Vol. 9, pp. 410–418.

Lilljebjörn, H., Henningsson, R., Hyrenius-Wittsten, A., Olsson, L., Orsmark-Pietras, C., von Palffy, S., Askmyr, M., Rissler, M., Schrappe, M., Cario, G., Castor, A., Pronk, C. J. H., Behrendtz, M., Mitelman, F., Johansson, B., Paulsson, K., Andersson, A. K., Fontes, M., and Fioretos, T. (2016). *Identification of ETV6-RUNX1-like and DUX4-rearranged subtypes in paediatric B-cell precursor acute lymphoblastic leukaemia.* Nature Communications, Vol. 7, pp. 11790.

Liu, Y.-F., Wang, B.-Y., Zhang, W.-N., Huang, J.-Y., Li, B.-S., Zhang, M., Jiang, L., Li, J.-F., Wang, M.-J., Dai, Y.-J., Zhang, Z.-G., Wang, Q., Kong, J., Chen, B., Zhu, Y.-M., Weng, X.-Q., Shen, Z.-X., Li, J.-M., Wang, J., Chen, S.-J. (2016). *Genomic Profiling of Adult and Pediatric B-cell Acute Lymphoblastic Leukemia.* EBioMedicine, Vol. 8, pp. 173–183.

Lu, Y., Xu, Q., Zuo, Y., Liu, L., Liu, S., Chen, L., Wang, K., Lei, Y., Zhao, X., and Li, Y. (2017). Isoprenaline/β2-AR activates Plexin-A1/VEGFR2 signals via VEGF

secretion in gastric cancer cells to promote tumor angiogenesis. BMC Cancer, Vol. 17(1), pp. 875.

Maan, K., Baghel, R., Dhariwal, S., Sharma, A., Bakhshi, R., and Rana, P. (2023). *Metabolomics and transcriptomics based multi-omics integration reveals radiation-induced altered pathway networking and underlying mechanism.* NPJ Systems Biology and Applications, Vol. 9(1), pp. 42.

Ma, J., Hou, L.-N., Rong, Z.-X., Liang, P., Fang, C., Li, H.-F., Qi, H., and Chen, H.-Z. (2013). *Antidepressant desipramine leads to C6 glioma cell autophagy: implication for the adjuvant therapy of cancer.* Anti-Cancer Agents in Medicinal Chemistry, Vol. 13(2), pp. 254–260.

Malard, F., and Mohty, M. (2020). *Acute lymphoblastic leukaemia*. The Lancet, Vol. 395(10230), pp. 1146–1162.

Malouf, C., and Ottersbach, K. (2018). *Molecular processes involved in B cell acute lymphoblastic leukaemia.* Cellular and Molecular Life Sciences: CMLS, Vol. 75(3), pp. 417–446.

Merico, D., Isserlin, R., Stueker, O., Emili, A., and Bader, G. D. (2010). *Enrichment map: a network-based method for gene-set enrichment visualization and interpretation.* PloS One, Vol. 5(11), pp. e13984.

Micheel, C. M., Nass, S. J., Omenn, G. S., Board on Health Care Services, Board on Health Sciences Policy, and Institute of Medicine. (2012). *Omics-Based Clinical Discovery: Science, Technology, and Applications.* 1st Edition. Washington (DC): National Academies Press (US).

Mudunuri, U., Che, A., Yi, M., and Stephens, R. M. (2009*). bioDBnet: the biological database network.* Bioinformatics, Vol. 25(4), pp. 555–556.

Mullighan, C. G. (2009). *Mutations of NOTCH1, FBXW7, and prognosis in T-lineage acute lymphoblastic leukemia Review of Mutations of NOTCH1, FBXW7, and prognosis in T-lineage acute lymphoblastic leukemia.* Haematologica, Vol. 94(10), pp. 1338–1340.

Mullighan, C. G. (2012). *Molecular genetics of B-precursor acute lymphoblastic leukemia.* The Journal of Clinical Investigation, Vol. 122(10), pp. 3407–3415.

Nazim, U. M., Moon, J.-H., Lee, Y.-J., Seol, J.-W., Kim, Y. J., and Park, S.-Y. (2017). *Glipizide sensitizes lung cancer cells to TRAIL-induced apoptosis via Akt/mTOR/autophagy pathways.* Oncotarget, Vol. 8(59), pp. 100021–100033.

Newman, D. J., and Cragg, G. M. (2020). *Plant Endophytes and Epiphytes: Burgeoning Sources of Known and "Unknown" Cytotoxic and Antibiotic Agents.* Planta Medica, Vol. 86(13-14), pp. 891–905.

O'Dwyer, K. M. (2022). *Optimal approach to T-cell ALL. Hematology / the Education Program of the American Society of Hematology.* American Society of Hematology. Education Program, Vol. 2022(1), pp. 197–205.

Ottmann, O. G., and Pfeifer, H. (2009). *First-line treatment of Philadelphia chromosome-positive acute lymphoblastic leukaemia in adults.* Current Opinion in Oncology, Vol. 21(1), pp. 43–46.

Oughtred, R., Rust, J., Chang, C., Breitkreutz, B.-J., Stark, C., Willems, A., Boucher, L., Leung, G., Kolas, N., Zhang, F., Dolma, S., Coulombe-Huntington, J., Chatr-Aryamontri, A., Dolinski, K., and Tyers, M. (2021). *The BioGRID database: A comprehensive biomedical resource of curated protein, genetic, and chemical interactions.* Protein Science: A Publication of the Protein Society, Vol. 30(1), pp. 187–200.

Pandita, V., Parihar, A., Parihar, D. S., Panda, S., Shanmugarajan, D., Kumari, L., and Badwaik, H. R A. Parihar, R. Khan, A. Kumar, A. K. Kaushik, and H. Gohel, (2022). *Computational Approaches for Novel Therapeutic and Diagnostic Designing to Mitigate SARS-CoV-2 Infection.* Academic Press, Vol. 13(1), pp. 267–290.

Parvathaneni, V., Kulkarni, N. S., Muth, A., and Gupta, V. (2019). *Drug repurposing: a promising tool to accelerate the drug discovery process.* Drug Discovery Today, Vol. 24(10), pp. 2076–2085.

Paul, S. M., Mytelka, D. S., Dunwiddie, C. T., Persinger, C. C., Munos, B. H., Lindborg, S. R., and Schacht, A. L. (2010). *How to improve R&D productivity: the*

pharmaceutical industry's grand challenge. Nature Reviews. Drug Discovery, Vol. 9(3), pp. 203–214.

Paulsson, K., Lilljebjörn, H., Biloglav, A., Olsson, L., Rissler, M., Castor, A., Barbany, G., Fogelstrand, L., Nordgren, A., Sjögren, H., Fioretos, T., and Johansson, B. (2015). *The genomic landscape of high hyperdiploid childhood acute lymphoblastic leukemia.* Nature Genetics, Vol. 47(6), pp. 672–676.

Pui, C.-H., and Evans, W. E. (2006). *Treatment of acute lymphoblastic leukemia.* The New England Journal of Medicine, Vol. 354(2), pp. 166–178.

Pushpakom, S., Iorio, F., Eyers, P. A., Escott, K. J., Hopper, S., Wells, A., Doig, A., Guilliams, T., Latimer, J., McNamee, C., Norris, A., Sanseau, P., Cavalla, D., and Pirmohamed, M. (2019). *Drug repurposing: progress, challenges and recommendations.* Nature Reviews. Drug Discovery, Vol. 18(1), pp. 41–58.

Qi, C., Zhou, Q., Li, B., Yang, Y., Cao, L., Ye, Y., Li, J., Ding, Y., Wang, H., Wang, J., He, X., Zhang, Q., Lan, T., Lee, K. K. H., Li, W., Song, X., Zhou, J., Yang, X., and Wang, L. (2014). *Glipizide, an antidiabetic drug, suppresses tumor growth and metastasis by inhibiting angiogenesis.* Oncotarget, Vol. 5(20), pp. 9966–9979.

Rafei, H., Kantarjian, H. M., and Jabbour, E. J. (2019). *Recent advances in the treatment of acute lymphoblastic leukemia*. Leukemia & Lymphoma, Vol. 60(11), pp. 2606–2621.

Rahman, M. R., Islam, T., Gov, E., Turanli, B., Gulfidan, G., Shahjaman, M., Banu, N. A., Mollah, M. N. H., Arga, K. Y., and Moni, M. A. (2019). *Identification of Prognostic Biomarker Signatures and Candidate Drugs in Colorectal Cancer: Insights from Systems Biology Analysis.* Medicina, Vol. 55(1), pp.20.

Ram, R., Gafter-Gvili, A., Vidal, L., Paul, M., Ben-Bassat, I., Shpilberg, O., and Raanani, P. (2010). *Management of adult patients with acute lymphoblastic leukemia in first complete remission: systematic review and meta-analysis.* Cancer, Vol. 116(14), pp. 3447–3457.

Rao, V. S., Srinivas, K., Sujini, G. N., and Kumar, G. N. S. (2014). *Protein-protein interaction detection: methods and analysis.* International Journal of Proteomics, Vol.

20, pp.147648.

Ravandi, F., and Kebriaei, P. (2009). *Philadelphia chromosome-positive acute lymphoblastic leukemia.* Hematology/oncology Clinics of North America, Vol. 23(5), pp. 1043–1063.

Reshmi, S. C., Harvey, R. C., Roberts, K. G., Stonerock, E., Smith, A., Jenkins, H., Chen, I.-M., Valentine, M., Liu, Y., Li, Y., Shao, Y., Easton, J., Payne-Turner, D., Gu, Z., Tran, T. H., Nguyen, J. V., Devidas, M., Dai, Y., Heerema, N. A., Hunger, S. P. (2017). *Targetable kinase gene fusions in high-risk B-ALL: a study from the Children's Oncology Group.* Blood, Vol. 129(25), pp. 3352–3361.

Ritchie, M. E., Phipson, B., Wu, D., Hu, Y., Law, C. W., Shi, W., and Smyth, G. K. (2015). *Limma powers differential expression analyses for RNA-sequencing and microarray studies.* Nucleic Acids Research, Vol. 43(7), pp. 47.

Roberts, K. G. (2018). *Genetics and prognosis of ALL in children vs adults. Hematology / the Education Program of the American Society of Hematology.* American Society of Hematology. Education Program, Vol. 2018(1), pp. 137–145.

Sabath, D. ,S. Maloy and K. Hughes, (2013). *Leukemia,* Brenner's Encyclopedia of Genetics. Vol. 2, pp. 226–227.

Safarzadeh Kozani, P., Safarzadeh Kozani, P., and O'Connor, R. S. (2021). *In Like a Lamb; Out Like a Lion: Marching CAR T Cells Toward Enhanced Efficacy in B-ALL.* Molecular Cancer Therapeutics, Vol. 20(7), pp. 1223–1233.

Saleh, K., Fernandez, A., and Pasquier, F. (2022). *Treatment of Philadelphia Chromosome-Positive Acute Lymphoblastic Leukemia in Adults.* Cancers, Vol. 14(7), pp. 1805

Samra, B., Jabbour, E., Ravandi, F., Kantarjian, H., and Short, N. J. (2020). *Evolving therapy of adult acute lymphoblastic leukemia: state-of-the-art treatment and future directions.* Journal of Hematology & Oncology, Vol. 13(1), pp. 70.

Sawada, R., Iwata, H., Mizutani, S., and Yamanishi, Y. (2015). *Target-Based Drug Repositioning Using Large-Scale Chemical-Protein Interactome Data.* Journal of

Chemical Information and Modeling, Vol. 55(12), pp. 2717–2730.

Sell, S. (2005). *Leukemia: stem cells, maturation arrest, and differentiation therapy.* Stem Cell Reviews, Vol. 1(3), pp. 197–205.

Shannon, P., Markiel, A., Ozier, O., Baliga, N. S., Wang, J. T., Ramage, D., Amin, N., Schwikowski, B., and Ideker, T. (2003). *Cytoscape: a software environment for integrated models of biomolecular interaction networks. Genome Research,* Vol. 13(11), pp. 2498–2504.

Smyth, G. K. (2004). Linear models and empirical bayes methods for assessing differential expression in microarray experiments. Statistical Applications in Genetics and Molecular Biology, 3, Article3.

Sobie, E. A., Lee, Y.-S., Jenkins, S. L., and Iyengar, R. (2011). *Systems biology-biomedical modeling.* Science Signaling, Vol. 4(190), pp. tr2.

Song, Y., Yang, X., and Yu, B. (2022). *Repurposing antidepressants for anticancer drug discovery*. Drug Discovery Today, Vol. 27(7), pp. 1924–1935.

Stathias, V., Turner, J., Koleti, A., Vidovic, D., Cooper, D., Fazel-Najafabadi, M., Pilarczyk, M., Terryn, R., Chung, C., Umeano, A., Clarke, D. J. B., Lachmann, A., Evangelista, J. E., Ma'ayan, A., Medvedovic, M., and Schürer, S. C. (2020). *LINCS Data Portal 2.0: next generation access point for perturbation-response signatures.* Nucleic Acids Research, Vol. 48(1), pp. 431–439.

Subramanian, A., Narayan, R., Corsello, S. M., Peck, D. D., Natoli, T. E., Lu, X., Gould, J., Davis, J. F., Tubelli, A. A., Asiedu, J. K., Lahr, D. L., Hirschman, J. E., Liu, Z., Donahue, M., Julian, B., Khan, M., Wadden, D., Smith, I. C., Lam, D., Golub, T. R. (2017). *A Next Generation Connectivity Map: L1000 Platform and the First 1,000,000 Profiles.* Cell, Vol. 171(6), pp.1437–1452.

Terwilliger, T., and Abdul-Hay, M. (2017). *Acute lymphoblastic leukemia: a comprehensive review and 2017 update*. Blood Cancer Journal, Vol. 7(6), pp. 577.

Thomas, P. D., Ebert, D., Muruganujan, A., Mushayahama, T., Albou, L.-P., and Mi, H. (2022). *PANTHER: Making genome-scale phylogenetics accessible to all*. Protein

Science: A Publication of the Protein Society, Vol. 31(1), pp. 8–22.

Thomas, X., and Heiblig, M. (2016a*). Diagnostic and treatment of adult Philadelphia chromosome-positive acute lymphoblastic leukemia.* International Journal of Hematologic Oncology, Vol. 5(2), pp. 77–90.

Thomas, X., and Heiblig, M. (2016b). *The development of agents targeting the BCR-ABL tyrosine kinase as Philadelphia chromosome-positive acute lymphoblastic leukemia treatment.* Expert Opinion on Drug Discovery, Vol. 11(11), pp. 1061–1070.

Turanli, B., Altay, O., Borén, J., Turkez, H., Nielsen, J., Uhlen, M., Arga, K. Y., and Mardinoglu, A. (2021). *Systems biology based drug repositioning for development of cancer therapy.* Seminars in Cancer Biology, Vol. 68, pp. 47–58.

Turanli, B., Grøtli, M., Boren, J., Nielsen, J., Uhlen, M., Arga, K. Y., and Mardinoglu, A. (2018). *Drug Repositioning for Effective Prostate Cancer Treatment*. Frontiers in Physiology, Vol. 9, pp.500.

Turanli, B., Gulfidan, G., and Arga, K. Y. (2017). *Transcriptomic-Guided Drug Repositioning Supported by a New Bioinformatics Search Tool: geneXpharma.* Omics: A Journal of Integrative Biology, Vol. 21(10), pp. 584–591.

Tusher, V. G., Tibshirani, R., and Chu, G. (2001). *Significance analysis of microarrays applied to the ionizing radiation response*. Proceedings of the National Academy of Sciences of the United States of America, Vol. 98(9), pp. 5116–5121.

Uchida, S., Kobayashi, K., Ohno, S., Sakagami, H., Kohase, H., and Nagasaka, H. (2019). *Induction of Non-Apoptotic Cell Death by Adrenergic Agonists in Human Oral Squamous Cell Carcinoma Cell Lines*. Anticancer Research, Vol. 39(7), pp. 3519–3529.

Vadillo, E., Dorantes-Acosta, E., Pelayo, R., and Schnoor, M. (2018). *T cell acute lymphoblastic leukemia (T-ALL): New insights into the cellular origins and infiltration mechanisms common and unique among hematologic malignancies.* Blood Reviews, Vol. 32(1), pp. 36–51.

Von Eichborn, J., Murgueitio, M. S., Dunkel, M., Koerner, S., Bourne, P. E., and

Preissner, R. (2011). *PROMISCUOUS: a database for network-based drug-repositioning.* Nucleic Acids Research, Vol. 39(1), pp. 1060–1066.

Wang, S., and He, G. (2016). *2016 Revision to the WHO classification of acute lymphoblastic leukemia.* Journal of Translational Internal Medicine, Vol. 4(4), pp. 147–149.

Wang, W.-Z., Lin, X.-H., Pu, Q.-H., Liu, M.-Y., Li, L., Wu, L.-R., Wu, Q.-Q., Mao, J.-W., Zhu, J.-Y., and Jin, X.-B. (2014). *Targeting miR-21 sensitizes Ph+ ALL Sup-b15 cells to imatinib-induced apoptosis through upregulation of PTEN*. Biochemical and Biophysical Research Communications, Vol. 454(3), pp. 423–428.

Wei, G., Wang, J., Huang, H., and Zhao, Y. (2017). *Novel immunotherapies for adult patients with B-lineage acute lymphoblastic leukemia.* Journal of Hematology & Oncology, Vol. 10(1), pp. 150.

Wieduwilt, M. J. (2022*). Ph+ ALL in 2022: is there an optimal approach? Hematology / the Education Program of the American Society of Hematology.* American Society of Hematology. Education Program, Vol. 2022(1), pp. 206–212.

Xing, H., Yang, X., Liu, T., Lin, J., Chen, X., and Gong, Y. (2012). *The study of resistant mechanisms and reversal in an imatinib resistant Ph+ acute lymphoblastic leukemia cell line.* Leukemia Research, Vol. 36(4), pp. 509–513.

Xiu, Y., Dong, Q., Li, Q., Li, F., Borcherding, N., Zhang, W., Boyce, B., Xue, H.-H., and Zhao, C. (2018). *Stabilization of NF-κB-Inducing Kinase Suppresses MLL-AF9-Induced Acute Myeloid Leukemia.* Cell Reports, Vol. 22(2), pp. 350–358.

Yang, D. K., and Kim, S.-J. (2017). *Desipramine induces apoptosis in hepatocellular carcinoma cells.* Oncology Reports, Vol. 38(2), pp. 1029–1034.

Yilmaz, M., Kantarjian, H., Ravandi-Kashani, F., Short, N. J., and Jabbour, E. (2018). *Philadelphia chromosome-positive acute lymphoblastic leukemia in adults: current treatments and future perspectives.* Clinical Advances in Hematology & Oncology: H&O, Vol. 16(3), pp. 216–223.

Zafar, S., Armaghan, M., Khan, K., Hassan, N., Sharifi-Rad, J., Habtemariam, S.,

Kieliszek, M., Butnariu, M., Bagiu, I.-C., Bagiu, R. V., and Cho, W. C. (2023). *New insights into the anticancer therapeutic potential of maytansine and its derivatives.* Biomedicine & Pharmacotherapy Biomedecine & Pharmacotherapie, Vol. 165, pp. 115039.

Zazuli, Z., Irham, L. M., Adikusuma, W., and Sari, N. M. (2022). *Identification of Potential Treatments for Acute Lymphoblastic Leukemia through Integrated Genomic Network Analysis.* Pharmaceuticals, Vol. 15(12), pp.1562

Zeisig, B. B., Fung, T. K., Zarowiecki, M., Tsai, C. T., Luo, H., Stanojevic, B., Lynn, C., Leung, A. Y. H., Zuna, J., Zaliova, M., Bornhauser, M., von Bonin, M., Lenhard, B., Huang, S., Mufti, G. J., and So, C. W. E. (2021). *Functional reconstruction of human AML reveals stem cell origin and vulnerability of treatment-resistant MLL-rearranged leukemia.* Science Translational Medicine, Vol. 13(582), pp.4822

Zhang, L., Habeebu, S. S. M., and Li, W. (2022). *Prognostic and Predictive Biomarkers in Precursor B-cell Acute Lymphoblastic Leukemia.* Exon Publications, Vol. 13.

Zhang, X., Rastogi, P., Shah, B., and Zhang, L. (2017). *B lymphoblastic leukemia/lymphoma: new insights into genetics, molecular aberrations, subclassification and targeted therapy.* Oncotarget, Vol. 8(39), pp. 66728–66741.

Zhang, Z., Zhou, L., Xie, N., Nice, E. C., Zhang, T., Cui, Y., and Huang, C. (2020). *Overcoming cancer therapeutic bottleneck by drug repurposing*. Signal Transduction and Targeted Therapy, Vol. 5(1), pp. 113.

Zhou, Y., Zhou, B., Pache, L., Chang, M., Khodabakhshi, A. H., Tanaseichuk, O., Benner, C., and Chanda, S. K. (2019). *Metascape provides a biologist-oriented resource for the analysis of systems-level datasets*. Nature Communications, Vol. 10(1), pp. 1523.

Zou, J., Zheng, M.-W., Li, G., and Su, Z.-G. (2013). *Advanced systems biology methods in drug discovery and translational biomedicine.* BioMed Research International, Vol. 13, pp.742835.